Contents

Organisation 2011

Scientific Committee

Ivan Stamenkovic
Institute of Pathology – CHUV

Liliane Michalik
Center for Integrative Genomics – UNIL

Lucia Mazzolai
Angiology – CHUV

François Pralong
Endocrinology, Diabetology and Metabolism – CHUV

Gérard Waeber
Internal Medicine - CHUV

Eric Eeckhout
Cardiology – CHUV

FBM Organisation Committee

Jovan Mirkovitch
Zadria Berzin
Nathalie Magnenat
Anne Tricot

Message of the Vice-Dean for Research

Dear Friends and Colleagues,

On behalf of the Organizing Committee I would like to welcome you to the ninth edition of the CHUV Research Day, which will be dedicated to cardiology and metabolism. Clinical and research development in both fields has been given high priority at the CHUV and UNIL, and the coming years should see significant progress toward the establishment of corresponding clinical and research centres.

Growing evidence indicates that inflammation is causally related to obesity and diabetes. Thus, obesity is associated with low grade systemic inflammation that constitutes one of the mechanisms underlying obesity-associated morbidity. Moreover, chronic inflammation is a significant risk factor for the development of cardiovascular and metabolic disease and continuous secretion of factors such as $TNF\alpha$ and IL-6 is associated with increased risk for numerous chronic diseases including insulin resistance, atherosclerosis and type 2 diabetes.

Given that obesity is a complex disorder, a mutidisciplinary approach is necessary to unravel its pathogenesis and underlying mechanisms. The use of numerous « omic » technologies including genomics, proteomics and metabolomics is becoming essential in order to identify inflammatory biomarkers that may be implicated in the pathogenesis of obesity and the mechanisms that link the increase in adipose mass to morbidity. Once identified, elucidation of the role of the relevant inflammatory factors in the various disorders related to obesity will be essential.

Among cardiovascular diseases, atherosclerosis is linked not only to inflammation but to an adaptive immune response as well. However, whereas the role of Th1 lymphocytes in atherogenesis is well established, less is known about the role of othee T cell subsets, including Th2 and Th17. Elucidation of the full repretoire of mechanisms whereby adaptive immunity enhances atherogenesis will no doubt be important.

The program to which you have been invited will cover a variety of aspects of the implication of inflammation and immunity in obesity and atherogenesis with a view as to possible novel therapeutic approaches down the line.

I would like to thank the Scientific Committee for putting together a high quality program with a superb panel of guest speakers and hope that you will find the event to be both stimulating and enjoyable.

Ivan Stamenkovic
Vice-Doyen for Research

Message du Vice-Doyen de la Recherche

Cher(e)s Collègues, Cher(e)s Ami(e)s,

Je vous souhaite la bienvenue à la neuvième édition de la Journée de Recherche CHUV dont les thématiques sont la cardiologie et le métabolisme. Ces thématiques représentent des domaines de développement prioritaires du CHUV et de l'UNIL et prennent une importance croissante dans notre Faculté.

Les développements récents dans le domaine du métabolisme indiquent que l'inflammation joue un rôle important dans l'obésité et dans le diabète. Ainsi, l'obésité est associée à un état inflammatoire systémique chronique de bas grade qui constitue l'un des mécanismes potentiels impliqué dans les complications de l'obésité. L'inflammation chronique de bas grade est un facteur de risque significatif pour les maladies cardiovasculaires et métaboliques, et la sécrétion continue des médiateurs tels que le TNFα et l'IL-6 est associée à un risque augmenté pour de nombreuses maladies chroniques y compris la résistance à l'insuline, l'artériosclérose et le diabète de type II.

La physiologie de l'obésité étant complexe, il est évident qu'une approche multidisciplinaire est nécessaire pour comprendre son processus et les mécanismes qui y conduisent. L'utilisation de nouvelles technologies, y compris la génomique, la protéomique et la métabolomique devient indispensable afin d'identifier les biomarqueurs inflammatoires qui pourraient être impliqués dans la pathogénèse de l'obésité ainsi que dans les mécanismes moléculaires qui lient l'augmentation la masse du tissu adipeux aux dysfonctions de l'organisme. Il est de ce fait essentiel de comprendre le rôle des différents facteurs inflammatoires dans les affections liées à l'obésité.

Parmi les maladies cardiovasculaires, la pathogénèse de 'artériosclérose est intimement liée à la réponse immune adaptative. Toutefois, alors que le rôle athérogène des lymphocytes Th1 est bien établi, celui des autres sous groupes lymphocytaires T, y compris Th2 et Th 17 l'est moins mais de plus en plus de données suggèrent que ces lymphocytes participent à la régulation de l'artériosclérose et l'élucidation de leur mécanisme d'action sera d'importance.

Le programme auquel vous êtes conviés fait le point sur les approches actuelles de l'analyse de la réponse inflammatoire et immune dans l'obésité et dans l'artériosclérose et examine les voies thérapeutiques possibles.

Je tiens à remercier les membres du comité scientifique pour avoir établi un programme stimulant et de très haute qualité et je vous souhaite de passer une journée agréable.

Ivan Stamenkovic
Vice-Doyen de la Recherche

*F*aculty of *B*iology and *M*edicine
FBM RESEARCH DAY 2011
Thursday, January 27th, 2011

César-Roux Auditorium, CHUV, Lausanne

Attendance is free - No registration is necessary

"Cardiovascular & Metabolic Disorders"

08:45 Ivan STAMENKOVIC
Vice Dean for Research

NUTRITION AND METABOLISM

09:00 Karine CLEMENT
Pierre & Marie Curie University, Paris, France
Human adipose tissue; pathological alteration in obesity and diabetes

09:45 Coffee & Poster presentations

10:15 PACTT and morning short talks

11:45 Johan AUWERX
EPFL, Lausanne, Switzerland
Integrating metabolic control by NAD+ sensors

12:30 Lunch, Coffee & Poster presentations

ATHEROSCLEROSIS & INFLAMMATION

13:30 Ziad MALLAT
Inserm U970, Paris, France
University of Cambridge, Cambridge, UK
Adaptive Immunity in Atherosclerosis

14:15 Euresearch and afternoon short talks

15:45 Coffee & Poster presentations

VASCULAR AGEING VASCULAR AGEING

16:15 Pierre BOUTOUYRIE
G. Pompidou European Hospital, Paris, France
Vascular ageing: patholophysiology and basis for therapeutics

17:00 Poster Prize Ceremony

17:30 Apéritif

Schedule	Names & Departments	Titles
Morning		
10h15 - 10h30	**Stefan KOHLER** PACTT – UNIL/CHUV	*From the lab to the market: Commercialisation of research results*
10h30 – 10h45	**Cécile JACOVETTI** Department of Cellular Biology and Morphology - UNIL	*The role of micro-RNAs in beta-cell mass expansion during pregnancy*
10h45 – 11h00	**Pedro MARQUES-VIDAL** Social and Preventive Medicine CHUV	*Prevalence and management of cardiovascular risk factors among migrants in Switzerland*
11h00 – 11h15	**Francesca AMATI** Department of Physiology - UNIL and Service of Endocrinology, Diabetology and Metabolism - CHUV	*Skeletal muscle mitochondrial content and electron transport chain activity in older adults at risk for type 2 diabetes: relationship to insulin sensitivity, metabolic flexibility and fatty acid oxidation*
11h15 – 11h30	**Evrim JACCARD** Departement of Physiology UNIL	*Involvement of the RasGAP-derived fragment N in the resistance of pancreatic beta cells towards apoptosis*
11h30 – 11h45	**Luca CARIOLATO** Institute of Pharmacology and Toxicology - UNIL	*Characterization of novel hypertrophic pathways activated by the AKAP-Lbc signalling complex in cardiomyocytes*
Afternoon		
14h15 – 14h30	**Sasha HUGENTHOBLER** Euresearch	*European funding opportunities for health and health related research*
14h30 – 14h45	**Mohammed NEMIR** Experimental Cardiology Unit CHUV	*Cardiac-specific overexpression of the Notch ligand Jagged1 reduces cardiac hypertrophy and fibrosis in response to hemodynamic stress*
14h45 – 15h00	**Hoshang FARHRAD** Service of Nuclear Medicine CHUV	*Myocardial Blood Flow Quantification with Rubidium-82 Cardiac PET has Incremental Prognostic Value in Patients with Known or Suspected Coronary Artery Disease*
15h00 - 15h15	**Muriel AUBERSON** Department of Pharmacology and Toxicology - UNIL	*GLUT9 and uric acid handling by the kidney*
15h15 - 15h30	**Fabienne MAURER** Service of Medical Genetics CHUV	*Mapping genetic variants associated to beta-adrenergic responses in inbred mice*
15h30 – 15h45	**Maxime PELLEGRIN** Service of Angiology CHUV	*Critical role of Angiotensin II type 1 receptor on bone marrow-derived cells in the development of vulnerable atherosclerotic plaque in 2-Kidney, 1-Clip ApoE-/- mice*

EHU
Human Environment

« Je sais pas si vous avez des plans pour l'avenir » ou les énoncés déclaratifs à valeur questionnante dans les entretiens oncologiques

[1]Bourquin C., [1]Stiefel F., [1]Singy P.

Psychiatric Liaison Service, DP-CHUV[1]

Si l'enseignement postgradué des compétences communicationnelles (*communication skills*) en médecine – et spécialement en oncologie – fait déjà l'objet d'un certain nombre d'évaluations, l'impact global de ce type d'enseignement au niveau prégradué reste encore largement à déterminer. Un fonds d'innovation pédagogique (FIP) visant à éclairer la portée d'un enseignement individualisé (en 1ère année de master), comparativement à un enseignement en petits groupes, consistant en une simulation de situation complexe (annonce de diagnostic d'une maladie oncologique – pouvant bénéficier d'une chimiothérapie soit curative, soit palliative – lors d'un entretien filmé avec un patient simulé) a constitué le cadre d'une première évaluation scientifique de la formation à la communication médecin/patient reçue par les étudiants en médecine de Lausanne.

Les compétences communicationnelles des étudiants ont été mesurées notamment au moyen du RIAS (Roter Interaction Analysis System), une méthode de codage qui permet d'associer l'ensemble des énoncés produits lors d'un entretien clinique à 42 catégories « de contenu » mutuellement exclusives. Les questions, « supercatégorie » qui nous intéresse ici, sont catégorisées sur la base de leur forme, ouverte vs fermée, et de leur contenu – en lien avec la condition médicale, le plan de traitement, le style de vie ou le psychosocial.

L'analyse des entretiens filmés menés par les étudiants (N=63) avec un patient simulé a fait ressortir l'usage récurrent d'énoncés de type *je sais pas si - vous avez déjà entendu parler des chimiothérapies / vous avez des plans pour l'avenir / …* ou *je sais pas comment - vous vous sentez aujourd'hui après cette opération / vous aimeriez que ça se passe / …* (26 étudiants (41%) recourent de 1 à 7 fois à ces énoncés durant leurs entretiens). Ces énoncés font question, pour ainsi dire, et sont l'objet d'une étude exploratoire en cours. Etude qui interroge notamment la particularité de ces énoncés interrogatifs (indirects) se présentant sous une forme déclarative, leur intentionnalité – spécifique (question fermée) vs exploratoire (question ouverte) – et la possible spécificité des contenus qu'ils véhiculent. Une comparaison de l'échantillon des étudiants avec un échantillon d'oncologues (N=31) ayant conduit de semblables entretiens montre que ce type d'énoncés est atypique chez ces derniers (4 oncologues y recourent de 1 à 2 fois au cours de leurs entretiens). Il s'agit donc aussi de tenter de saisir les raisons de la récurrence de ces formulations en *je sais pas* parmi les étudiants : expression d'un sentiment d'insécurité relativement au sujet discuté, marqueur d'atténuation ou générationnel, mécanisme de défense ?

Exposition au virus de l'hépatite E dans les STEP

[1]Masclaux F., [2]Duquenne P., [3]Hotz P., [1]Oppliger A.

Institut universitaire romand de Santé au Travail (IST)[1], INRS Nancy, France[2], Département de médecine du travail, Université de Zürich[3]

L'hépatite E est une inflammation du foie provoquée par un virus à ARN appelé VHE. L'hépatite E est très répandue dans la plupart des pays en développement et fréquente dans tous les pays au climat chaud. Elle se propage principalement par le biais de la contamination fécale de l'approvisionnement en eau ou en nourriture. Dans les pays développés comme la Suisse ou la France, il y a peu de personnes touchées par une hépatite E. Cependant, les statistiques montrent que les cas sont en forte augmentation dans ces pays, sans qu'il soit pour le moment possible d'expliquer cette augmentation.

En Suisse, une étude longitudinale montre une incidence non négligeable de séroconversion pour le VHE chez des travailleurs avec 26 nouveaux cas apparus en 5 ans dans une cohorte de 667 travailleurs (Tschopp et al 2008). L'eau contaminée par les matières fécales est un vecteur de transmission de beaucoup de maladies virales, bactériennes ou parasitaires. La recherche du VHE dans ce type d'eau peut permettre de mesurer le niveau de circulation du virus tout en identifiant les différentes souches en circulation. De plus, travailler à proximité des eaux usées pourrait être une situation de risque pour les employés des STEP. Les voies possibles de contamination dans ces STEP n'ont pas encore été identifiées : la contamination peut se produire par contact direct avec l'eau, par contact avec des surfaces contaminées (transfert au niveau de lésion cutanées ou par ingestion) ou par inhalation ou déglutition d'aérosols contaminés.

Une méthode de détection du VHE a été développée : c'est une méthode moléculaire de type RT-PCR en temps réel TaqMan (RTi RT-PCR - TaqMan). Des STEP suisses ont été sélectionnées afin d'avoir un échantillonnage représentatif de leur grande variété d'environnements (urbain, rural,). La recherche du VHE a été entreprise dans ces STEP en analysant les eaux et l'air environnant, prélevés à différents niveaux de traitement. Ce travail permettra d'évaluer l'exposition professionnelle aux VHE dans les STEP. Il permettra aussi de fournir des informations sur les réservoirs du virus et sur les voies de propagation.

Good implementation of a smoking ban in public places in the Seychelles

[1]Plumettaz C., [2]Viswanathan B., [2]Shamlaye C., [2]Gedeon J., [1]Bovet P.

Institute of Social and Preventive Medicine - CHUV[1], Ministry of Health, Republic of Seychelles[2]

Background Following two decades of continued tobacco control activities, a smoking ban in all enclosed public places was initiated in August 2009 in the Seychelles (African region), as part of a comprehensive tobacco control legislation. After nine months of a "grace period" (penalties were not issued against for offenders), we assessed the level of implementation of the ban.

Methods Seven survey officers visited, during a two-week period, 38 most popular hospitality venues in the country, including all bars and discotheques. In each venue, a survey officer observed compliance with the smoking ban for 15 minutes and subsequently administered a structured questionnaire to two customers, two workers and one manager.

Results In the 38 venues, information was gathered from 63 patrons, 66 workers and 34 managers. Survey officers witnessed virtually no smoking in the indoor premises. 88% of managers but only 65% of workers "often" or "always" requested customers to stop smoking. 88% of workers and 98% of managers reported that smoking customers "generally agree smoothly" to stop smoking when requested. The smoking ban was supported by approximately 90% of the patrons, workers and managers. Health improvement was reported by 20% of workers. Respectively 21% of managers and 9% of workers reported a decrease in business but 17% of managers reported new customers since the smoking ban took effect.

Conclusion We found good compliance with the smoking ban in hospitality venues in the Seychelles. Despite a few weaknesses in the implementation processes, suggesting the need for further training of workers and application of enforcement measures, our findings suggest that a smoking ban has a large potential for self-implementation, conditional on favorable circumstances, i.e. previous tobacco control activities likely to mould social support to clean air policy. This study also provides an example of a simple and inexpensive methodology to evaluate the implementation and impact of clean air policy.

Aménagement d'un laboratoire de production cellulaire selon les GMP au CHUV

CALMET G.

CHUV

Le Centre Universitaire Vaudois souhaite créer un laboratoire de production cellulaire, appelé Centre de Production Cellulaire du CHUV ou CPC2.

Ce centre sera un laboratoire destiné à la production de cellules selon les réglementations GMP, dans des domaines variés tels que la production de peau pour le Centre Romand des Grands Brûlés, et des applications liées à la recherche clinique (production de cellules neurales, mésenchymateuses, …).

La réglementation suisse impose aux laboratoires qui souhaitent se lancer dans le développement technique de la thérapie cellulaire, de respecter les « Good Manufacturing Practice for medicinal Products » (GMP). Cela implique des contraintes relativement sévères dans différents domaines.

Pour respecter ces recommandations, l'équipe d'ingénierie biomédicale du CHUV ainsi que les responsables du projet CPC2 ont travaillé sur plusieurs concepts, puis à l'élaboration d'un cahier des charges techniques pour une étude de marché. Plusieurs solutions techniques ont été envisagées, mais après mûres réflexions, il s'avère que l'installation d'isolateurs « ultra-propres » semble la meilleure, tant au niveau des contraintes techniques que financières. Un appel d'offres fut envoyé pour l'acquisition de tels modules.

En parallèle, d'autres outils sont mis en places afin de faciliter la certification du laboratoire, telle qu'un logiciel LIMS (pour *Laboratory Information Management System*).

Mots clés : thérapie cellulaire ; production cellulaire ; classe de propreté ; CHUV ;
grands brûlés ; peau ; monitoring, air, réglementation suisse.

De novo sequencing of the genome of the human pathogenic fungus *Pneumocystis jirovecii* from lung microbiome

[1-2]Cissé O., [1]Hauser P., [2]Pagni M.

Institute of Microbiology -CHUV[1], Vital-IT group - SIB[2]

Pneumocystis jirovecii is an opportunistic fungus, which causes life-threatening pneumonia in immunocompromised patients. The lack of a culture method *in vitro* has hampered progress in the understanding of its biology. Sequencing *P. jirovecii* genome is complicated by the fact that its DNA can be isolated only from bronchoalveolar lavage specimens, which implies small amounts and contamination from other organisms. These difficulties can now be overcome using the new techniques of random DNA amplification and high throughput sequencing, as well as appropriate bioinformatics strategy. The main problem in this approach is the reconstruction of the whole genome out of a mixture of DNA sequences from diverse organisms. We are using the following procedure in order to obtain a high-quality genome assembly. First, we performed an enrichment of the BAL in *P. jirovecii* cells using immuno-precipitation. Multiple displacement amplification was then used to obtain large amounts of DNA. 1'192'988 sequence reads were analysed by comparison to other relevant genomes, including the *Pneumocystis* species infecting rats. Currently, 20% of reads had a high homology with *P. carinii* and were considered as being from *P. jirovecii*. Remaining reads considered, as non-*Pneumocystis* using rigorous control will be removed before assembly of *P. jirovecii* genome. Recent updates will be presented.

Gender and communicative competence in medical setting: a case study

[1]SULSTAROVA B., [1]SINGY P.

Liaison Psychiatry Service[1]

Background: Although we can observe a rise in number of women in medical profession, they are still less present in the high ranking positions. Some researches have shown the impact of physician gender on medical communication with patients. They revealed that female physicians engage in more patient-centered communication than do their male peers. Few researches, however, have examined how the gender affect the backstage communication, where the health care professionals learn to gain communicative competences through discourse and to present themselves as future candidate for professional careers.

Aims: An ongoing Ph.D. study in sociolinguistics attempts to show the linguistic practices used by health care providers when they discuss amongst themselves in a formal setting. The study aims mainly to find gender differences in these linguistics practices and to investigate the perceptions of health care providers on the importance of backstage communication and on the gender linguistic patterns in this context.

Methods: Data are collected in the Liaison Psychiatry Service (CHUV) in two phases. In the first phase, eight meetings with several male and female physicians, psychologists, nurses and social workers supervised by an expert psychiatrist, were filmed. In the second phase, 25 semi-directive interviews were conducted with members of all professions in this service. All the data are transcribed and submitted to quantitative and qualitative discourse analyses.

Results and discussion: The preliminary results reveal the impact of gender in gaining communicative competence in medical settings. The evaluation of speaking time in the recorded meetings shows an evident asymmetry between male and female health care professionals. The male dominate the verbal exchange independently of their professional status. Gender differences are also observed in linguistic practices used by male and female health care professionals during medical communication. It seems that the participants in the meetings choose strategically the linguistics practices according to the norms of a particular community and according to the linguistic behaviors considered appropriate to women and men. When asked about their experiences and linguistic behavior in medical settings, some physician women insist on the barriers they are facing as speakers in institutional settings. They are more likely to experience "anxiety" when speaking in such formal settings than their male colleagues.

Influence of individual factors on occupational solar UV exposure - for a targeted prevention

[1]Milon A., [1]Vernez D., [2]Bulliard J.-L., [3]Bonneau J.

Institute for Work and Health, DUMSC[1], Institute of Social and Preventive Medicine, DUMSC[2], EHESP School of Public Health[3]

BACKGROUND

UV is a carcinogenic agent involved in both the initiation and promotion of skin cancers. Over the last decades, skin cancer rates have markedly increased in Caucasian populations worldwide. And Switzerland has one of the highest rates of melanoma and non-melanoma skin cancers in Europe. Outdoor workers, such as agricultural workers, are at increased risk of skin cancer. The lag time between sun exposure and severe cutaneous damage, along with the positive social perception of tanning, render compliance with sun protection messages challenging. Specific educational messages and prevention strategies focusing on the work place and occupational exposure appear to be a key reinforcement to reach this highly sun-exposed subgroup.

MATERIAL AND METHODS

A questionnaire has been used to obtain information on sun-related behaviour during occupational and leisure activities (use of sun protective measures, history of skin cancers, sun sensitivity, knowledge and understanding of UV Index). Through the collaboration with professional farmers' associations, 4000 questionnaires were sent to farmers in Vaud, Valais, Neuchâtel and Jura cantons,.

In addition, field measurements using biological film dosimeters were performed to estimate the daily UV dose associated to several agricultural activities (vineyard, arboriculture, cereal and agriculture).

RESULTS

This study (answer rate = 29%) indicated a better knowledge of UV risk in this specific population compared to the general population. However, this awareness did not translate into a systematic use of sun-protective measures and showed an under-estimation of the personal UV risk, especially at work. If farmers knew the UV index and could describe it better than the general population, it was scarcely used to plan outdoor activities. Surprisingly, significant differences between vineyard/arboriculture workers and farmers were evidenced on risk perception and protective measures used at work.

Personal solar UV exposure measurements indicated an elevated acute and chronic exposure associated to agricultural activities. Combined with postural activity recordings, these results confirmed a risk of over-exposing specific anatomical parts where cutaneous carcinomas tend to appear.

CONCLUSION

This study was the first broad-scaled description of the knowledge and UV risk perception, and use of sun protective measures in an occupational activity in Switzerland. The differences in sun exposure modalities between leisure and occupational activities reinforce the need for specific prevention messages on occupational solar UV exposure for outdoor workers.

Incidence of colorectal cancers and polyps in Vaud, 1983-2007:
Trends and determinants

F. Bruchez[1], F. Levi[2,3], J-L. Bulliard[2]

[1]   Faculty of Biology and Medicine (FBM), Lausanne, Switzerland
[2]   Cancer Epidemiology Unit, University Institute of Social and Preventive Medicine (IUMSP), Centre Hospitalier Universitaire Vaudois (CHUV) and University of Lausanne, Switzerland
[3]   Vaud Cancer Registry, Lausanne, Switzerland

Background:

Colorectal cancer is the second most lethal cancer and third most common neoplasm in Switzerland, with about 1600 deaths and 4000 new cases per year, respectively. A prior study in the canton of Vaud showed an increase in rates of polyps but a stable incidence of colorectal cancer between 1979 and 1996 with however diverging trends according to subsite.

Objectives:

To examine recent trends (1983-2007) in colorectal polyps and cancers, and explore determinants of these trends in a rare population-based series on polyps in the world.

Methods:

16,308 first polyps and 7063 primary cancers of the colon and rectum registered between 1983 and 2007 were extracted from the Vaud Cancer Registry. Standardised (European population) rates as well as sex, age- and site-specific incidence rates were computed.

Results:

A fourfold increase was observed in the detection rate of polyps (from 46/100,000 in 1985-89 to 188/100,000 in 2003-07) while colorectal cancer incidence remained constant (35-40/100,000) over the 25-year period studied. Rates of polyps increased exponentially since the late 1980s. The proportion of polyps in the right side of colon doubled (17% to 35%) whereas a commensurate decrease was seen in the percentage of polyps in the rectum. No statistically significant change occurred in the sex, grade or site distribution of colorectal cancer over time, and trends by stage at diagnosis were inconsistent. However, a concomitant shift to younger age at diagnosis was found both for polyps and cancers, with a higher risk of polyp and cancer in males than females.

Conclusion:

The large increase in detection rate of polyps, along with shifts to right-sided adenomas and younger age at diagnosis support the effect of an increasing use of colonoscopy as a screening and diagnostic tool. In a multifactorial and evolving context, the stable incidence of colorectal cancer can be explained by several concomitant and antagonistic factors which may mask the impact of the increasing practice of opportunistic screening in the Vaud population.

ENA
Natural Environment

Exposure to microorganisms and endotoxins in crop workers

[1]Niculita-Hirzel H., [1]Oppliger A.

Institute for Work and Health [1]

Microorganisms are biotic factors that may strongly affect farmers' health. They may be present at a particularly high concentration in the air when they are mechanically aerosolized during harvesting and post-harvesting operations. Regular inhalation of these microorganisms and of their constituents (e.g. endotoxins, β-glucans, mycotoxins) has been proposed to be responsible of the high prevalence of respiratory syndromes among farmers. For this raison, general preventive strategies are needed in order to decrease farmer exposure to these bioaerosols. This study aims to identify the factors that reduce the growth of fungi and bacteria in crops.

In agroecosystem, the composition of soil fungal and bacteria communities is greatly influenced by agriculture practices such as the usage or not of tilling, of nutritional additives or of different fungicides. A change in soil microbial community composition may directly affect the concentration in bacteria, fungal particles and mycotoxins deliver in air. In order to test this hypothesis, we sampled soil, plant, grain and air during harvesting from 100 sites randomly distributed through Vaud canton representative of the different agriculture practices. Genomic DNA has been extracted from these samples and fungal and bacteria concentration has been evaluated by Q-PCR on the ITS2 and 16S respectively. The results are interpreted by taking in account the agriculture practice, the Phosphorus : Carbon : Nitrogen ratio of the soil, the altitude and the average of rainy days per year.

Estrella lausannensis, a new species within the Chlamydiales order

[1]LIENARD J., [1]CROXATTO A., [1]GREUB G.

Institute of Microbiology - CHUV[1]

Originally, the *Chlamydiales* order was represented by a single family, the *Chlamydiaceae*, composed of several pathogens, such as *Chlamydia trachomatis*, *C. pneumoniae*, *C. psittaci* and *C. abortus*. Recently, 4 new families have been added to the order. *Chlamydia*-related bacteria are strict intracellular bacteria, able for the most to replicate in free-living amoebae. Amoebal co-culture that selectively isolates amoeba-resisting bacteria allowed the discovery of the strain CRIB 30, from an environmental water sample. Based on the 16S ribosomal RNA gene sequence similarity, strain CRIB 30 was affiliated as a new genus in the *Criblamydiaceae* family. Morphologic analyses revealed peculiar star-shaped elementary bodies similar to that of *Criblamydia sequanensis* and we proposed to call this new strain "*Estrella lausannensis*". Phylogenetic analyses of the genes *gyrA*, *gyrB*, t*opA*, *rpoA, rpoB* and 23S rRNA and MALDI TOF assay confirmed the taxonomic affiliation of *E. lausannensis*. Furthermore, *E. lausannensis* showed a large amoebal host range and a very efficient replication rate in *Acanthamoeba* species.

A Numeric Model to Simulate Solar Individual Ultraviolet Exposure

[1]Milon A., [1]Vernez D., [2]Francioli L., [3]Bulliard J.-L., [4]Moccozet L., [5]Vuilleumier L.

Institute for Work and Health, DUMSC[1], ZOOM Créations[2], University Institute of Social and Preventive Medicine, DUMSC[3], Faculty of Social and Economic Sciences, UniGe[4], Federal Office of Meteorology and Climatology MeteoSwiss[5]

Exposure to solar Ultra-Violet (UV) light is the main causative factor for skin cancer. UV exposure depends on environmental and individual factors. Individual exposure data remain scarce and development of alternative assessment methods is greatly needed. We developed a model simulating human exposure to solar UV. The model predicts the dose and distribution of UV exposure received on the basis of groud irradiation and morphological data. A 3D rendering visualisation tool illustrates UV exposure over the body surface. Computer graphic techniques (3D rendering) were adapted to reflect solar exposure conditions. A virtual manikin, depicted as a 3D triangular mesh, represented the body skin. The amount of solar energy received by each triangle was calculated, taking into account reflected, direct and diffuse radiation, and shading from other body parts. Dosimetric measurements (n=54) were conducted in field conditions using a foam manikin as surrogate for an exposed individual. Dosimetric results were compared to the model predictions. The model predicted exposure to solar UV adequately. The symmetric mean absolute percentage error was 13%. Half of the predictions were within 17% range of the measurements. This model provides a tool to assess outdoor occupational and recreational UV exposures, without necessitating time-consuming individual dosimetry, with numerous potential uses in skin cancer prevention and research.

GEN
Genes and Environment

Variant within the promoter region of the CHRNA3 gene associated with nicotine dependence is not related to willingness to quit smoking

[1]Marques-Vidal P., [2]Kutalik Z., [1]Paccaud F., [2]Bergmann S., [3]Waeber G., [3]Vollenweider P., [4]Cornuz J.

CHUV and University of Lausanne[1], Department of Medical Genetics, University of Lausanne[2], Department of Medicine, CHUV[3], Department of Ambulatory Care and Community Medicine, University of Lausanne[4]

Introduction: Common variation in the *CHRNA5-CHRNA3-CHRNB4* gene region is robustly associated with smoking quantity. Conversely, the association between one of the most significant SNPs (rs1051730 within the *CHRNA3* gene) with difficulty or willingness to quit smoking is unknown.

Methods: cross-sectional study including current smokers, 502 women and 552 men. Heaviness of smoking index (HSI), difficulty, attempting and intention to quit smoking were assessed by questionnaire.

Results: the rs1051730 SNP was associated with increased HSI (age, gender and education-adjusted mean ± standard error: 2.6 ± 0.1, 2.2 ± 0.1 and 2.0 ± 0.1 for AA, AG and GG genotypes, respectively, $p < 0.01$). Multivariate logistic regression adjusting for gender, age, education, leisure-time physical activity and personal history of cardiovascular or lung disease showed rs1051730 to be associated with higher smoking dependence (OR and 95% confidence interval for each additional A-allele: 1.38 [1.11-1.72] for smoking over 20 cigarette equivalents per day; 1.31 [1.00-1.71] for a HSI≥5 and 1.32 [1.05-1.65] for smoking 5 minutes after waking up) and borderline associated with difficulty to quit (OR=1.29 [0.98-1.70]), but this relationship was no longer significant after adjusting for nicotine dependence. Also, no relationship was found with willingness (OR=1.03 [0.85-1.26]), attempt (OR=1.00 [0.83-1.20]) or preparation (OR=0.95 [0.38-2.38]) to quit.

Conclusions: these data confirm the effect of rs1051730 on nicotine dependence but failed to find any relationship with difficulty, willingness and motivation to quit.

The nuclear hormone receptor PPARβ and microRNA as a regulators of skin carcinogenesis

[1]Degueurce G., [2]Schütz F., [2]Ibberson M., [1]Wahli W., [2]Xenarios I., [1]Michalik L.

UNIL[1], SIB[2]

The three isotypes of peroxisome proliferator-activated receptors (PPARs), PPARα, β and γ, are ligand-inducible transcription factors that belong to the nuclear hormone receptor family.

While they are best known as transcriptional regulator of lipid and glucose metabolism, PPARs are also implicated in the control of inflammatory responses.

We have described a number of roles for PPARβ in skin homeostasis. We showed that the activation of PPARβ triggers keratinocyte survival, directional sensing and migration, and proliferation. Our ongoing work demonstrates that PPARβ is involved in skin tumor development after UV irradiation, through the control of c-Src expression and downstream signaling pathways. Interestingly, microRNA (miRNA) were shown to be involved in the UV stress response. Based on these observations, we explore the interaction between miRNAs and PPARβ in the development of UV-induced skin cancer. PPARβ wt and null mice were exposed to UV during a maximal period of 30 weeks, and mRNA and miRNA expression was analysed in UV-exposed skin at various time points using microarrays. Our data suggests that miRNAs are indeed involved in the PPARβ response to UV in dorsal skin. We are currently validating some of the miRNA/mRNA interactions and their involvement in PPARβ-mediated UV-stress response pathways.

Understanding the mechanism of RasGAP cleavage by caspase-3 derived fragment N on Survivin induction.

Peltze N.

Department of Physiology

RasGAP, a regulator of the Ras and Rho small G proteins, is cleaved by caspase-3 into two fragments in low stress conditions. The N-terminal fragment, called fragment N, displays potent anti-apoptotic properties, protecting a variety of cell types against many death stimuli. Fragment N protects cells by activating the Ras-PI3K-Akt pathway. Which of the many Akt effectors is participating in fragment N-induced protection is unclearly defined at the moment, although we have recently observed that survivin, a member of the inhibitor of apoptosis (IAP) family, is induced by fragment N in an Akt-dependent manner.

Moreover we observed that when survivin is silenced, even though fragment –N is produced in the cell under a mild stress, cells are no longer protected against apoptosis suggesting that indeed survivin is a key mediator in fragment N - mediated protection.

Survivin is an antiapoptotic protein but also a chromosomal passenger and so it is highly regulated at different levels, suffering from transcriptional to post-translational modifications. In this study we would like to characterize the mechanism of activation of survivin by fragment N and try to understand better this antiapoptotic pathway as a whole.

Transgenic Animal Facility (TAF) of the Faculty of Biology and Medicine and the University Hospitals, UNIL/CHUV

[1]Dénéréaz M.-L., [1]Maison D., [1]Merillat A.-M., [1]Hummler E.

Institut de Pharmacologie et Toxicologie[1]

The Transgenic Animal Facility (TAF) is now in its 6th year of activity. The platform generates genetically-engineered mouse models for biomedical research. In principle, the Platform generates transgenic mice using BACs and mini-genes, knock-out and Knock-in mice and performs rederivation of established mouse strains. Additionally, we offer thawing of frozen embryos. The TAF actively participates in the continued formation and offers thereby a platforme open to the local scientific community in order to answer questions concerning the generation and analysis of these mice.

Since August 2010, the Transgenic Animal Facility is part of the technical platforms of the NCCR Kidney :CH (Kidney Control of Homeostasis) and will develop complex engineered rat and mouse animal models using novel techniques like zinc finger nuclease technology.

IMI
Immunity and Infectiology

DNA topology alterations induced by a bacterial volatile excreted molecule promote antibiotic tolerance in prokaryotes

[1]Que Y., Hazan R., He J., Zhang J., Kesarwani M., Giddey M., Rahme L.

Service de Médecine Intensive Adulte[1]

Bacterial persistence, observed in a broad range of microbial species, is the capacity of bacteria sub-populations to tolerate exposure to normally lethal concentrations of bactericidal antibiotic. This ability, which is not due to antibiotic-resistant mutants, has been implicated in antibiotic treatment failures and may account for latent, chronic and relapsing infections that can be suppressed, but not eradicated. Drugs that target such infections are lacking, as the phenomenon of antibiotic tolerance remains poorly understood. The low frequency and transience of the persister trait has complicated the elucidation of the mechanism that controls persister cell formation. We show that 2' amino-acetophenone (2-AA), a small, volatile odorant molecule produced by the recalcitrant Gram-negative human pathogen *Pseudomonas aeruginosa* promotes persister production in response to quorum-sensing (QS) signalling in an epigenetic manner. 2-AA modulates DNA topology via its effects on topoisomerase I (TopA) activity, leading to persister accumulation in an SOS response-independent manner. Our findings provide a new perspective on the functions of QS regulated small molecules and the first demonstration of a natural topology auto-altering molecule being involved in the promotion of antibiotic tolerant cells formation. As QS and TopA are evolutionarily conserved among bacteria, our findings suggest that QS auto-regulated molecules altering DNA topology may be a universal mechanism by which prokaryotes produce persisters.

Pancreatic Stone Protein (PSP): an Acurate Biomarker of Sepsis

[1]Eggimann P., [2]Liaudet L., [2]Que Y.-A., [3]Lajaunias F., [4]Graf R., [4]Bain M., [5]Moreillon P., [6]Roger T., [6]Calandra T., [2]Eggimann P.

Service de Medecine Intensive Adulte[1], Service de Medecine Intensive Adulte, CHUV, Lausanne[2], Lascco SA, Geneva[3], Visceral and Transplant Surgery, Univ. Hosp. Zürich[4], Institut de microbiologie fondamentale, Université de Lausanne[5], Service des maladies infectieuses, CHUV, Lausanne[6]

BACKGROUND: Serum levels of pancreatic stone protein/regenerating protein (PSP) increased transiently in septic polytrauma patients without pancreatic injury (Crit Care Med 2009; 37:1642). PSP acts as an activator of neutrophils suggesting that it may be a biomarker of sepsis.

METHODS: Serum levels of PSP (ELISA) and other sepsis biomarkers (procalcitonin [PCT], IL-8, IL-6, TNF-alpha) were measured in samples collected prospectively at admission, day 3, day 7, and weekly thereafter until discharge or death in ICU in a cohort of 108   patients with severe sepsis (n=33) and septic shock (n=75).

RESULTS: Median age was 63 years (19-85). Respiratory tract (n=37) and abdomen (n=38) were the most common sources of infection, which were microbiologically documented in 91 cases (82%). Overall, 2 (6%) and 17 (25%) patients with severe sepsis and septic shock died, respectively. At admission IL-6, IL-8, IL-10, PSP, and PCT were significantly more elevated in septic shock. At admission, PSP and IL-8 were significantly more elevated in non survival (Table)

Median values at entry (IQR)	Survival (n=87)	Death (n=21)	P values
Cytokines			
TNF-alpha	2.35(6.7)	2.1(10.3)	0.67
IL-1beta	7.32(20.4)	1.59(34)	0.44
IL-6	737(6483)	2901(15801)	0.056
IL-8	412(1616)	818(10358)	0.046
IL-10	135(500)	570(1390)	0.06
Acute phase protein			
PCT	4.22(22)	6.2(28.8)	0.92
PSP	211(397)	398(1627)	0.007

To predict survival at entry areas under the ROC curves, were 0.68 (95% CI: 0.56-0.81), 0.64 (0.49-0.79) and 0.49 (0.34-0.64), for PSP, IL-8, and PCT, respectively. The evolution of PSP and PCT differed significantly over time in patients with severe sepsis and septic shock.

These data suggests that PSP serum levels is an accurate biological marker of the clinical severity of infections requiring ICU admission. Moreover, it predicts outcome and then may potentially allow early stratification of septic patients.

CONCLUSIONS: We conclude that Pancreatic Stone Protein (PSP), an acute phase protein, is an early and accurate biomarker reflecting severity and outcome in patients with severe sepsis and septic shock requiring ICU admission.

Rapid detection of *Staphylococcus aureus* strains with reduced susceptibility to vancomycin by isothermal microcalorimetry

[1]Bizzini A., [2]Kasas S., [3]Trampuz A.

Institute of Microbiology - CHUV[1], Laboratory of Physics of Living Matter - EPFL[2], Department of Infectious diseases - CHUV[3]

Objectives: Methicillin-resistant *Staphylococcus aureus* (MRSA) is an increasing cause of morbidity and mortality. Vancomycin (VAN) is the first-line antibiotic for serious and invasive MRSA infections. MRSA can be either vancomycin-susceptible (VSSA) or exhibit reduced susceptibility to VAN. The latter can be expressed as a heterogeneous-intermediate (hVISA), homogeneous-intermediate (VISA) or resistant (VRSA) phenotype. Current microbiological detection techniques are either inaccurate (e.g. macrobroth, Etest) or laborious and time-consuming (e.g. population analysis profile). We investigated the potential of microcalorimetry to detect subpopulations of reduced susceptibility to VAN by detection of growth-related heat production in the presence of VAN.

Methods: Representative strains were used for VSSA (ATCC 29213, ATCC 43300), hVISA (Mu3, PC1), VISA (Mu50, PC3) and VRSA (SA510) phenotypes. Microcalorimetry was performed by inoculating 5×10^7 CFU of overnight cultures into vials containing 3 ml of brain heart infusion broth with serial dilutions of VAN. Heat production was measured at 37°C and time to detection was determined.

Results: No heat production was detected in the VSSA strains at VAN concentration >3 µg/mL during the 72 hours of incubation. hVISA and VISA strains showed heat production with a dose-proportional delay up to 6 µg/mL in 48h and up to 12 µg/mL in 72h, respectively. The VRSA strain showed heat production up to 16 µg/mL in 12h.

Conclusions: Microcalorimetry was able to detect strains with reduced susceptibility to VAN and distinguish hVISA, VISA and VRSA strains in less than 12 h. Measuring of bacterial heat production might represent a simple and rapid method for detection of heteroresistant bacterial phenotypes.

Monitoring of 1,3-Beta-D-Glucan (BDG) for Early Diagnosis of Abdominal Candidiasis (AC) in High-Risk Surgical ICU Patients

[1]Tissot F., [2]Hauser P., [3]Lamoth F., [4]Eggiman P., [5]Flueckiger U., [6]Siegemund M., [5]Orasch C., [7]Zimmerli S., [3]Calandra T., [3]Marchetti O.

Infectious Diseases Service[1], Institute of Microbiology, CHUV[2], Infectious Diseases Service, CHUV[3], Intensive Care Unit, CHUV[4], Infectious Diseases Service, Basel University Hospital[5], Intensive Care Unit, Basel University Hospital[6], Infectious Diseases Institute, Bern University Hospital[7]

Background : The aim of study was to assess the utility of monitoring serum 1,3-beta-D-glucan (BDG) for early diagnosis of abdominal candidiasis (AC) in high-risk surgical ICU patients.

Methods : serum BDG (Fungitell®) was monitored 3x/week in a 3-year prospective observational cohort of surgical ICU patients at high-risk for AC (recurrent abdominal perforation/leakage, acute necrotizing pancreatitis). The *Candida* score (CS) was assessed during the first week after inclusion and the *Candida* colonization index (CI) monitored 2x/week. Endpoint was the occurrence of microbiologically documented AC. The diagnostic performance of BDG cut-offs ranging from 60 to 500 pg/ml for diagnosis of AC was compared to that of CS and CI.

Results : 89 patients (67% males; median age 62y, range 22-86) with recurrent abdominal perforation/leakage (68) and acute necrotizing pancreatitis (21) were followed during 19d (3-63): 87 were colonized during the first week (IC ≥ 0.5 in 51) and the CS was ≥ 3 in 44. AC occurred in 29 cases (76% *C. albicans*). 9 (2-28) blood samples were collected per patient. Median BDG values at inclusion were significantly higher in AC (n=29) vs. colonized patients who received antifungal therapy (n=18) vs. colonized patients who were not treated (n=40): 176 pg/ml (11.85-3866), 78.87 (18.19-439.77) and 70.95 (7.81-240.66), respectively. A BDG cut-off ≥ 80 at inclusion as well as at the time of microbiological diagnosis of AC had the best sensitivity / specificity (76% / 59% and 76% / 78%, respectively) for differentiating infected from colonized patients. Sensitivity / specificity of a CI ≥ 0.5 and a CS ≥ 3 were 79% / 34% and 62% / 64%, respectively. The first BDG value ≥ 80 preceded by a median of 5 days the microbiological documentation of AC.

Conclusion : 1,3-beta-D-glucan early differentiates abdominal candidiasis from colonization in high-risk surgical ICU patients and may be used for guiding pre-emptive antifungal therapy.

Impact of chlorhexidine-impregnated sponges on catheter-related infections rate

[1]Joseph C., [2]Thévenin M.-J., [3]Voirol P., [2]Bellini C., [2]Zanetti G., [1]Pagani J.-L., [1]Revelly J.-P., [1]Eggimann P.

Service de Médecine Intensive Adulte[1], Service de Médecine Préventive Hospitalière, CHUV, Lausanne[2], Service de Pharmacie, CHUV, Lausanne[3]

INTRODUCTION

Multimodal strategy targeted at prevention of catheter-related infection combine education to general measures of hygiene with specific guidelines for catheter insertion and dressing [1].
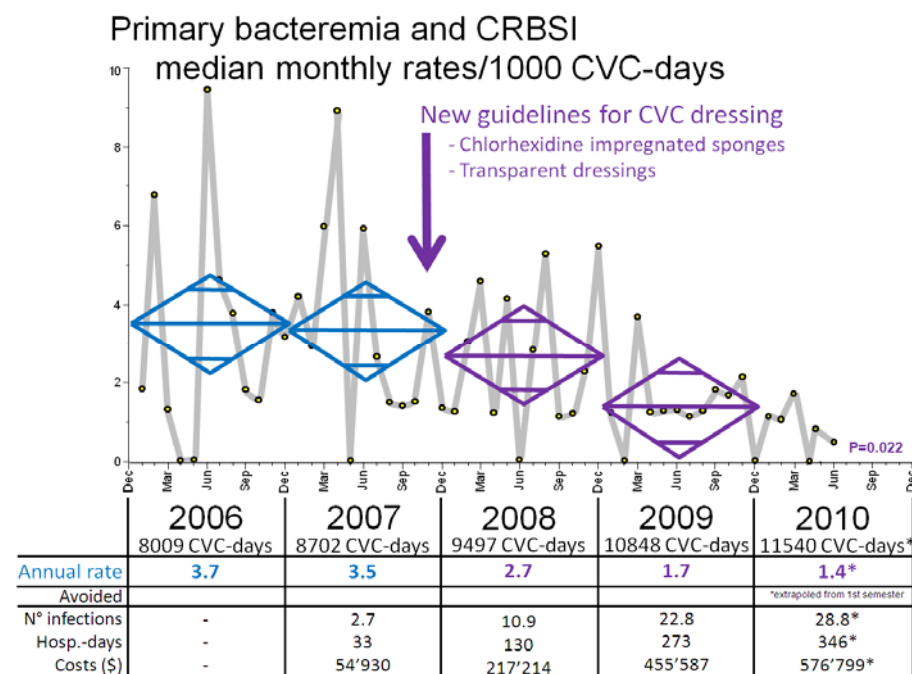
OBJECTIVES

In this context, we tested the introduction of chlorhexidine(CHX)-impregnated sponges [2].

METHODS

In our 32-beds mixed ICU, prospective surveillance of primary bacteremia and of microbiologically documented catheter-related bloodstream infections (CRBSI) is performed according to standardized definitions. New guidelines for central venous catheter (CVC) dressing combined a CHX-impregnated sponge (BioPatch®) with a transparent occlusive dressing (Tegaderm®) and planning for refection every 7 days. To contain costs, Biopatch® was used only for internal jugular and femoral sites. Other elements of the prevention were not modified (overall compliance to hand hygiene 65 to 68%; non coated catheters except for burned patients [173 out of 9542 patients]; maximal sterile barriers for insertion; alcoholic solution of CHX for skin disinfection).

RESULTS

Median monthly CVC-days increased from 710, to 749, 855 and 965 in 2006, 2007, 2008 and 2009, respectively (p<0.01). Following introduction of the new guidelines (4Q2007), the average monthly rate of infections decreased from 3.7 (95%CI: 2.6-4.8) episodes/1000 CVC-days over the 24 preceding months to 2.2 (95%CI: 1.5-2.8) over the 24 following months (p=0.031). Dressings needed to be changed every 3 to 4 days

	2006 8009 CVC-days	2007 8702 CVC-days	2008 9497 CVC-days	2009 10848 CVC-days	2010 11540 CVC-days*
Annual rate	3.7	3.5	2.7	1.7	1.4*
Avoided					*extrapoled from 1st semester
N° infections	-	2.7	10.9	22.8	28.8*
Hosp.-days	-	33	130	273	346*
Costs ($)	-	54'930	217'214	455'587	576'799*

The decrease of catheter-related infections we observed in all consecutive admitted patients is comparable to that recently showed in a placebo- randomized trial [2]. Further generalization to all CVC and arterial catheters access may be justified.

CONCLUSIONS

Our data strongly suggest that combined with occlusive dressings, CHX-impregnated sponges for dressing of all CVC catheters inserted in internal jugular and/or femoral sites, significantly reduces the rate of primary bacteremia and CRBSI.

Cambinol, an inhibitor of Sirtuin 1 and Sirtuin 2, inhibits innate immune responses

[1]Lugrin J., [1]Grandmaison G., [1]LeRoy D., [1]KnaupReymond M., [1]Calandra T., [1]Roger T.

Infectious Diseases - CHUV - UNIL[1]

Background: The mammalian family of histone deacetylases (HDACs) is composed of HDAC1-11 and sirtuins (Sirt) 1-7. Sirt1-7 display deacetylase and/or ADP-ribosyl transferase activities, and have been involved in the control of cell metabolism, proliferation and survival. Pharmacological inhibitors and activators of sirtuins are currently been evaluated for the treatment of metabolic, neurogenerative and oncologic disorders. We have recently shown that inhibitors of HDAC1-11 strongly inhibit innate immune responses and protect from mice from septic shock. The aim of this study was to analyze the impact of cambinol, an inhibitor of Sirt1-2 that exhibits antitumor activity, on innate immune responses *in vitro* and *in vivo*.

Methods: Bone marrow-derived macrophages (BMDMs), RAW 264.7 macrophages and human whole blood were incubated for 1 h with cambinol and stimulated with microbial products (LPS, Pam_3CSK_4, CpG DNA, and heat-killed *E. coli* and *S. aureus*). TNF, IL-6 and IL-12p40 mRNA and protein levels were quantified by RT-PCR, bioassay and ELISA. The activation of intracellular signalling pathways was analyzed by Western blotting. Mice were injected with LPS (LPS 17.5 mg/kg i.p.) and treated with cambinol (10 mg/kg). Blood was collected after 3 h, and mouse survival followed over 6 days.

Results: Cambinol dose-dependently inhibited the secretion of TNF, IL-6 and IL-12p40 by macrophages and whole blood stimulated with microbial products. In agreement, cambinol inhibited LPS- and Pam_3CSK_4-induced cytokine mRNA expression in macrophages. Yet, cambinol did not affect the activation of the NF-kB and MAPKs intracellular signaling pathways. Finally, cambinol reduced TNF blood levels (P = 0.05) and increased survival (from 0% to 42%; P = 0.03) of mice injected with LPS.

Conclusion: Cambinol has potent anti-inflammatory activity *in vitro* and *in vivo*. Although the molecular mechanisms by which cambinol interferes with innate immune responses remain to be identified, our data suggest that drugs targeting sirtuin activity could represent promising adjunctive therapy for the treatment of acute or chronic inflammatory disorders.

Histone deacetylase inhibitors impair innate immune responses through the induction of the Mi-2/NuRD transcriptional repressor

[1]Lugrin J., [1]LeRoy D., [2]Schrenzel J., [2]François P., [1]Calandra T., [1]Roger T.

Infectious Diseases - CHUV - UNIL[1], Infectious Diseases - HUG[2]

Background: Histone deacetylase (HDAC) inhibitors are potent anticancer agents. Several HDAC inhibitors are currently being tested in phase II-III clinical trials in cancer patients, and two drugs of this class have recently been introduced in the clinic. We have previously shown that HDAC inhibitors impair innate immune responses *in vitro* and *in vivo*. The aim of this study was to identify the molecular mechanisms underlying these effects.

Methods: Mouse bone marrow-derived macrophages and RAW 264.7 macrophage (in selected experiments transfected with Mi-2b siRNAs) were incubated for 1 h with the HDAC inhibitors trichostatin A (TSA) or valproate (VPA), and then stimulated for 15 min to 24 h with bacterial products (lipopolysaccharide and Pam_3CSK_4 lipopetide). The expression of cytokines, the activation of intracellular signalling pathways and the binding of transcription regulatory factors to DNA were analyzed by RT-PCR, ELISA, luminex, Western blotting and chromatin immunoprecipitation.

Results: TSA and VPA inhibited cytokine (TNF, IL-6, IL-12p40, and IL-10) and chemokine (CCL2, CCL5, CCL8, CXCL2, CXCL10) mRNA and protein expression induced by microbial products in macrophages. Although TSA did not interfere with the activation of the intracellular signal transduction pathways (NF-kB, ERK1/2 and p38 MAPKs, IRF3 and STAT-1), it strongly impaired the recruitment of RNA polymerase II and NF-kB p65 to the promoter region of TSA-repressed repressed genes. TSA enhanced the expression and DNA binding activity of Mi-2b, the catalytic subunit of the Mi-2/NuRD complex which acts as a transcriptional repressor of pro-inflammatory gene expression. Moreover, siRNA-mediated silencing of Mi-2beta increased LPS-induced IL-6 mRNA expression in RAW 264.7 macrophage.

Conclusions: We describe a new molecular mechanism by which HDAC inhibitors impair cytokine production in macrophages through an increased expression and DNA-binding activity of the transcriptional repressor Mi-2b. Overall, our data identify an essential role for HDACs inhibitors in the regulation of the expression of innate immune genes and host defenses against microbial pathogens.

EVALUATION OF A PCR-RFLP ASSAY FOR DERMATOPHYTES IDENTIFICATION IN SITU

[1]Verrier J., [1]Bontems O., [1]Fratti M., [1]Monod M.

Service of Dermatology and Venereology - CHUV[1]

Background: Dermatophytes are the main cause of superficial mycoses. These fungi have the capacity to invade keratinized tissue of humans or animals to produce infections that are generally restricted to the corneocytes of the skin, hair, and nails.

Statement of the problem: It is common to obtain negative results from fungal cultures of dermatological specimens where direct mycological examination showed fungal elements (≈30-40%). However, correct identification of the isolated dermatophytes from Tinea is important to choose the appropriate treatment.

Objectives: To develop a rapid polymerase chain reaction – restriction fragment length polymorphism (PCR-RFLP) assay based on 28S rDNA that is able to identify dermatophytes species in positive dermatological samples.

Results: PCR-RFLP identification of dermatophytes in skin or hair allowed validation of the results obtained in culture. It was also possible to identify the infectious dermatophytes when direct hair/skin mycological examination showed fungal elements, but negative results were obtained from fungal culture.

Conclusion: PCR methods may provide significant benefits in the rapid diagnosis of *Tinea*. First, there is an increase in sensitivity of dermatophytes identification when enough material is available. Secondly, identification of the infecting agent can be obtained in 24h with PCR-RFLP or sequencing, whereas results from fungal cultures can take 3–4 weeks.

Keywords: dermatophytes, identification *in situ*, PCR-RFLP assay

Macrophages from Crohn's disease patients exhibit deficient pro-repair functions

[1]D'Angelo F., [1]Bernasconi E., [1]Maillard M., [1]Pythoud C., [1]Bachmann D., [2]Michetti P., [1]Velin D.

Department of gastroenterology- CHUV[1], Gastroentérologie La Source-Beaulieu[2]

Background: We previously reported that myeloid cells can induce mucosal healing in a mouse model of acute colitis. Promotion of mucosal repair is becoming a major goal in the treatment of Crohn's disease. Our aim in this study is to investigate the pro-repair function of myeloid cells in healthy donor (HD) and Crohn's disease patients (CD).

Methods: Peripheral blood mononuclear cells (PBMC) from HD and CD patients were isolated from blood samples by Ficoll density gradient. Monocytic $CD14^+$ cells were positively selected by Macs procedure and then differentiated ex-vivo into macrophages (Mφ). The repair function of PBMC, $CD14^+$ monocytic cells and macrophages were evaluated in an in vitro wound healing assay.

Results: PBMC and $CD14^+$ myeloid cells from HD and CD were not able to repair at any tested cell concentration. Remarkably, HD Mφ were able to induce wound healing only at high concentration (10^5 added Mφ), but, if activated with heat killed bacteria, they were able to repair even at very low concentration. On the contrary, not activated CD Mφ were not able to promote healing at any rate, but this function was restored upon activation.

Conclusion: We showed that CD Mφ in their steady state, unlike HD Mφ, are defective in promoting wound healing. Our results are in keeping with the current theory of CD as an innate immunodeficiency. Defective Mφ may be responsible to the mucosal repair defects in CD patients and to the subsequent chronic activation of the adaptive immune response.

Immunotherapeutic strategies to induce vaccine-specific cytotoxic T lymphocytes (CTL) in mice bladder and tumor regression

[1]Domingos-Pereira S., [1]Decrausaz L., [1]Bobst M., [1]Jichlinski P., [1]Nardelli-Haefliger D.

Service d'urologie - CHUV[1]

Introduction: Non musculo-invasive bladder cancer (NMIBC) can respond to immunomodulation as demonstrated by intravesical (ives) treatments with Bacillus Calmette-Guerin (BCG) after transurethral resections. Although quite effective, about one-third of patients fail to respond and/or suffer from side effects. Vaccines against tumor associated antigens (TAA) are able to eradicate tumors growing subcutaneously in animal models. However, it is yet unclear how to target vaccine-specific cell mediated immune responses to the bladder. Here we are investigating in mice a novel immunotherapeutic approaches that combines vaccines against TAA and local application of immunomodulators to increase local CTL responses. As the bladder is part of the immune mucosal network, we have examined whether mucosal immunization routes may better target vaccine-specific cell mediated immune responses to the bladder and induce local tumor protection. In parallel, we will examine how the local instillation of different immunostimulants may increase the vaccine-specific CD8 T cells responses locally in the bladder.

Methods: Mice were immunized by different routes with an adjuvanted synthetic polypeptide vaccine encoding for a human papillomavirus oncogene (E7), as a model antigen. The specific immune response was investigated by tetramer staining (TetE7) and ex-vivo IFN-gamma ELISPOT. Bladder tumor regression was evaluated in an orthotopic murine model where tumor cells co-expressing E7 and luciferase (TC-1-luc) were instilled intravesically (ives) and followed with a Xenogen in vivo imaging system. Synthetic (CpG, Poly I:C) or bacterial (Ty21a or BCG) immunostimulants were used ives in combination with subcutaneous (s.c.) vaccination route, in order to increase vaccine-specific immune responses in bladder.

Results: Comparison of s.c., intranasal (i.n.) and intravaginal (ivag) vaccinations showed that both sc and ivag routes were able to induce similar number of TetE7 CD8 T cells in the bladder mucosa, while s.c. immunization induced higher responses in the spleen. Interestingly, i.n. immunization did not induce detectable responses in the bladder. Orthotopic bladder cancer model with ives TC-1-luc instillation resulted in 85% tumor-take. Tumor protection assay in a prophylactic setting shows that a single vaccination by all three routes was able to efficiently protect the mice against a tumor challenge 8 days later, as well as at long term. In a therapeutic setting ivag vaccination route efficiently regressed established tumors (7/9), whereas s.c. vaccination route transiently regressed 8/9 tumors, though only 3 remained tumor free at long term. All the immunostimulants tested increased 5-30 fold the number of vaccine induced E7-specific CD8 T cells locally in the bladder, highest responses being obtained with live Ty21a bacteria. The effect of the immunostimulant was only local as it did not affect the vaccine-specific response in draining lymph nodes and in the spleen.

Conclusion: Our results shows that both s.c. and ivag vaccination routes can efficiently induced vaccine-specific CD8 T cells able to both prevent and regress at least small established tumor in the bladder. S.c. vaccinaton in combination with ives application of immunostimulants significantly increase vaccine-specific CD8 T cells in the murine bladder. We anticipate that this will result in regression of larger bladder tumors, as we have shown in the case of genital tumors in mice. This represents a valuable immunotherapeutic strategy to investigate in NMIBC patients.

Rapid Enterovirus PCR in Cerebrospinal Fluid Reduces Duration of Antimicrobial Therapy and Hospital Stay in Adults with Aseptic Community-Acquired Meningit

[1]Chapuis-Taillard C., [2]Manuel O., [3]Jaton K., [3]Meylan P., [2]Marchetti O.

Service of Infectious diseases [1], Service of Infectious diseases[2], Institute of Microbiology[3]

Background. Enterovirus (EV) is the most frequent cause of aseptic meningitis (AM). Lack of differentiation of self-limited EV AM from bacterial meningitis results in unnecessary antimicrobial therapy and prolonged hospitalisation. We assessed the impact of rapid PCR for detecting EV in cerebrospinal fluid (CSF) (GeneXpert EV assay, [GXEA]) on management of patients with suspected AM.

Methods. Observational study in adult patients with AM defined by all of the followings: 1) headache plus fever and/or meningeal signs, 2) CSF pleocytosis and 3) negative bacterial cultures. Three periods were analyzed according to the use of EV PCR in addition to standard CSF tests: Period A = no PCR, Period B = home-made real-time PCR (a two-step reverse transcriptase TaqMan PCR using the ABI 7900 Detection system), and Period C = GXEA. Demographics, clinical and laboratory data were compared.

Results. Eighteen AM patients in Period A, 25 in Period B and 22 in Period C were studied. Demographics, clinical presentation, and CSF parameters were similar in the 3 groups. EV was identified in CSF in 0/18 cases (0%) of Period A, 20/25 cases (80%) of Period B, and in 22/35 cases (63%) of Period C. Median time to PCR result was 58h (15.5-118.5) in period B vs. 5.3h (3.5-20) in period C (p<0.001). Aciclovir was empirically administered in 50%, 36%, and 0% of patients in Period A, B, and C, respectively (p=0.001) and antibacterial therapy was started in 67%, 60%, and 54% of cases. Duration of antibiotics was 3d (1-12), 1d (1-3), and 0.5d (single dose in all patients) in period A, B, and C, respectively (p<0.001). Median length of hospital stay was 96h (24-288) in period A, 48h (18-624) in period B, and 11h (5-28) in period C (p<0.001).

Conclusions. Routine detection of enterovirus by PCR in cerebrospinal fluid of patients with suspected aseptic meningitis significantly reduces the use of empirical antimicrobial therapy and length of hospital stay.

Determination of oseltamivir and oseltamivir carboxylate in human plasma by liquid chromatography-tandem mass spectrometry

Aouri M.

Clinical Pharmacology-CHUV

Introduction: Oseltamivir phosphate (OP), the prodrug of oseltamivir carboxylate (OC; active metabolite), is marketed since 10 years for the treatment of seasonal influenza flu. It has recently received renewed attention because of the threat of avian flu H5N1 in 2006-7 and 2009-10 A/H1N1 pandemics. However, relatively few studies have been published on OP and OC clinical pharmacokinetics. The disposition of OC and the dosage adaptation of OP in specific populations, such as young children or patients undergoing extrarenal epuration, have also received poor attention. An analytical method was thus developed to assess OP and OC plasma concentrations in patients receiving OP and presenting with comorbidities or requiring intensive care.

Methods: A high performance liquid chromatography coupled to tandem mass spectrometry method (HPLC-MS/MS) requiring 100-µL aliquot of plasma for quantification within 6 min of OP and OC was developed. A combination of protein precipitation with acetonitrile, followed by dilution of supernant in suitable buffered solvent was used as an extraction procedure. After reverse phase chromatographic separation, quantification was performed by electro-spray ionization–triple quadrupole mass spectrometry. Deuterated isotopic compounds of OP and OC were used as internal standards.

Results: The method is sensitive (lower limit of quantification: 5 ng/mL for OP and OC), accurate (intra-/inter-assay bias for OP and OC: 8.5%/5.5% and 3.7/0.7%, respectively) and precise (intra-/inter-assay CV%: 5.2%/6.5% and 6.3%/9.2%, respectively) over the clinically relevant concentration range (upper limits of quantification 5000 ng/mL). Of importance, OP, as in other previous reports, was found not to be stable *ex vivo* in plasma on standard anticoagulants (i.e. EDTA, heparin or citrate). This poor stability of OP has been prevented by collecting blood samples on commercial fluoride/oxalate tubes.

Conclusions: This new simple, rapid and robust HPLC-MS/MS assay for quantification of OP and OC plasma concentrations offers an efficient tool for concentration monitoring of OC. Its exposure can probably be controlled with sufficient accuracy by thorough dosage adjustment according to patient characteristics (e.g. renal clearance). The usefulness of systematic therapeutic drug monitoring in patients appears therefore questionable. However, pharmacokinetic studies are still needed to extend knowledge to particular subgroups of patients or dosage regimens.

Antimicrobial Activity against Propionibacterium acnes Biofilms Determined by Microcalorimetry

[1]Furustrand U., [2]Trampuz A.

Infectious diseases service - CHUV[1], nfectious diseases service - CHUV[2]

Objectives: *Propionibacterium acnes* is a low-virulent, facultative anaerobe organism, which is part of the normal skin flora. *P. acnes* typically causes infections associated with implants on which they grow in biofilms and manifest delayed (3-24 months after surgery). *P. acnes* is difficult to eradicate because of decreased antimicrobial susceptibility in the biofilm state. We tested antimicrobial activity against *P. acnes* biofilms on large-surface beads by measuring growth-related heat production (microcalorimetry).

Methods: *P. acnes* (ATCC 11827) was used. The minimal inhibitory concentration (MIC) for daptomycin, rifampicin, levofloxacin and clindamycin was determined by Etest. *P. acnes* biofilm was formed on porous sintered glass beads (diameter 2mm, surface ~2.65m^2) in reduced Brain Heart Infusion supplemented with 0.5% glucose (rBHI+g) at 37°C under anaerobic conditions without agitation. After 72 h, beads were washed in sterile normal saline trice and incubated in rBHI+g containing serial dilution of antimicrobials (or combinations) for 24 h. Beads were then washed as before and placed in 4ml rBHI+g. Recovering bacteria were detected by measuring heat production at 37°C for 5 days. The minimal biofilm inhibition concentration (MBIC) was defined as the lowest antimicrobial concentration inhibiting heat production during 72 h. The minimal biofilm eradication concentration (MBEC) was determined as the lowest concentration showing no heat production during 5 days and absent growth on subsequently plated on blood agar plates. Experiments were repeated twice.

Results: The MIC, MBIC and MBEC of tested antimicrobials are shown in Table 1. Rifampicin and clindamycin were most active against planktonic bacteria (MIC <0.5 µg/ml). In biofilm, 256x (for daptomycin) to 16,384x higher concentration (for clindamycin) were needed to inhibit growth of *P. acnes*. For eradication of *P. acnes* biofilms, rifampin was the most effective (MBEC 128 µg/ml). In combination at sub-MBIC concentrations, daptomycin and rifampin showed improved activity against biofilms (Figure 1).

Conclusions: The activity of antibiotics was significantly decreased in *P. acnes* biofilms, especially for clindamycin. In combination, daptomycin and rifampicin showed an improved activity against biofilms. Microcalorimetry allowed the investigation of most promising antimicrobial combinations for in vivo experiments in a foreign-body infection animal model.

Table 1. MIC, MBIC, MBEC and MBIC/MIC ratio of antimicrobials tested against   *P. acnes* biofilm

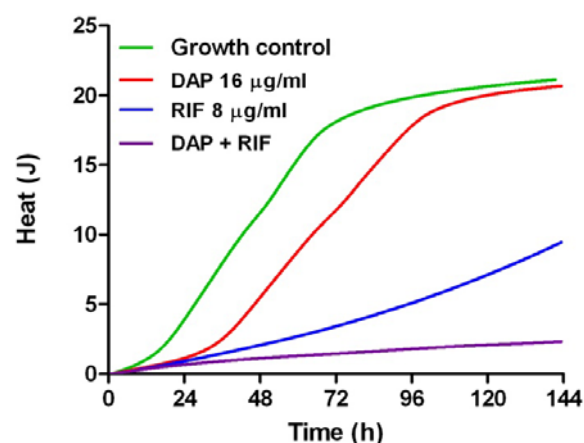| Antibiotic	MIC (µg/ml)	MBIC (µg/ml)	MBEC (µg/ml)	MBIC/ MIC ratio
Daptomycin	1	256-512	> 1024	256-512
Levofloxacin	0.75	512-1024	>1024	341-682
Clindamycin	0.125	> 1024	> 1024	>8192
Rifampin	0.004	16-32	128	4000-8000

Figure 1. Activity of daptomycin (DAP) and rifampin (RIF) alone and in combination against *P. acnes* biofilms on sintered beads evaluated by microcalorimetry.

Activity of Daptomycin and Vancomycin (alone or in combination with gentamicin) against Enterococcus faecalis in a Experimental Foreign-Body Infection Mode

[1]Furustrand U., [1]Majic I., [2]Zimmerli W., [1]Trampuz A.

Infectious diseases service - CHUV[1], Kantonspital Liestal, Switzerland[2]

Background. The optimal antimicrobial regimen enterococcal implant-associated infections has not been defined. We investigated the activity of daptomycin (DAP), vancomycin (VAN) and gentamicin (GEN) against *E. faecalis* in a foreign-body infection model.

Methods. A guinea pig model with subcutaneously implanted cages was used. Infection was established by injection of 10^4 *E. faecalis* (ATCC 19433) in the cage. Treatment for 4 days with intraperitoneal DAP (1 x 40 mg/kg) or VAN (2 x 15 mg/kg), alone or combined with GEN (2 x 10 mg/kg) was started 3 h (early biofilm) or 24 h (established biofilm) after infection. Animals were sacrificed 5 days after end of treatment, cages were removed and cultured in TSB for 48 h to determine the cure rate (%).

Results. The MIC and MBC (broth macrodilution) was for DAP 1.25 and 5 µg/ml, for VAN 1 and >64 µg/ml, and 16 and 32 µg/ml, respectively. Figure shows cure rates of treatment regimens. DAP cured 33% of early (3 h) and 0% of established (24 h) biofilms, which was improved in combinations with GEN to 58% and 8%, respectively ($p < 0.05$).

Conclusion. DAP was more active against *E. faecalis* foreign-body infection than VAN, which was further improved by GEN. Delaying treatment from 3 h to 24 h, the cure rate was significantly reduced, highlighting the importance of early treatment of implant-associated infections.
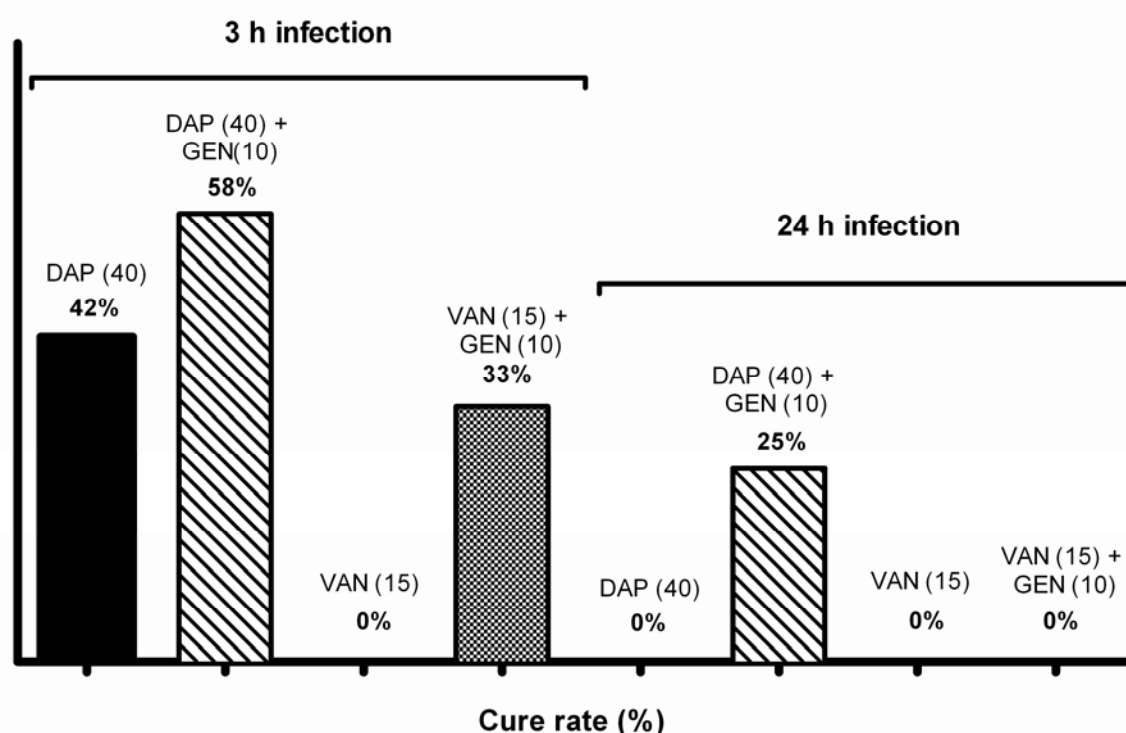
The role of TLR1 and TLR6 in the Innate Immune Response to A. fumigatus in Mouse and Human

[1]Rubino I., [2]coste a., [1]leroy d., [1]roger t., [3]monod m., [4]Latgé J., [1]Calandra T., [1]Bochud P.-Y.

Infectious Diseases Service, CHUV[1], Insitute of Microbiology, CHUV[2], Service of Dermatology, CHUV[3], Department of Parasitology and Mycology, Pasteur Institute, Paris, France[4]

Background: *Aspergillus fumigatus (A. fumigatus)* is an opportunistic pathogen that causes invasive aspergillosis (IA), a potentially fatal infection in onco-hematological patients. Toll-like receptors (TLRs) are key detectors of pathogens, which interact with adaptor proteins such as MyD88 or TRIF to trigger innate immune response. While TLR2 and TLR4 were shown to influence innate immune response to *A. fumigatus*, the role of TLR1 and TLR6 has not been established. The aim of this study was to determine the role of TLR1 and TLR6 in the immune response to *A. fumigatus* in mice and in human.

Methods: Bone marrow derived macrophages (BMDMs) from wild type (WT), TLR1, TLR2, TLR4, TLR6, MyD88 and TRIF-deficient mice were stimulated with two strains of 2% PFA inactivated *A. fumigatus*, a wild-type strain (CBS144-89) and a strain deficient in the RodA protein, known to be highly immunogenic (ΔrodA-47). CXCL-2 and IL-12p40 expression and secretion were measured after 4h by RT-PCR and after 24h by ELISA. *In vivo* expression of cytokines in response to 10^7 CFU of *A. fumigatus* ΔrodA-47 and fungal burden in lungs of intranasally injected WT and TLRs-deficient mice were assessed by RT-PCR and lungs plating, respectively. HEK293T cells were transiently transfected with 50 ng of ELAM-1 plasmid, together with 5 ng of a pRL-TK plasmid and 10 ng of human or murine MD2 and TLR4 or CD14 together with TLR2 and TLR1 or TLR6. Twenty-four hours after transfection, cells were stimulated with 10^7 CFU of *A. fumigatus* WT and Δrod A and appropriate controls. Luciferase and Renilla Luciferase activities were measured 4 hours latter using the Dual-LuciferaseTM Reporter Assay System (Promega Corporation, Madison USA). Results were expressed as relative Luciferase activity (the ratio of Luciferase to Renilla Luciferase activity).

Results: The expression and secretion of CXCL-2 and IL-12p40 by BMDMs in response to both strains of *A. fumigatus* were strongly reduced in cells from mice deficient in TLR1, TLR2, TLR4, TLR6 and MyD88, but not in TRIF, as compared to cells from WT mice. *In vivo* expression of CXCL-2 and CXCL-1 in response to *A. fumigatus* ΔrodA-47 was abolished in lungs from TLR1, TLR2, TLR4, TLR6 and MyD88-deficient mice compared to WT mice. *In vivo* fungal burden was higher in lungs collected from TLR1, TLR2, TLR4, TLR6 and MyD88-deficient mice, but not from TRIF KO mice, compared to WT mice. *A. fumigatus* induced NF-κB activation in cells transfected with TLR4 from both mice and human, TLR2/TLR1 combinations from both mice (mTLR2/mTLR1) and humans (hTLR2/hTLR1), as well as TLR2/TLR6 combination from mouse (mTLR2/mTLR6), but not human (hTLR2/hTLR6).

Conclusion: These data suggest that TLR1 is involved in the innate immune detection of *A. fumigatus* in human and mouse, while TLR6 seems to play a role in mouse but not in human. They confirm the role of TLR2 and TLR4, and show a role for MyD88, but not TRIF, both in human and mice, in this detection.

Cross-reactivity between myelin oligodendrocyte glycoprotein (MOG) and Epstein-Barr virus (EBV)-specific T cells in multiple sclerosis patients

[1]Jilek Terrasse S., [2]Schluep M., [1]Pantaleo G., [3]DuPasquier R.

Division of Immunology and Allergy - CHUV[1], Service of Neurology - CHUV[2], Service of Neurology and Division of Immunology and Allergy - CHUV[3]

Introduction: Myelin oligodendrocyte glycoprotein (MOG) is a serious potential target antigen in MS, as MOG-specific antibodies and T cell responses were detected in the blood of MS patients. Another myelin protein, the myelin-associated oligodendrocyte basic protein (MOBP), was reported to cause experimental autoimmune encephalomyelitis (EAE) in susceptible mice and MOBP-specific cellular T cells were found in MS patients. On the other hand, EBV has been repeatedly associated with MS. We and others have shown that humoral and cellular immune responses are increased in patients with MS as compared to control subjects. Furthermore, recent studies demonstrated the existence of T cells in MS patients which recognize both EBV and myelin proteins, revealing a role for viral-specific T cells in the autoimmunity processes. Thus, we analysed the MOG- and MOBP-specific T cell responses in a large population of MS patients and controls and study the putative cross-reactivity between myelin proteins and EBV.

Methods: We enrolled 78 patients with MS, 24 patients with other neurological diseases (OND) and 20 healthy controls (HC) and analysed their MOG-, MOBP- and EBV-specific T cell responses by proliferation and ELISPOT assays. Cross-reactivity between MOG and EBV peptides was tested with a crossed functional CFSE Cytotoxic T Lymphocyte (CTL) assay in a subset of study subjects.

Results: We found that a fraction of the subjects have a myelin-specific cellular immune response (36% for MOG and 14% for MOBP) with no difference between the different groups of subjects. There was no correlation between myelin- and EBV-specific T cell responses in the proliferation or ELISPOT assay. However, by crossed CTL assay, we found that 2/16 MS patients and 0/4 control subjects who had EBV-specific T cells that recognized MOG-specific targets.

Conclusions: Myelin-specific T cells are not increased in MS patients as compared to controls. However, there may be a molecular mimicry between EBV and MOG in some MS patients.

Phenotypical characterization of GILZ-deficient mice.

Suarez P.

Department of Pharmacology and Toxicology

The glucocorticoid-induced leucine zipper (GILZ) is a X-linked transcription factor and was originally described as a dexamethasone-induced transcript in murine thymocytes. It is a member of the transforming growth factor b1-stimulated clone 22 domain (TSC22D) family. GILZ is known as TSC22D3 and described as 4 isoforms. GILZ is widely expressed and an important role in immunity, adipogenesis, renal sodium handling has been proposed.

Using the Cre-Lox recombination technique, we generated mice constitutively lacking the vital region of the GILZ gene, thus abolishing the function of this gene in mice. The expression of GILZ mRNA transcripts and protein is completely abolished in all the tissues tested from knockout mice. Knockout mice are viable, but the males are sterile and present a severe testis hypoplasia. Although different processes in inflammation and immune system have been tested, only minor defects were observed. Changes in fat metabolism and adipogenesis are observed with age. Following sodium and water deprivation experiments, water and salt homeostasis is conserved. Sterility of knockout males is associated with a severe testis dysplasia. Generally, seminiferous tubules are smaller and the number of Sertoli and germ cells is reduced while apoptosis is increased as evidenced by TUNEL staining. The interstitial Leydig cell population is augmented, and higher plasma FSH and testosterone levels are found.

In summary, these new GILZ-deficient mice allow to proof *in vivo* its implication in various glucocorticoid-dependent and -independent biological processes.

The role of NOX proteins in chlamydial growth in the model organism Dictyostelium discoideum

[1]Rusconi B., [1]Greub G.

Institute of Microbiology[1]

The various species of the *Chlamydiales* order differ in their ability to infect phagocytic cells. *Waddlia chondrophila* infects macrophages and replicates within them. *Parachlamydia acanthamoebae* infects macrophages and causes a rapid apoptosis of the host cell without productive infection. Macrophages are refractory to *Chlamydia pneumoniae* infection. Since *D. discoideum* is used as a model amoebae to determine basal functions of the phagocytic machinery, we wanted to investigate the role of the Nox genes in the outcome of various chlamydial infections. The model organism *D. discoideum* encodes three members of the NADPH oxidase (Nox) family. NoxA and NoxB are homologous to Nox2, an enzyme responsible for the respiratory burst in phagocytic cells. NoxC is homologous to Nox5 that contains two EF-hand domains. *D. discoideum* does not encode for any homologues to DUOX the third member of the Nox family. So far the role of these Nox proteins has only been studied in the development of the multicellular structure of *D. discoideum*, the fruiting body. Preliminary results with *W. chondrophila* show a resistance to infection independent on the presence of Nox genes. Upon infection of both the wild-type and Nox mutants the bacteria enter the cell, but rapidly the number of infected cells decreases. Even though the infected cells were observed over an extend period of time the replication of *W. chondrophila* was very low. Immunofluorescence observations showed that the bacteria differentiate from elementary bodies to reticulate bodies, but then their replication stops. Some reticulate bodies even become large aberrant bodies. So far the absence of Nox genes seems not to influence the resistance of *D. discoideum* to infection. Further investigations with the other members of the *Chlamydiales* will allow to better understand the role of Nox genes in the phagocytic cells.

Role of Hepatitis C Virus Genotype 3 in Liver Fibrosis Progression - A Systematic Review and Meta-Analysis

[1]Probst A., [2]Dang T., [3]Bochud M., [4]Egger M., [5]Negro F., [1]Pierre-Yves B.

Infectious Disease Service - CHUV[1], Internal Medicine Service - CHUV[2], Institute for Social and Preventive Medicine - CHUV[3], Institute for Social and Preventive Medicine - Bern[4], Division of Gastroenterology and Hepatology - HUG[5]

Background: It has long been considered that the progression rate of liver fibrosis among chronic HCV patients is not influenced by the viral genotype. However, recent studies suggested an association between viral genotypes 3 and rapid progression. We performed a systematic review and meta-analysis of published studies evaluating the association between HCV genotypes and fibrosis progression.

Methods: We searched PubMed, Embase and ISI Web of Knowledge databases for studies on treatment naïve HCV infected-adults with an estimated date of HCV infection, at least one liver biopsy, and an estimated fibrosis progression rate (FPR). A random-effect model was used to derive FPR among the different HCV genotypes.

Results: Eight single biopsy studies (3182 patients, mean/median duration of infection ranging from 9-21 years) and 8 paired biopsies studies (678 patients, mean interval between biopsies 2-12 years) met the selection criteria. Most patients included in the studies were males (62%), the most frequent ethnicity was Caucasian (95%, data available in 5 studies) and the mean age was 42 years. The most frequent routes of infection were intravenous drug use (41%) and blood transfusion (31%). The odds ratio for the association of genotype 3 with accelerated fibrosis progression was 1.52 (95% CI 1.12-2.07, P=0.007) in single biopsy studies. The odds ratio for the association of genotype 3 with fibrosis progression was 1.37 (95% CI 0.87-2.17, P=0.17) in paired biopsy studies.

Conclusion: Viral genotype 3 was significantly associated with faster fibrosis progression when analyzing single biopsy studies. There was a trend toward the same direction when analyzing paired biopsy studies. Paired biopsies studies may have reduced power to detect such associations, due to an important indication bias, small sample size and use of arbitrary dichotomization criteria to assess progression. This observation may have important consequences for the decision to start therapy among genotype 3-infected patients.

Contact Information:
Pierre-Yves Bochud, Infectious Disease Service, Department of Medicine, Rue du Bugnon 46, 1011 Lausanne, Switzerland, mail: pierre-yves.bochud@chuv.ch, Phone: +41213144379

Single cell analysis reveals similar functional competence of dominant and non-dominant CD8 T-cell clonotypes

[1]Gupta B., [2]Speiser D., [1]Wieckowski S., [1]Iancu E., [2]Baumgaertner P., [2]Michielin O., [2]Romero P., [1]Rufer N.

Department of Research, CHUV, UNIL, Lausanne, Switzerland[1], Ludwig Institute for Cancer Research, UNIL, Lausanne, Switzerland[2]

The properties of CD8 T-cells required for protection from infectious disease and cancer are only partially characterized, and only limited data is available regarding T-cell clonotypes. It has been proposed that dominant T-cell clonotypes may have higher protective potential than their non-dominant counterparts. Our objectives were to assess memory and effector functions, stage of differentiation and clonotype selection of tumor-reactive T lymphocytes following peptide vaccination in melanoma patients. We also characterized dominant versus non-dominant clonotypes to further understand the in vivo function of these T-cells based on their prevalence. Using a novel single-cell approach for simultaneous ex vivo molecular and functional analysis, we report the preferential selection and expansion of several tumor-specific co-dominant clonotypes of intermediate to high frequencies, irrespective of whether native or analog peptide was used for vaccination. These clonotypes made up 40 to 95% of the differentiated "effector-like" T-cells, but only 25% of the less-differentiated "effector-memory" cells. Both subsets also contained non-dominant T-cell clonotypes, but these were significantly more frequent in the less-differentiated cells. Thus, cell differentiation was clonotype-dependent. Surprisingly however, the acquisition of memory and effector T-cell properties was clonotype independent, as we found similar functional profiles in dominant and low/non-dominant T-cell clonotypes. In contrast to analog peptide vaccination, native peptide vaccination induced T-cell functions that were more comprehensive, with more pronounced effecter functions combined with memory cell properties. In summary, this study reveals that T-cell functions are determined primarily by the antigen and the stage of T-cell differentiation, but are similar in dominant and non-dominant clonotypes participating in a CD8 T-cell response. The identified clonotypic basis of T-cell responses contributes to the rational development of vaccines.

Determination of daptomycin postantibiotic and postantibiotic sub-MIC effect in *Staphylococcus aureus* by isothermal microcalorimetry : comparison with the conventional gold standard

[1]Belkhodja Zalila C., [1]Trampuz A., [2]Bizzini A.

Laboratoire des maladies infectieuses - CHUV[1], Institut de Microbiologie - CHUV[2]

Objectives : The postantibiotic effect (PAE) and the postantibiotic sub-minimal inhibitory concentration effect (PA-SME) represent important pharmacodynamic parameters for the establishement of an optimal antibiotic dosing regimen. The current gold standard for the determination of PAE and PA-SME is the viable counts method, which is laborious and time consuming. We developed a new method based on the measurement of bacterial growth-related heat production to determine the PAE and the PA-SME.

Methods : All experiments were performed with either a methicillin-sensitive (SA1) or methicillin-resistant (SA3) *Staphylococcus aureus*. Exponential growth cultures (OD_{600} = 0.3) were exposed to 10 times the minimal inhibitory concentration (MIC) of daptomycin for 1 hour. At the end of exposure, antibiotic was removed by dilution. Microcalorimetry was performed on a 48-channel isothermal microcalorimeter (TAM III, TA Instruments, USA) by adding 30 μl of the antibiotic-exposed cultures into ampoules containing 3 ml of Mueller Hinton broth. For PA-SME determination, subinhibitory concentrations of the drug were added to the ampoules after antibiotic removal. Heat production (in μW) was followed at 37 °C. Duration of the PAE and PA-SME was defined as the time required for cultures to reach a 10 μW heat flow threshold. All experiments were performed in triplicate.

Results : The PAE and PA-SME (in hours) of the tested strains towards daptomycin determined either by microcalorimetry (present work) or by conventional method (Pankuch et al. AAC, 2007) are shown in the Table 1.

Conclusion : Microcalorimetry is a new method that allows a simple and precise determination of the PAE and the PA-SME. In comparison with the gold standard, this method is less labor-and time-consuming. Further experiments will aim at determining the PAE and PA-SME of various drug/pathogen combinations.

Table 1. PAE and PA-SME of daptomycin against *S. aureus* strains

	Determination by microcalorimetry				Determination by conventional method			
	PAE	PA-SME (0.2x MIC)	PA-SME (0.3x MIC)	PA-SME (0.4x MIC)	PAE	PA-SME (0.2x MIC)	PA-SME (0.3x MIC)	PA-SME (0.4x MIC)
S. aureus **strain**								
SA1 (MSSA)	4.27 ± 0.87	5.16 ± 1.19	8.46 ± 4.98	18.71 ± 8.48	1.2-4.2	1.2-4.3	10.1->12	10.6->12
SA3 (MRSA)	5.28 ± 0.69	6.2 ± 1.02	8.63 ± 2.44	18.29 ± 12.37	4.8-7.6	>12	>12	>12

Reassessing the Pathogenic Role of Staphylococcus aureus Fibronectin-Binding Protein A (FnBPA) in a Realistic Model of Infective Endocarditis Using Prolong

[1]Veloso T., [2]Que Y., [1]Giddey M., [1]Vouillamoz J., [1]Moreillon P., [1]Entenza J.

DMF[1], Massachusetts General Hospital, Boston, MA, USA[2]

Background: Recurring low-grade bacteremia following tooth brushing, or even mastication, is likely to cause infective endocarditis (IE) in patients at risk. This was recently confirmed in a new animal model of IE, in which prolonged low-grade inoculation of *S. aureus* was as infective as bolus injection of large bacterial numbers ($\geq 10^4$ CFU; Entenza *et al*. ICAAC 2009). Since this model mimics more closely the human situation, it is relevant to use it to reassess the role of *S. aureus* virulence factors involved in IE. Here used it to study the role of FnBPA, which was expressed individually in surrogate *Lactococcus lactis*.

Methods: Rats with sterile aortic vegetations (Veg) were inoculated with 10^6 or 10^7 CFU of *L. lactis* WT (lacking surface adhesins) or recombinant *L. lactis* expressing FnBPA (Que et al. IAI 2001; Que et al. JEM 2005). Identical inoculum sizes of each strain were given by continuous i.v. infusion, at a rate of 0.0017 ml/min over 10 h. Bacteremia levels 2 h after inoculation [expressed as mean (range) CFU/ml of blood] and Veg infection 24 h later were determined.

Results:

Inoculum	Strain	Bacteremia (CFU/ml)	Infected veg/total (%)
10^6 CFU	*L. lactis* WT	7 (2-18)	4/14 (28,5)
	L. lactis FnBPA	12 (0-40)	9/12 (75)[*]
10^7 CFU	*L. lactis* WT	267 (1-360)	9/18 (50)
	L. lactis FnBPA	39 (0-100)	18/19 (95)[*]
* *P*<0.05 vs *L. lactis* WT			

Conclusions: Recombinant *L. lactis* expressing FnBPA were more infective parent *L. lactis* WT in this realistic low-grade inoculation model. This confirms FnBPA as a critical virulence factor in IE, and as potential target for andi-adhesin strategies. Reassessing the role of other virulence factors, such as that of fibrinogen-binding protein (ClfA), is currently in progress.

Positive Impact of a Nurse Intervention Program over a 3.5-Year Period on Hepatitis B Immunity in an HIV clinic.

[1]Boillat Blanco N., [1]Probst A., [1]WaeltiDaCosta V., [1]Giulieri S., [1]Cavassini M., [1]Bochud P.-Y.

Infectious Disease Service - CHUV[1]

Background: Hepatitis B infection among HIV-infected patients is more frequent than in the general population, and associated with an increased severity, making vaccination particularly important. We assessed the impact of a nurse intervention over a 3.5-year period (2007-2010) on hepatitis B (HBV) immunity in patients from the Lausanne center of the Swiss HIV Cohort Study (SHCS).

Methods: All participants from the SHCS in the Lausanne center with a negative AgHbs and anti-HBc followed between 2007 and 2010 were included. Non immune patients (anti-HBs < 10 IU/L) and patients with unknown immunity were eligible for nurse intervention, consisting of (1) documenting HBV serostatus in all patients with previously missing information, (2) providing vaccination (3 doses with a minimal interval of 1 and 6 months) to all non-immune patients, (3) measuring vaccination effectiveness ≥ 1 month after the 3rd dose and (4) providing a second course of vaccination to non-responders (anti-HBs < 10 IU/L).

Results: The study included 245 patients, of whom 169 were included in the intervention. The number of patients with undocumented HBV serostatus before intervention declined from 40 (16%) to 1 (1%) (P<0.001), the number of patients with immunity increased from 76 (31%) to 178 (73%) (P<0.001), and 2 patients categorized as non-immune before intervention acquired HBV infection.

Conclusions: HBV immunity in the HIV population is insufficient in Switzerland and can be significantly improved by nurse intervention.

Subversion of the host cell's innate immune defense by human pathogenic arenaviruses

Pythoud C.

Institute of Microbiology

A hallmark of fatal arenavirus infections in humans is the inability of the patient's innate immune system to contain the virus resulting in uncontrolled infection, shock and death. The nucleoprotein (NP) of the prototypic arenavirus lymphocytic choriomenengitis virus (LCMV) was shown to counteract the host type I interferon (IFN) response by inhibiting activation of the IFN regulatory factor 3 (IRF3). In this study we show that the NPs of different arenaviruses (LCMV, Lassa virus, Junin virus, and Tacaribe virus) block signaling via the RNA-sensing retinoic acid-inducible gene (RIG-I) helicase. Arenavirus NPs intercept signal transduction leading to IRF3 activation downstream of the mitochondrial-bound CARD protein Cardif (IPS-1/MAVS/VISA). Using a co-immunoprecipitation approach, our preliminary experiments show that arenavirus NPs interact with one of the kinases involved in RIG-I/Cardif-mediated activation of IRF3, IKKε, but not with the closely related kinase TBK1. The interaction of NP with IKKε may interfere with the phosphorylation of IRF3, which is an essential step in IRF3 activation and type-I IFN induction. Moreover, the specific interaction with IKKε, but not TBK1, is striking and suggests selective perturbation of some, but not other pathways involved in innate anti-viral defense by arenaviruses.

Lymphodepletion by short-term chemotherapy does not alter the highly stable and persistent EBV specific CD8 T cell repertoire

[1]Iancu E., [2]Laurent J., [1]Wieckowski S., [1]Gupta B., [2]Leyvraz S., [3]Meylan P., [4]Romero P., [2]Michelin O., [4]Speiser D., [1]Rufer N.

Department of Research, CHUV[1], Multidisciplinary Oncology Center (CEPO), CHUV[2], Department of Microbiology, CHUV[3], Ludwig Institute for Cancer Research, CHUV-UNIL[4]

Protective T cell responses against persistent viruses like Epstein-Barr virus in healthy individuals are characterized by a remarkable stability of the T cell receptor (TCR) clonotypic repertoire, with highly preserved clonotype selection and persistence over time. Here, we extended recent work to the study of EBV-specific CD8 T cell responses in melanoma patients treated by short-term chemotherapy for transient lymphodepletion, followed by adoptive cell transfer (ACT) and immune reconstitution for cancer therapy. After this treatment, we observed increased proportions of virus-specific T cells in 3/5 patients, accompanied by a more differentiated phenotype (EMRA/CD28^{neg}), compared to specific cells of healthy individuals. Yet, similarly to healthy donors, clonotype selection and composition of virus-specific T cells varied along the pathway of cell differentiation, with some clonotypes that were selected with late differentiation, while others were not. After treatment, we did not observe novel dominant clonotypes, likely related to absence of EBV reactivation measured as viral load levels by quantitative PCR in PBMCs and antibody levels in plasma samples. Furthermore, public TCR BV signatures were frequently found within T cell clonotypes that dominated the repertoires of patients, in line with those observed in healthy individuals. Our findings indicate that even in situations where the immune system is strongly challenged such as following lymphodepletion and homeostatic repopulation, cytotoxic T cells specific for EBV remain strikingly stable in terms of clonotype selection and composition along T cell differentiation. We are currently characterizing the clonotype selection and gene expression profiles of single EBV-specific CD8 T lymphocytes sorted ex-vivo in one patient who underwent two cycles of lymphodepletion with escalading doses of chemotherapy over one-year interval. Observations made from this setting will provide additional insight into the degree of stability of virus specific T cells, and changes in the expression levels of genes important for cytolytic function and long-term survival of T cells.

Hepatitis E Virus Seroprevalence among Blood Donors in Switzerland

[1]Kaufmann A., [2]Kenfak-Foguena A., [3]André C., [4]Canellini G., [3]Bürgisser P., [5]Moradpour D., [2]Darling K., [2]Cavassini M.

Faculty of Biology and Medicine, University of Lausanne[1], Infectious Diseases Service, Centre Hospitalier Universitaire Vaudois[2], Service of Immunology and Allergy, Centre Hospitalier Universitaire Vaudois[3], Service Régional Vaudois de Transfusion Sanguine, Epalinges[4], Division of Gastroenterology and Hepatology, Centre Hospitalier Universitaire Vaudois[5]

Aim

The aim of this study was to determine the seroprevalence of Hepatitis E virus (HEV) among blood donors in Switzerland.

Background

HEV has emerged as a food-borne disease in various developed countries, transmitted mainly through pork meat. Cases of transmission through blood transfusion have been reported. Recent studies revealed seroprevalence rates of 13.5%, 16.6% and 20.6% among blood donors in England, France and Denmark, respectively.

Methods / Materials

We analyzed 550 consecutive blood donor samples collected in the canton of Vaud in Switzerland for the presence of anti-HEV IgG (MP Diagnostics HEV ELISA). For each donor, we obtained the following variables: age, sex and alanine aminotransferase (ALT) values.

Results

The study panel was composed of 332 men (60.4 %) and 218 women (39.6%). Overall, anti-HEV IgG was found in 27 of 550 samples (4.9%). The seroprevalence was 5.4% (18/332) in men and 4.1% (9/218) in women. The presence of anti-HEV IgG was not correlated with age, gender or ALT values.

Conclusions

Compared with other European countries, the HEV seroprevalence among blood donors in Switzerland is low. Possible explanations include 1) the strict regulation of animal and meat imports and 2) the sensitivity of commercial tests used.

Optimal CD8 T cell responsiveness is controlled within a defined TCR affinity window

[1]Hebeisen M., [2]Irving M., [2]Schmid D., [3]Zoete V., [4]Romero P., [4]Speiser P., [2,3,4]Michielin O., [1,2,4] Rufer N.

Dep. Formation & Recherche - CHUV[1], Multidisciplinary Oncology Center - CHUV[2], Swiss Institute of Bioinformatics - UNIL[3], Ludwig Institute for Cancer Research - UNIL[4]

Milk fat globule-EGF factor 8 (MFG-E8) is a secreted glycoprotein that is expressed in breast carcinomas and is present in the serum of patients with aggressive breast cancer. By performing a meta-analysis of publicly available gene expression data of breast cancer biopsies we have found that MFG-E8 is highly expressed in breast cancer and its expression is significantly associated with low levels of ErbB2 and of Estrogen receptor. We have then confirmed MFG-E8 expression in a series of breast cancer biopsies by immunohistochemistry analysis. To investigate the function of MFG-E8 we have overexpressed it in non-transformed mouse mammary epithelial cells NMuMG. We have observed that MFG-E8 increases in vitro proliferation and anchorage-independent growth of NMuMG cells and it promotes their proliferation and branching in Collagen I gels. Moreover, overexpression of of MFG-E8 in mouse mammary carcinoma cells that have low endogenous levels of the protein promotes their in vivo growth when injected orthotopically in immunosuppressed mice. In line with these results, we have also found that MFG-E8 downregulation enhances the epithelial phenotype of mammary carcinoma and Ras-transformed mammary cells, and decreases the in vivo growth of the latter. In addition, expression of a mutated version of MFG-E8 unable to bind integrins decreases in vivo tumorigenicity of mammary carcinoma cells. These results demonstrate that MFGE8 promotes mammary gland carcinoma growth in vivo and and identify this molecule as a potential therapeutic target in breast cancer.

Rapid Detection and Susceptibility Testing of Mycobacterium abscessus by Microcalorimetry

[1]Boillat Blanco N., [1]Furustrand U., [2]Jaton K., [1]Trampuz A.

Infectious Disease Service - CHUV[1], Institute of Microbiology - CHUV[2]

Background: Susceptibility testing of mycobacteria is time-consuming and not well standardized. We evaluated a new method for rapid detection and susceptibility testing of mycobacteria by real-time measurement of their growth-related heat production in comparison with the standard microbroth dilution method.

Methods: A clinical isolate of *M. abscessus* was used. MIC was determined by microbroth dilution method after 120 h-incubation. Microcalorimetry was performed by adding 50 µl containing 2 ± 0.7 $\times 10^7$ CFU/ml (= $1 \pm 0.5 \times 10^6$ CFU/ampoule) *M. abscessus* on Middlebrook 7H10 agar supplemented with 10% OADC. For susceptibility testing, serial two-fold antibiotic dilutions were added to agar. Heat production was measured at 37°C and defined positive at 5 µW. The minimal heat inhibition concentration (MHIC) was defined as the lowest concentration delaying the heat detection (compared to growth control) for 24 h. Experiments were performed in duplicate.

Results: The mean detection time of *M. abscessus* without antibiotics was 12.8 h (range, 10.4-15.2 h), reaching a peak of 109 µW (range, 104.8-114.1 µW) after 62.9 h (range, 60.8-65.0 h). With antibiotics, the heat production was delayed proportionally to antibiotic concentration. The MHIC / MIC were (µg/ml): 2 / 4 (clarithromycin), 4-8 / 8 (amikacin), 12 / 8 (linezolid) and 2 / >4 (ciprofloxacin).

Conclusion: Microcalorimetry allowed rapid detection (within 1 day) and susceptibility testing (within 2 days) of *M. abscessus.* The MHIC correlated with MIC values within one two-fold dilution, except for ciprofloxacin. Microcalorimetry might be extended to other mycobacteria, including slow-growing such as *M. tuberculosis*. This method has the potential to accelerate the current diagnosis and antibiotics susceptibility testing of mycobacteria.

In vivo inhibition of the membrane-bound serine protease CAP1/Prss8 (channel-activating protease-1)

[1]Crisante G.

DPT-UNIL[1]

Serine proteases are involved in the regulation of many biological processes. Their activities are controlled by different specific inhibitors. Any alteration of this balance may result diseases. CAP1/Prss8 is a serine protease involved in the physiology of several organs including the skin. In our study, we have used an *in vitro* Xenopus oocyte assay where we can test the effect of potential inhibitory candidates on CAP1/Prss8 induced ENaC-mediated sodium currents. Using this technique, a specific CAP1/Prss8 inhibitor has been identified. To verify whether this inhibition can occur also *in vivo,* we have generated mice transgenic for CAP1/Prss8 and mice transgenic for this inhibitor in the skin. Animals transgenic for CAP1/Prss8 exhibit a scaly skin phenotype, an increase in epidermal thickness and an excessive loss of water through the skin. Strikingly, this phenotype can be prevented in double transgenic mice that over-express both CAP1/Prss8 and its inhibitor. Therefore, we show that skin abnormalities caused by CAP1/Prss8 over-expression can be abolished when its inhibitor is also co-expressed. In conclusion, CAP1/Prss8 inhibition could be confirmed in an *in vivo* model as well showing the importance of a controlled CAP1/Prss8 balance expression for the normal skin physiology.

An NKT cell-independent, innate immune signaling role for CD1d in UV skin pathogenesis

[1]Ryser S., [2]Hohl D., [3]Moodycliffe A.

Service of Dermatology[1], Service of Dermatology, CHUV[2], Service of Dermatology, CHUV ; Department of Immunology, Nestle Research Center[3]

Sunburn, an acute inflammatory response to UVB-induced epithelial skin injury represents a clinical marker for non-melanoma skin cancer (NMSC) risk. Here we investigated the role of CD1d, a MHC class-1-like receptor for lipid antigen, in sunburn development. We show that sunburn, signified by cutaneous tissue injury and inflammation, is abolished in CD1d-/- mice compare to wt mice. In epidermal tissues, the activation of NKT cells by CD1d-lipids has an important role in the regulation of innate and adaptive immune responses. We thus investigated if CD1d has an NKT cell-independent signaling role in human and mouse keratinocyte in response to UVB. We analyzed the release of pro-inflammatory cytokines in normal and CD1d-deficient keratinocyte after different doses of UVB radiation and indentify cell signaling pathways regulated by CD1d in an UVB-time and –dose dependent manner. In mouse and human epithelial cells, CD1d is critical for the expression of many genes that promote inflammation and skin tumor development. In summary, our findings identify an NKT cell-independent signaling role for CD1d in regulating the response of keratinocyte to UVB.

SLPI expression along the reproductive tract of postmenopausal women: effect of hormone treatment.

[1]Canny G., [1]Kumar R., [1]Vicari M., [2]Gori I., [2]Achtari C., [2]Fiche M., [1]Surbeck I., [2]Damnon F.

Dept. of Gynaecology & Obstetrics- CHUV [1], Gynaecology & Obstetrics- CHUV [2]

Introduction : Immunity in the reproductive tissues of postmenopausal women is poorly understood. SLPI (Secretory leukocyte protease inhibitor), a multifunctional antimicrobial protein expressed at mucosal surfaces, is thought to play a key role in infectious and inflammatory contexts. The aim of this study was to measure SLPI production along the female reproductive tract in postmenopausal women with and without hormonal treatment. We additionally examined ER alpha expression in these tissues as it is the main receptor through which oestrogen is thought to signal in this environment.

Methods : SLPI and estrogen receptor alpha mRNA expression was quantified using realtime PCR and protein was quantified using an ELISA or Western blot. SLPI cellular localisation was shown using Immunohistochemistry.

Results : SLPI tissue expression was highest in the endocervix and lowest in the vagina. SLPI is prominently expressed by epithelial cells.

SLPI expression was decreased in the ectocervix of women under hormonal treatment and increased in the vagina, while production in the endocervix and endometrium remained unchanged. ER alpha expression correlated with SLPI expression in general, with a differential regulation being observed in vaginal tissue.

Conclusion : We demonstrate a compartmentalised expression of this antimicrobial protein and hormone receptor along the female reproductive tract in postmenopausal women and that expression is altered after hormonal administration.

Characterization of CD4 T cell responses to a long synthetic Melan-A peptide in vaccinated patients

[1]Braun M., [1]Baumgaertner P., [2]Schwarz K., [2]Bachmann M., [1]Speiser D., [1]Romero P.

Ludwig Center for Cancer Research of the University of Lausanne[1], Cytos Biotechnology[2]

CD4 T cell help is required for the generation and maintenance of long-lasting, robust cytolytic T lymphocyte (CTL) responses for many antigens. Here, patients were vaccinated with a virus like particle (VLP) linked, long Melan-A peptide containing the immunodominant Melan-A$_{26-35}$ epitope with an introduced amino acid exchange for improved HLA-class I binding. We previously reported on the vaccination-driven CTL response in five of six patients based on *ex vivo* analysis of Melan-A-multimer specific CD8 T cells. Now, we found that four of these five patients also elicited a CD4 T cell response to the vaccine peptide, but the amino acid exchange greatly reduced or impeded recognition of the natural counterpart. So far, one of those responses was characterized in detail and revealed that repeated vaccinations induced a Th1 dominated response to the vaccine peptide and, to an even higher extent, to the VLP derived peptides. Vaccination also drove the expansion of CD4 T cells specific for the natural Melan-A peptide, but their functional profile was Th2 biased. These results may already suggest that peptide vaccination protocols should include strong, natural CD4 T cell epitopes that maximally support sustained polyfunctional CD8 T cell responses.

MCV
Metabolism and
Cardiovascular

Non-invasive assessment of coronary artery disease progression using magnetic resonance imaging (MRI)

Stuber M.

Radiology/CIBM

Cardiovascular disease is still the leading cause of death in industrialized nations. According to the AHA statistical update in 2010, more than 50% if these deaths are attributable to coronary heart disease in the United States. The current gold standard for the assessment of coronary artery disease is x-ray angiography. However, early atherosclerosis progression that precedes luminal narrowing cannot easily be identified with this test, and repeated studies aimed at guiding and monitoring therapy in a low risk population cannot ethically be justified due to invasiveness and x-ray exposure. For these reasons, a non-invasive, safe and repeatable means that provides information about both early atherosclerosis progression and luminal disease would not only significantly advance diagnosis but also therapy. In theory, magnetic resonance imaging (MRI) fits that profile perfectly since a high soft tissue contrast can be obtained without ionizing radiation and with relatively high spatial and temporal resolution. While significant technical challenges exist for imaging the small and constantly moving coronary arteries, advanced methods still permit the assessment of coronary *endothelial dysfunction*, the quantification of *positive arterial remodeling* of the coronary vessel wall, characterization of plaque components using *targeted contrast agents*, and the identification of proximal *luminal coronary artery disease*. Therefore, MRI does not only have the ability to characterize different stages of the atherosclerotic cascade, but it also offers novel biological insights in the local progression of coronary disease.

BORN AT 27 WEEKS OF GESTATION WITH CLASSICAL PKU: CHALLENGES OF DIETETIC MANAGEMENT IN A VERY PRETERM INFANT.

[1]Ballhausen D., [2]Egli D., [3]Bickle-Graz M., [2]Bianchi N., [1]Bonafé L.

Pédiatrie Moléculaire, DMCP, CHUV[1], Unité de Nutrition clinique, CHUV[2], Unité de Développement, DMCP, CHUV[3]

Only few cases of classical phenylketonuria (PKU) in premature infants have been reported. Treatment of these patients is challenging due to the lack of a phenylalanine-free amino acid solution for parenteral infusion. The boy was born at 27 weeks of gestation with a weight of 1000 g (P10). He received parenteral nutrition with a protein intake of 3 g/kg/day. On day 7 he was diagnosed with classical PKU (genotype IVS10-11G>A/IVS12+1G>A) due to highly elevated phenylalanine (Phe) level in newborn screening (2800 micromol/L). His maximum plasma Phe level reached 3696 micromol/L. Phe intake was stopped for 4 days. During this time the boy received intravenous glucose and lipids as well as little amounts of Phe-free formula by a nasogastric tube. Due to a deficit of essential amino acids and insufficient growth, a parenteral nutrition rich in branched-chain amino-acids and relatively poor in Phe was added, in order to promote protein synthesis without overloading in Phe. Under this regimen, Phe plasma levels normalized on day 19 when intake of natural protein was started. The boy has now a corrected age of 2 years. He shows normal growth parameters and psychomotor development. Despite a long period of highly elevated Phe levels in the postnatal period our patient shows good psychomotor development. The management of premature infants with PKU depends on the child's tolerance to enteral nutrition. It demands an intensive follow-up by an experienced team and dedicated dietician. Appropriate Phe-free parenteral nutrition would be necessary especially in case of gastro-intestinal complications of prematurity.

DIFFERENTIAL EXPRESSION OF GLUTARYL-COA DEHYDROGENASE IN ADULT RAT CNS, PERIPHERAL TISSUES AND DURING EMBRYONIC DEVELOPMENT

[1]Ballhausen D., [2]Bonafé L., [3]Braissant O.

Pédiatrie Moléculaire, DMCP, CHUV[1], Pédiatrie Moléculaire, DMCP, CHUV [2], Laboratoire Chimie Clinique, CHUV[3]

Glutaryl-CoA dehydrogenase (GCDH, EC 1.3.99.7) deficiency, known as glutaric acidemia type I, is one of the more common organic acidurias. To investigate the role of this pathway in different organs we studied the tissue-specific expression pattern of rat Gcdh. The open reading frame cDNA of the rat Gcdh gene was cloned from rat brain mRNA by RT-PCR, allowing the synthesis of digoxigenin-labeled in situ hybridization (ISH) riboprobes. Gcdh mRNA expression was analyzed by ISH on cryosections of adult rat brain, kidney, liver, spleen and heart muscle, as well as on E15 and E18 rat embryos. Gcdh was found expressed in the whole rat brain, almost exclusively in neurons. Gcdh was absent from astrocytes but expressed in rare oligodendrocytes. Strong Gcdh expression was found in liver and spleen, where expression appears predominant to lymphatic nodules. In kidney, the highest Gcdh expression is found in the juxtamedullar cortex (but not in glomerula), and at lower levels in medulla. Heart muscle was negative. During embryonic development, Gcdh was found well expressed in liver, intestinal mucosa and skin, as well as at lower levels in CNS. Further studies are ongoing to provide evidence on the presence of the entire pathway in CNS in order to understand the mechanisms leading to neurotoxicity in glutaric aciduria. The high expression of Gcdh in kidney may explain why certain patients with residual enzyme activity are low excretors at the urine metabolite level.

DETERMINATION OF CELL-SPECIFIC NEUROTOXICITY OF MALONATE, METHYLMALONATE AND PROPIONATE IN A 3D RAT BRAIN CELL AGGREGATE SYSTEM

[1]Ballhausen D., [2]Henry H., [1]Bonafé L., [2]Braissant O.

Pédiatrie Moléculaire, DMCP, CHUV[1], Laboratoire Chimie Clinique, CHUV[2]

Malonate, methylmalonate and propionate are potentially neurotoxic metabolites in branched-chain organic acidurias. Their effects were tested on cultured 3D rat brain cell aggregates, using dosages of 0.1, 1.0 and 10.0 mM with a short but intense (twice a day over 3 days) and a longer but less intense treatment (every 3rd day over 9 days). CNS cell-specific immunohistochemical stainings allowed the follow-up of neurons (axons, phosphorylated medium-weight neurofilament), astrocytes (glial fibrillary acidic protein) and oligodendrocytes (myelin basic protein). Methylmalonate and malonate were quantified by tandem mass spectrometry. Tandem mass spectrometry analysis of harvested brain cell aggregates revealed clear intracellular accumulation of methylmalonate and malonate. In immunohistochemical stainings oligodendrocytes appeared the most affected brain cells. The MBP signal disappeared already at 0.1 mM treatment with each metabolite. Mature astrocytes were not affected by propionate, while immature astrocytes on intense treatment with propionate developed cell swelling. 1 mM methylmalonate induced cell swelling of both immature and mature astrocytes , while 1 mM malonate only affected mature astrocytes. Neurons were not affected by methylmalonate, but 10.0 mM malonate on less intense treatment and 0.1, 1.0 and 10.0 mM propionate on intense treatment affected axonal growth. Our study shows significant uptake and deleterious effects of these metabolites on brain cells, principally on astrocytes and oligodendrocytes. This may be explained by the absence of the pathway in glial cells, which thus are not able to degrade these metabolites. Further studies are ongoing to elucidate the underlying mechanisms of the observed neurotoxic effects.

Isolation, culture and characterisation of human endothelial progenitor cells.

[1]ROSENBLATT-VELIN N., [2]RIGNAULT S., [3]LIAUDET L., [4]RAFFOUL W., [3]BERGER M., [2]WAEBER B., [2]FEIHL F.

Division of Physiopathology-CHUV[1], Division of Clinical Pathophysiology-CHUV[2], Department of Intensive Care Medicine -CHUV[3], Burns Center-CHUV[4]

In the adult organism, the ability to form new blood vessels via angiogenesis or vasculogenesis is essential to wound healing. Endothelial progenitor cells (EPCs) have the capacity to differentiate into mature endothelial cells and to secrete angiogenic factors *in vitro* and *in vivo*. Thus, their therapeutic potential may be important, notably in the management of skin wounds or ischemic myocardial injury.

The aim of our study was to determine whether EPCs can be isolated in large number from peripheral blood of healthy or burned patients and expanded *in vitro*. In a second step, we characterized these cells and tested their capacity to induce angiogenesis in a mouse model of ischemic limb *in vivo*.

Mononuclear cells were isolated from peripheral blood samples obtained from either healthy donors (100 ml) or severly burned patients (45 ml)and cultured in specific medium. EPC colonies appeared after 2 weeks and could be cultured up to 10 passages. They formed tubelike structures on matrigel, took up acetylated low-density lipoprotein and bound Ulex lectin. They expressed the surface antigens CD34, VEGFR-2, CD31, and E-cadherin, as well as the von Willbrand factor and the endothelial isoform of nitric oxide synthase (eNOS). After 5 passages of a single clone, cells were generated in sufficient number to allow 5×10^5 of them to be injected to nude mice. The evaluation of the angiogenic properties of these cells *in vivo* is ongoing.

In conclusion, it is possible to isolate endothelial precursor cells from a limited amount of peripheral blood from healthy donors or burned patients. These cells can be obtained in large number after culture expansion. If their angiogenic potential is valuated *in vivo*, these cells could be re-injected in patients in order to treat ischemic damages by cellular therapy.

Identification of cardiac precursor cells in human adult atrial appendages

[1]Gonzales C., [1]Plaisance I., [2]Ullrich N., [1]Perruchoud S., [3]Ruchat P., [1]Demcik N., [1]Pedrazzini T.

Experimental Cardiology Unit[1], Institute of Physiology, University of Bern[2], Department of Cardiovascular Surgery[3]

In the western world, cardiovascular disease remains a leading cause of mortality and morbidity. Heart failure is a progressive disorder that is initiated by a loss of functional cardiomyocytes leading to the weakening of the pumping capacity of the heart. In this context, cell replacement therapies to induce myocardial regeneration represent attractive alternatives to classical drug approaches for maintaining cardiac function. In a first study, we isolated cardiac precursor cells (CPCs) from human fetal ventricles. These mesenchymal cells can proliferate in vitro and express early cardiac markers (Nkx2.5 and Gata4) but no cardiac proteins expressed in functional cardiomyocytes, such as contractile proteins of the sarcomere. In appropriate conditions, these cells can differentiate into functional cardiomyocytes and smooth muscle cells (SMC). In order to identify a suitable source of cardiomyocyte precursors that could be used in autologous cell replacement therapy in humans, we established the conditions to isolate a mesenchymal non-myocyte fraction from human adult atrial appendages. Biopsies were obtained from adult patients undergoing right atrial appendage resection during surgery. Minced tissue was subjected to enzymatic digestion (protease XXIV and Collagenase V), and the non-myocyte fraction (containing putative precursor cells) was isolated and expanded in vitro. These cells are adherent, can be expanded for several passages and stored frozen. Flow cytometry analysis of cells in expansion showed no expression of hematopoietic markers (c-kit and CD45) and low or no expression of the endothelial stem cell markers CD34 (<10%) and CD31 (0%). In contrast, 100% of the cells expressed the mesenchymal stem cell markers CD73, CD90 and CD105. Cells under expansion conditions expressed early cardiac markers such as Mef2c, GATA4, and Nkx2.5 but no contractile proteins of the sarcomere and no SMC markers. This pattern of expression is consistent with a CPCs phenotype. Induction of differentiation in vitro stimulated the expression of β-MHC and sm-MHC in CPCs. When injected into the temporal vein of new born SCID mice, cells were able to home back to the heart, to engraft and to differentiate into cardiomyocytes 12 days after transfer. Taken together, these data demonstrate that we successfully isolated mesenchymal CPCs from human atrial appendages. These cells are able to proliferate and differentiate into cardiomyocytes in vitro and in vivo, and might, therefore, represent a suitable source of precursors for autologous cell replacement therapy.

Impaired Na+ and K+ excretion in inducible renal tubule-specific Nedd4-2 knockout mice

[1]Ronzaud C., [2]Loffing D., [3]Yang B., [4]Stokes J., [5]Koesters R., [6]Loffing J., [1]Staub O.

Department of Pharmacology and Toxicology - UNIL[1], Institute of Anatomy - Zurich University[2], Obstetrics and Gynecology - Iowa University, USA[3], Department of Internal Medicine - Iowa University, USA[4], INSERM UMRS 702 - UPMC, Tenon Hospital, Paris, France[5], Institute of Anatomy - Zurich University, Switzerland[6]

Generation of Nedd4-2 total knockout (KO) mice revealed that Nedd4-2 inactivation leads to Na^+ retention and hypertension. To determine the role of renal Nedd4-2 in mediating salt-sensitive hypertension *in vivo*, inducible renal tubule-specific Nedd4-2 KO mice were generated by combining the TetOn and CreLoxP systems. Pax8-rtTA transgenic mice expressing the reverse tetracycline (Tet)-dependent transactivator (rtTA) along all renal tubules were bred with TRE-LC1 transgenic mice expressing the Cre recombinase under the control of an rtTA-response element (TRE). Double transgenic Pax8-rtTA/TRE-LC1 mice (Pax8/LC1) allowing Tet-inducible renal tubule-specific Cre-mediated recombination were bred with mice homozygous for the Nedd4-2 floxed allele to obtain mutants (Nedd4-2$^{fl/fl}$/Pax8/LC1). Controls (Nedd4-2$^{fl/fl}$/Pax8 or Nedd4-2$^{fl/fl}$/LC1) and mutants were treated with doxycyclin (Dox, 2mg/ml) for 11d and fed with high-Na^+ diet for 8d. Western-blot on total kidney lysates revealed complete loss of Nedd4-2 in Dox-treated mutants. Daily urine volume was increased in mutants, whereas plasma aldosterone, urine Na^+ and absolute urinary Na^+ excretion were decreased. Interestingly, mutants showed impaired urinary K^+ excretion, paralleled with hyperkalemia. Western blot on kidneys showed increased α-, β-, γ-ENaC, and NCC protein abundance in mutants. In addition, immunofluorescence revealed increased ROMK protein expression in distal convoluted tubules and connecting tubules in mutants, which might be secondary to the hyperkalemia. Taken together, these data suggest that inducible Nedd4-2 ablation in renal tubules of adult mice leads to Na^+ retention, likewise via ENaC and NCC over-activation. The impaired K^+ excretion in mutants suggests that Nedd4-2 is important for maintaining K^+ balance. The mechanisms behind this regulation remain to be elucidated.

Cardiorespiratory fitness prevents high blood pressure in obese adolescents

[1]Marques-Vidal P., [2]Marcelino G., [2]Melich-Cerveira J., [1]Paccaud F.

CHUV and University of Lausanne[1], Faculdade de Medicina de Lisboa[2]

Objective: to assess the relationships between body mass index (BMI), body fat (BF), and fitness on blood pressure (BP) levels.

Methods: cross-sectional study in 2041 boys and 1995 girls aged 10-18 living in the Lisbon area, Portugal. BMI and BP were measured as recommended. BF was assessed by bioimpedance. Fitness was assessed by the 20-meter shuttle run and the participants were classified as fit/ unfit. Obesity and high blood pressure were defined according to international criteria.

Results: in both genders, BMI and BF were positively related with systolic (BMI only) and diastolic BP z-scores. No interaction was found between being fit and BMI categories regarding BP levels, while for BF a significant interaction (lower BP levels among fit participants) was found. Being fit reduced the BF-induced increase in the Odds ratio (OR) of presenting with high BP: OR (95% confidence interval) 1.01 (0.73-1.40) and 0.99 (0.70-1.38) for overweight and obese fit boys, respectively, the corresponding values for unfit overweight and obese boys being 1.33 (0.94-1.90) and 1.75 (1.34-2.28), respectively. The values were 0.88 (0.57-1.35) and 1.66 (0.98-2.80) for overweight and obese fit girls, respectively, the corresponding values for unfit overweight and obese being 1.63 (1.12-2.37) and 1.90 (1.32-2.73) respectively. Conversely, no interaction was found between fitness and BMI-defined overweight and obesity.

Conclusion: Being fit reduces the negative impact of BF on BP levels in both genders. This protective effect was not found with BMI. Our results emphasize the importance of fitness in the paediatric age.

Prevalence and management of cardiovascular risk factors among migrants in Switzerland

[1]Marques-Vidal P., [2]Vollenweider P., [2]Waeber G., [1]Paccaud F.

CHUV and University of Lausanne[1], Department of Medicine, CHUV[2]

Background: in industrialized countries, migrants tend to present higher cardiovascular risk factor (CVRF) levels than nationals. Whether these differences are due to inadequate management of CVRFs among migrants has seldom been studied. Hence, we assessed CVRF (hypertension, dyslipidaemia and diabetes) management according to nationality in Switzerland.

Methods: four cross-sectional studies: three nationwide interview surveys (Swiss Health Surveys – SHS) from 1997, 2002 and 2007 (N=49,245) and one local examination (CoLaus study, 2004-2006, N=6,710). Subjects were separated into Swiss, French, German, Italian, Portuguese, Spanish, former Republic of Yugoslavia, other European and other countries.

Results: most CVRFs were unevenly distributed between migrants and Swiss nationals. Among hypertensive subjects, lower treatment rates were found in participants from Portugal and Spain and to a lesser degree from the former Republic of Yugoslavia, Germany and other countries in the SHS. Multivariate analysis adjusting for sex, age, educational level, body mass index and leisure-time physical activity showed lower treatment rates among Italian and Spanish participants. In CoLaus, lower treatment rates were found for participants from France and Portugal, but the differences were not significant after multivariate adjustment. Among dyslipidamic subjects, lower treatment rates were found in participants from Italy, Portugal and Spain in the SHS. In CoLaus, lower treatment rates were found for participants from Germany, Portugal and other countries; in both settings the differences were not significant after multivariate adjustment. No differences were found regarding treatment of diabetes.

Conclusion: most CVRFs are unevenly distributed among migrants in Switzerland, but these differences are mainly due to disparities in age, leisure-time physical activity, overweight/obesity and education. Screening and management of CVRFs in Switzerland do not appear to differ significantly between Swiss nationals and migrants, suggesting that there is no need to specifically target migrant populations regarding CVRFs.

Burden of disease attributable to obesity and overweight in Switzerland

[1]Marques-Vidal P., [1]Davin C., [2]Vollenweider P., [2]Waeber G., [1]Paccaud F.

CHUV and University of Lausanne[1], Department of Medicine, CHUV[2]

Background/Introduction: Obesity increases the risk for cardiovascular risk factors (hypertension, dyslipidemia and type 2 diabetes). The contribution of overweight and obesity to those risk factors at the population level should be assessed using data from the same population.

Methods: The number of cases of cardiovascular risk factors that could have been prevented if the increase in overweight and obesity in Switzerland had been contained were estimated using gender-specific, age and smoking-adjusted PAFs for overweight and obesity. PAFs were estimated from the Swiss Health Survey 2007 (self-reported) and the CoLaus study (measured) data.

Results: PAFs calculated using self-reported data were lower than using measured data. Using measured data, overweight and obesity contributed to 38% of hypertension cases in men (32% in women). In men, being overweight contributed more to hypertension than obesity (22.2% and 15.6%, respectively), while the opposite was observed for women (13.6% and 18.1%, respectively). Also, 36% of dyslipidemia in men (30% in women) could be attributed to overweight and obesity. In both genders, being overweight had a higher contribution than being obese (21.2% and 15.2% in men; 15.9% and 14.3% in women, respectively). Lastly, 57% of type 2 diabetes in men (62% in women) was attributable to overweight and obesity, with obesity having a larger impact than overweight in both sexes (39.2% and 17.7% in men; 48.0% and 14.1% in women, respectively). Circa 61,500 cases of hypertension, 37,500 cases of dyslipidemia and 26,500 cases of type 2 diabetes could have been prevented if overweight and obesity levels were maintained at 1992 levels.

Conclusion: In Switzerland, a large proportion of cardiovascular risk factors is attributable to overweight and/or obesity. A substantial amount of them could have been prevented by containing the overweight/obesity epidemic.

Nothing lethal: no relationship between Euro/World football cup matches and coronary heart disease deaths in Switzerland

Marques-Vidal P.

CHUV and University of Lausanne

Background: several authors have suggested that watching football matches might increase the risk of developing coronary heart disease (CHD).

Objective: to assess the relationship between football matches and CHD mortality in Switzerland.

Methods: Swiss mortality data was collected for the periods of European cups 1980 to 2004 and World cups 1982 to 2006 (385,238 deaths). CHD was assessed using the following ICD definitions: acute myocardial infarction (AMI) + unstable angina + acute ischaemic heart disease, unspecified + cardiac arrest + other cardiac arrhythmias. Matches carrying a potential extra stress, i.e. where the Swiss national team played or with over time or penalties, where flagged.

Results: after adjusting for year, age and gender, no increase in the risk of dying from CHD was found in days when matches occurred (table). Similarly, no increase in the risk of dying from CHD was found for matches with extra time or with penalties, or after stratification on gender (table). Restricting deaths to AMI only also did not change the results (not shown).

Conclusion: no relationship was found between Euro or World cup football matches and CHD mortality in Switzerland. Matches with extra time or with penalties do not carry any additional risk.

Table 1: risk of dying of CHD according to football matches

	All (n=385,238)	Men (n=196,023)	Women (n= 189,215)
Year	0.995 (0.993 – 0.997)	1.000 (0.997 – 1.002)	0.992 (0.988 - 0.997)
Gender			
Women	1 (ref.)	-	-
Men	0.86 (0.84 - 0.88)	-	-
Age group			
18-44	1 (ref.)	1 (ref.)	1 (ref.)
45-64	2.56 (2.34 - 2.80)	2.70 (2.44 - 2.98)	2.36 (1.90 - 2.92)
65-74	2.97 (2.73 - 3.24)	2.57 (2.34 - 2.83)	4.62 (3.77 - 5.64)
75+	3.20 (2.93 - 3.50)	2.56 (2.31 - 2.84)	5.11 (4.18 - 6.25)
Match day			
No	1 (ref.)	1 (ref.)	1 (ref.)
Yes	1.01 (0.96 - 1.05)	1.03 (0.97 - 1.09)	0.98 (0.92 - 1.04)
Swiss team plays			
No	1 (ref.)	1 (ref.)	1 (ref.)
Yes	0.90 (0.75 - 1.07)	0.97 (0.77 - 1.23)	0.80 (0.60 - 1.06)
Extra time or penalties			
No	1 (ref.)	1 (ref.)	1 (ref.)
Yes	0.93 (0.82 - 1.05)	0.91 (0.77 - 1.08)	0.95 (0.79 - 1.14)

Prevalence of overweight and obesity among migrants in Switzerland: association with country of origin

[1]Marques-Vidal P., [2]Vollenweider P., [2]Waeber G., [1]Paccaud F.

CHUV and University of Lausanne[1], Department of Medicine, CHUV[2]

Background: Migrants tend to present higher overweight/obesity levels, but whether this relationship applies to all nationalities has seldom been studied. In this study, we assessed the prevalence of overweight/obesity according to nationality in Switzerland.

Methods: data from a five-year nationwide cross-sectional interview survey (Swiss Health Surveys - SHS) from 1992 to 2007 (N=63,766) and from local cross-sectional examination survey (CoLaus study in Lausanne 2004-2006, N=6,743) were used. Subjects were separated into Swiss, French, German, Italian, Portuguese, Spanish, former Republic of Yugoslavia, other European and other countries.

Results: compared to Swiss, German and French nationals presented lower prevalence of overweight and obesity, while nationals from Italy, Spain, Portugal and the former Republic of Yugoslavia presented higher levels. Adjusting the SHS data for age, gender, education, smoking, leisure-time physical activity and survey year, a lower odds for overweight + obesity was found for German (Odds ratio=0.80, 95% confidence interval [0.70-0.92]) and French (0.74 [0.61-0.89]) nationals, while higher odds were found for participants from Italy (1.45 [1.33-1.58]), Spain 1.36 [1.15-1.61], Portugal (1.25 [1.06-1.47]) and the former Republic of Yugoslavia (1.98 [1.69-2.32]). Similar findings were observed in the CoLaus study for Italian (1.63 [1.29-2.06]), Spanish (1.54 [1.17-2.04]), Portuguese (1.49 [1.16-1.91]) and former Republic of Yugoslavia (5.34 [3.00-9.50]).

Conclusion: overweight and obesity are unevenly distributed among migrants in Switzerland. Migrants from Southern Europe and former Republic of Yugoslavia present higher prevalence rates. This suggests that preventive messages should be tailored to these specific populations.

Prevalence and factors associated with difficulty and intention to quit smoking in Switzerland

[1]Marques-Vidal P., [2]Melich-Cerveira J., [1]Paccaud F., [3]Waeber G., [3]Vollenweider P., [4]Cornuz J.

CHUV and University of Lausanne[1], Faculdade de Medicina de Lisboa[2], Department of Medicine, CHUV[3], Department of Ambulatory Care and Community Medicine, University of Lausanne[4]

Background: recent data indicate a slight decrease in the prevalence of smoking in Switzerland, but little is known regarding the intention and difficulty to quit smoking among current smokers. Hence, we aimed to quantify the difficulty and intention to quit smoking among current smokers in Switzerland.

Methods: cross-sectional study including 607 female and 658 male smokers. Difficulty, intention and motivation to quit smoking were assessed by questionnaire.

Results: 90% of women and 85% of men reported being "very difficult" or "difficult" to quit smoking. Almost three quarters of smokers (73% of women and 71% of men) intended to quit; however, less than 20% of them were in the preparation stage and 40% were in the precontemplation stage. On multivariate analysis, difficulty to quit was lower among men (Odds ratio and 95% [confidence interval]: 0.51 [0.35-0.74]) and increased with nicotine dependence and number of previous quitting attempts (OR=3.14 [1.75 - 5.63] for 6+ attempts compared to none). Intention to quit decreased with increasing age (OR=0.48 [0.30-0.75] for ≥65 years compared to <45 years) and increased with nicotine dependence, the number of previous quitting attempts (OR=4.35 [2.76 - 6.83] for 6+ attempts compared to none) and among subjects with personal history of lung disease (OR=1.73 [1.00 - 2.99]). Motivation to quit was inversely related with nicotine dependence and positively related with the number of previous quitting attempts and personal history of lung disease.

Conclusion: over two thirds of Swiss smokers want to quit. However, only a small fraction wishes to do so in the short term. Nicotine dependence, previous attempts to quit or previous history of lung disease are independently related with difficulty and intention to quit.

Please die within working hours: periodicity of cardiovascular deaths in Switzerland

[1]Marques-Vidal P., [2]Reavey M.

CHUV and University of Lausanne[1], Faculty of Biology and Medicine, University of Lausanne[2]

Purpose: Several studies have previously suggested periodical patterns in mortality rates from cardiovascular disease (CVD), acute myocardial infarction (AMI) and stroke. The aim of this study was to see if there was such a phenomenon and its significance in the Swiss population between the years 1969 and 2007.

Methods: Swiss mortality data from 1969 to 2007 (2'362'430 deaths) were used. Number of deaths and mortality rates due to CVD, AMI and stroke were computed for the time of day, day of the week, and month. A further stratification on gender or age (<65 and ≥65 years old) was also performed.

Results: There was a clear variability on CVD, AMI and stroke mortality rates according to the time of day, day of the week and the month. In general, mortality peaked in the morning (8h00-12h00) and also in the late afternoon (14h–18h), while the nadir occurred during the nightly hours. Both males and females showed similar hourly patterns, although the trend diminished in older patients, particularly regarding death from stroke. Weekly variation of mortality rates was also found for the younger (<65 years) subjects, with the lowest mortality rates on Sundays and the highest on Mondays. Conversely, seasonal variation according to month was stronger in the elder subjects, with the highest mortality rates during the winter and the lowest in the summer (July/August).

Conclusion: There is a timely pattern to death rates for CVD, AMI and stroke in Switzerland depending on the age and sex of the patients. Knowing this trend, its triggering factors and consequences, measures could put in place to prevent, diagnose and treat the population at certain times.

Trends of body image and desire to lose weight in the adult swiss population, 1997-2007

[1]Marques-Vidal P., [2]Melich-Cerveira J., [2]Marcelino G., [1]Paccaud F.

CHUV and University of Lausanne[1], Faculdade de Medicina de Lisboa[2]

Background/Introduction: Studies have shown that, in the USA, body dissatisfaction has decreased among overweight and obese subjects. Knowledge of trends on how current body weight relates to both weight satisfaction and desire to change weight among Swiss adults is limited.

Methods: Cross-sectional data from three National health interview surveys conducted in representative samples of the Swiss adult population: 1997 (n=12,474), 2002 (n=18,908) and 2007 (n=17,879). Weight, height, body dissatisfaction and desire to change weight were assessed by questionnaire.

Results: In 1997, 2002 and 2007 the percentages of overweight individuals dissatisfied with their weight was 63%, 67% and 63% in women and 41%, 46% and 42% in men respectively. Among obese subjects, the percentages were 77%, 82% and 79% in women and 63%, 73% and 67% in men. In overweight men, desire to change weight was 62.9% and 69.9% in 1997 and 2007, respectively (79.7% and 88.5% in women). Among obese men the percentages were 82.7% and 86.2% (86.3% and 91.6% in women). Most (>97%) of the desired changes were towards a decrease. Still, a significant percentage (36.1% in 2007) of normal weight men reported a desire to increase weight (9.1% in normal weight women). Multivariate analysis revealed that female gender, younger age, migrant status, high educational level, former smokers and increased BMI were independently and positively associated with body dissatisfaction and desire to change weight, while no relationship was found for survey year.

Conclusion: Contrary to the USA, body dissatisfaction and desire to lose weight remained stable in Switzerland between 1997 and 2007.

Relationship between cardiovascular risk factors, atherosclerosis burden and diameter of abdominal aorta.

[1]Glauser F., [1]Mazzolai L., [2]Darioli R., [1]Depairon M.

CHUV[1], UNIL[2]

Objective: The contribution of atherosclerosis (ATS) in the development of abdominal aortic aneurysm (AAA) remains controversial. The aim of this study was to investigate the correlation between the traditional cardiovascular risk factors (CVRF), the burden of subclinical ATS, and the diameter of the abdominal aorta (AA).

Patients and methods: 2052 consecutive patients (P) (39% female), mean age 52 ± 13 years, were prospectively screened for the burden of subclinical ATS and the diameter of AA. B-mode ultrasonography was used to detect the presence of atherosclerotic plaques on carotid and femoral arteries and to evaluate the greatest diameter of the AA.

Results: The mean abdominal aortic diameter (AAD) was 15.2 ± 2.8 mm. We detected atherosclerotic plaques in 71 % of P. We found significant correlations between the AAD and the Framingham coronary heart disease-risk score ($p = 0.001$; $r = 0.35$). A multiple regression analysis showed that the subclinical ATS and only 4 CVRF were significantly correlated with the variability of AAD, namely gender, age, BMI and smoking. With this model, all the CVRF accounted for 27% ($R^2 = 0.27$) of the variability of AAD.

The prevalence of enlarged AA and AAA in this population was very low (1% and 0.44% respectively). To further analyze our data we used a multivariate logistic analysis to evaluate the impact of the CVRF among the P with enlarged AA D as compared to the other P with AAD less than 25 mm. Five CVRF are significantly associated with the increased of AAD: age, sub-clinical atherosclerosis, current smoking, hypertriglyceridemia and gender. Here again, these results indicate that these CVRF play a role for the risk of dilatation of AAD, but that accounting no more than 30 %, as given by the pseudo R^2 coefficient. Thus impact of these CVRF was no greater on the general variability of AAD than on the AA dilatation.

Conclusion: Our results suggest that CVRF and the burden of subclinical ATS play a role in the increase of the AAD and that other major factors should be involved in the development of a dilation of aorta then aneurysm.

Mice generated by assisted reproductive technologies, a model organism for the study of epigenetic mechanisms of vascular dysfunction in vivo

[1]Rexhaj E., [1]Rimoldi S., [2]Giacobino A., [1]Dessen P., [1]Bichat A., [1]Nicod P., [1]Sartori C., [1]Scherrer U.

Internal Medicine - CHUV[1], Department of Genetic Medicine - Geneva University Medical School[2]

Background: Environmental influences acting early in life predispose to premature cardiovascular disease. Assisted reproductive technologies (ART) involve the manipulation of early embryos at a time when they may be particularly vulnerable to external disturbances. We recently found that vascular function in both children and mice conceived by ART is defective. In mice, this vascular dysfunction is transmitted to their progeny, suggesting an epigenetic mechanism.

Methods: To test this hypothesis, we assessed vascular function and the vascular DNA methylation pattern of imprinted genes and the eNOS gene promoter in male ART and control mice. We then tested the effects of a histone deacetylase inhibitor on these variables.

Results: As expected, ART mice displayed marked mesenteric-artery endothelial dysfunction in vitro and arterial hypertension in vivo. Most importantly, the methylation pattern of imprinted genes H19 (P<.01, vs. ctrl), Gtl2 (P<.01, vs. ctrl), Peg3 (P=.02, vs. ctrl) and of the eNOS promoter (P=.01, vs. ctrl) was altered in the aorta of ART mice. The dysmethylation of the eNOS gene promoter in ART mice was of functional importance, since it was associated with decreased eNOS expression in carotid arteries and decreased NOx plasma concentration (9.1 ± 10.4 vs. 32.3 ± 9.6 μM, X±SD, P<.001, ART vs. ctrl). DNA dysmethylation can be reversed by histone deacetylase inhibitors. Administration of such an inhibitor (Butyrate, 2 mg/kg/d, i.p. for 2 wks) to male ART mice normalized the vascular methylation pattern of imprinted genes H19, Gtl2 and Peg3 (all P<.05 vs. vehicle), of the eNOS promoter (P=.04 vs. vehicle) and NOx plasma concentration (29.0 ± 12.4 μM, P<.001 vs. vehicle). The normalization of the vascular DNA methylation pattern by Butyrate was associated with normalization of the vascular function in ART mice and prevention of the transmission of this defect to their progeny.

Conclusion: ART induces premature systemic vascular dysfunction in mice by an epigenetic mechanism. ART mice represent a model organism for the study of epigenetic mechanisms of vascular dysfunction. We speculate that epigenetic mechanisms also play a role in ART-induced vascular dysfunction and predisposition to premature cardiovascular disease in humans.

Association between cardiovascular risk factors and markers of adiposity in young adults in the Seychelles

[1]Arlabosse T., [2]Viswanathan B., [1]Lyngdoh T., [3]Myers G., [1]Bovet P.

Institute of Social and Preventive Medicine, University of Lausanne & University Medical Center, Switzerland[1], Ministry of Health, Section of Noncommunicable diseases, Republic of Seychelles[2], University of Rochester Medical Center, NY, USA[3]

Objective: In view of increasing prevalence of obesity worldwide, we examined the associations between cardiovascular risk factors (CVRF) and several adiposity markers among young adults in the Seychelles.

Methods: In 549 participants aged 19-20 years from a population-based cohort study (Seychelles Child Development Study), we assessed health behaviors through questionnaire and measured weight, height, waist, fat mass (bioimpedance), blood pressure (BP), as well as blood lipids and glucose and uric acid on fasting blood. Analyses were made separately in males and females.

Results: The prevalence of several CVRFs was elevated. BMI was strongly associated with CVRFs. The standardized regression coefficients ranged between 0.25-0.40 for systolic and diastolic BP, triglycerides, uric acid, and blood glucose (females) and between 0.15-0.26 for HDL-cholesterol and LDL-cholesterol (males). The odds ratios (contrasting the highest vs. two other tertiles for both BMI and the considered CVRFs) ranged between 6-12 for systolic/diastolic BP and between 2.5-6 for glucose, triglyceride and uric acid. Overall, associations with the CVRFs were not markedly different based on BMI, waist circumference or fat mass but tended to be weaker with waist/hip ratio. Estimates were only minimally altered upon adjustment for smoking, alcohol intake, physical activity and parents' socio economic status.

Conclusion: The elevated prevalence of several main CVRFs in youths emphasizes the importance of a life course approach to cardiovascular disease prevention. Our findings show strong associations between adiposity and several CVRFs in this population in the African region and suggest that BMI and waist circumference are equally useful markers.

Participation of connexin-based channels in the control of vascular function

[1]Alonso F., [2]Boittin F.-X., [2]Bény J.-L., [3]Mazzolai L., [4]Meda P., [2]Waeber G., [2]Haefliger J.-A.

Service de Médecine Interne[1], Service de Médecine Interne, CHUV[2], Service d'Angiologie, CHUV[3], Département de Biolgie Cellulaire et Métabolisme, CMU, Genève[4]

The cardiovascular connexins (Cx), forming the gap junctions, play a role in the contractility of the vessel wall and in the control of blood pressure. To evaluate the role of Cx of the endothelial cells (EC; Cx37, Cx40) and smooth muscle cells (SMC; Cx43, Cx45) in the adaptation of the vascular wall during chronic hypertension, we investigated how connexins of the aorta change during renin-dependent and -independent hypertension. We subjected wild type (WT) mice and mice invalidated for the gene encoding Cx40 (Cx40-/- mice representing a genetic model of renin-dependent hypertension), to either a 2-kidney, 1 clip procedure or to N-nitro-arginine-methyl-ester treatment, which induce renin-dependent and -independent hypertension, respectively. All hypertensive mice featured a thickened aortic wall, increased levels of Cx37 and Cx45 in SMC, and of Cx40 in EC (except in Cx40-/- mice). Cx43 was only upregulated in the SMC of renin-dependent models of hypertension. Blockade of the renin-angiotensin system of Cx40-/- mice normalized blood pressure, and prevented both aortic thickening and Cx alterations. *Ex vivo* exposure of WT arteries (aortas, carotids, and mesenteric) to angiotensin II (AngII), increased the levels of Cx43, but not of other Cx. In the A7r5 aortic SMC line, AngII activated kinase-dependent pathways and induced binding of the Nuclear Factor-kappa B (NFKB) to the Cx43 gene promoter, increasing Cx43 expression.

Using isometric tension measurements in precontracted aortic rings, we demonstrated that endothelium-dependent relaxations depend on NO release in both WT and Cx40-/- mice, but are markedly weaker in Cx40-/- mice. Consistently, NO production was decreased in the aorta of Cx40-/- mice. Altered relaxations and NO release from aorta of Cx40-/- mice were associated with lower expression levels of eNOS in the aortic endothelium of Cx40-/- mice, which also exhibit a marked decrease of Cx37 in EC. We further showed that eNOS, Cx40 and Cx37 tightly interact with each other at intercellular junctions in the aortic endothelium of WT mice, suggesting that the absence of Cx40 in association with altered Cx37 levels in EC from Cx40-/- mice participate to the decreased levels of eNOS. Altogether, our data demonstrate that 1) Cx37, Cx40 and Cx45 are upregulated by the increased mechanical forces impinging on the wall of arteries, whereas Cx43 is selectively increased in renin-dependent hypertension, via an AngII activation of the extracellular signal-regulated kinase and NFKB pathways and 2) the endothelial connexins participate in the control of eNOS expression levels and function.

Birth Weight, Weight Change, and Blood Pressure throughout Childhood and Adolescence: a School-Based Multiple Cohort Study

[1]Chiolero A., [2]Paradis G., [3]Madeleine G., [2]Hanley J., [1]Paccaud F., [1]Bovet P.

Institute of Social and Preventive Medicine (IUMSP)[1], Department of Epidemiology, Biostatistics, and Occupational Health, McGill University, Montreal, Canada[2], Ministry of Health and Social Development, Victoria, Republic of Seychelles[3]

Background: The relative contribution of body weight change at different ages on the level of current blood pressure (BP) during childhood and adolescence remains unclear. We assessed the association between birth weight, weight change, and current BP across the entire age-span of childhood and adolescence in large school-based cohorts in the Seychelles, an Island state in the African region. **Method:** Three cohorts of children were analyzed: 1606 whose weight was measured at age 5.5 and 9.1 years, 2557 at 9.1 and 12.5, and 2065 at 12.5 and 15.5, respectively. Birth and one year data were gathered from medical files. The outcome was BP at age 5.5, 9.1, 12.5 or 15.5 years, respectively. **Results:** At all ages, the association between birth weight z-score and current BP was either null or weakly positive without adjustment for current weight and generally weakly negative upon adjustment for current weight. Current BP was strongly associated with current body weight z-score. Conditional linear regression analysis indicated that changes in body weight z-score during each successive period of growth since birth contributed substantially to current BP at all ages. The strength of the association between weight change and current BP increased throughout successive periods of growth. **Conclusion:** During childhood and adolescence, BP is more responsive to recent than earlier weight changes.

Key words: blood pressure, birth weight, growth, life course, children

Renal sodium retention in cholestatic mice is independent of ENaC in CCD

[1]MORDASINI D., [2]LOFFING J., [3]HUMMLER E., [4]WANG Q., [4]MAILLARD M., [4]BURNIER M., [4]VOGT B.

NEPHROLOGY[1], Institute of Anatomy, university of Zurich[2], Departement de Pharmacologie et de Toxicologie, University of Lausanne[3], SERVICE DE NEPHROLOGIE ET D'HYPERTENSION, CHUV[4]

The renal site of sodium retention in cirrhosis as well as the transporters involved and the way they are activated, although extensively studied in rats and dogs, is still a matter of debate. Our previous study using the cholestatic mouse model revealed an aldosterone independent stimulation of the basolateral Na^+,K^+ATPase activity exclusively in the cortical collecting duct (CCD). In order to explore the role of the apical amiloride sensitive sodium channel (ENaC) in the CCD we took advantage of existing CCD specific αENaC KO (Hoxb7 cre; scnn1a^{loxlox}).

Control (CTL) and CCD specific αENaC KO (KO) mice underwent bile duct ligation (BDL) or sham operation. Urinary sodium and potassium excretion was measured every 3 days in metabolic studies over 3-hours period and αENaC expression analyzed by immunofluorescence.

Two to three weeks after BDL, 30% (CTL and KO) mice displayed ascites (~20 ml, BDL(+)) whether the remaining ones did not (BDL(-)). Six groups were distinguished subsequently for analysis: CTL and KO; with sham operation, BDL without ascites (BDL(-)) and BDL with ascites (BDL(+)). At the time of evident ascites the urinary Na/K ratio (mean±SEM) was as follow: CTL-sham 0.9±0.2 (n=6), CTL-BDL(-) 0.8±0.3 (n=7; ns vs CTL-sham), CTL-BDL(+) 0.1±0.1 (n=4; p<0.05 vs CTL-sham) and KO-sham 1.3±0.2 (n=6), KO-BDL(-) 1.2±0.3 (n=7; ns vs KO-sham), KO-BDL(+) 0.2±0.1 (n=5; p<0.01 vs KO-sham). The differences observed between CTL and KO groups were not significant. Macroscopically kidneys of non ascitic mice are more affected by the disease. Immunofluorescence confirmed cre-mediated deletion of αENaC in the collecting duct of floxed mice. Aside from altered ENaC abundance in CD, no other obvious changes were seen by immunofluorescence between CTL and KO mice.

In conclusion, ENaC activity in the CCD is not required for renal sodium retention in cholestatic mice. The urinary Na/K ratio reflects that aldosterone can be involved in the development of Na^+ retention.

Myocardial Blood Flow Quantification with Rubidium-82 Cardiac PET has Incremental PrognosticValue in Patients with Known or Suspected Coronary Artery Disease

[1]Farhad H., [1]Dunet V., [1]Prior J.

Service de Médecine Nucléaire - CHUV[1]

AIM: Cardiac PET allows non-invasively assessment of myocardial blood flow (MBF) and myocardial flow reserve (MFR). The impact of MBF and MFR in predicting major adverse cardiovascular events (MACE) has not been investigated in a prospective study, which was our aim.

MATERIAL AND METHODS: In total, 313 patients (65±11y, 36% women) with known or suspected CAD underwent both a rest and adenosine stress cardiac PET/CT with Rubidium-82. Dynamic acquisitions were analyzed semi-quantitatively computing the summed difference score (SDS) and quantitatively using the FlowQuant 2.1.3 software (MBF, MFR). Patients were stratified according to SDS, and allocated into groups of tertiles of stress MBF and MFR. For each group, annualized event rates were computed by dividing the number of annualized MACE (cardiac death, myocardial infarction, revascularisation or hospitalisation for cardiac-related event) by the sum of individual follow-up periods in years. Outcome were analyzed for each group using Kaplan-Meier event-free survival curves and compared using the logrank test. Multivariate analysis was performed in a stepwise fashion using Cox proportional hazards regression models.

RESULTS: The median follow-up was 256 days (range 168-494d) during which 42 MACE were observed. Ischemia (SDS≥2) was observed in 85 patients for whom annualized MACE rate was higher as compared to those without (60% vs. 8%, p<0.0001). The group with the lowest MFR tertile (MFR<1.7) had higher MACE rate than the two highest tertiles (44% vs.9% and 12%, p<0.0001). Besides, the group with the lowest stress MBF tertile (MBF<1.8mL/min/g) had the highest annualized MACE rate as compared to the two others (37% vs. 21% and 3%, p=0.0001). On multivariate analysis, the addition of MFR or stress MBF to SDS significantly increased the global χ2 (from 60 to 65, p=0.02; and from 60 to 66, p=0.01). The best prognostic power was obtained by combining SDS (p<0.0001) and stress MBF (p=0.006). Interestingly, integrating stress MBF enhanced risk stratification even in absence of ischemia.

CONCLUSIONS: Quantification of MBF or MFR in Rb-82 cardiac PET/CT, over semi-quantitative assessment, provides independent and incremental prognostic information and is of significant value for risk stratification.

Characterization of novel hypertrophic pathways activated by the AKAP-Lbc signalling complex in cardiomyocytes

[1]Cariolato L., [1]Diviani D.

Institute of Pharmacology and Toxicology[1]

In response to various pathological stresses, the heart undergoes a remodelling process that is associated with cardiomyocyte hypertrophy. Since cardiac hypertrophy can progress to heart failure, one of the major cause of lethality worldwide, the intracellular signalling pathways that control cardiomyocyte growth have been subjected of intensive investigation. We have previously shown that AKAP-Lbc, an A-kinase anchoring protein (AKAP) with an intrinsic Rho specific guanine nucleotide exchange factor activity, is critical for activating RhoA and transducing hypertrophic signals downstream of the α1-adrenergic receptors (ARs). During the characterization of the hypertrophic signalling pathways activated by AKAP-Lbc, we have discovered that in rat neonatal ventricular cardiomyocytes the anchoring protein maintains a signalling complex that is required for the activation of the mitogen activated protein kinase (MAPK) p38, which is known to promote hypertrophic cardiomyocyte growth.

It is well established that activated p38 can promote hypertrophic gene transcription through the activation of transcription factors such as GATA-4 and MEF2C. In this context, we could show that suppression of AKAP-Lbc expression by infecting rat neonatal ventricular cardiomyocytes with lentiviruses encoding AKAP-Lbc specific short hairpin RNAs strongly reduces α1-AR mediated GATA-4 transcriptional activation.

Altogether these results indicate that in cardiomyocytes AKAP-Lbc assembles a transduction complex that includes PKN, MLTK, MKK3 and p38 that is required for the activation of p38 and of the hypertrophic transcription factor GATA-4.

Urinary calcium excretion is controlled by the circadian gene clock

[1]Zavadova V., [1]Nikolaeva S., [1]Centeno G., [1]Firsov D., [2]Bonny O.

Department of Pharmacology and Toxicology[1], Department of Pharmacology and Toxicology and Service of Nephrology, CHUV[2]

Circadian rhythms have been described for plasma calcium, parathormone (PTH) and for urinary calcium in constant conditions, and may play a role in kidney stone formation and osteoporosis. The mechanisms underlying these rhythms remain however largely unknown. Entrainment by systemic cues or regulation by the local intracellular molecular clock have been proposed. Here, we aimed (i) at describing the physiological circadian rhythms for calcium in the mouse, (ii) at measuring the diurnal variations in mRNA levels of the main renal calcium transporters and (iii) at assessing the role of the molecular clock in the regulation of calciuria. We first studied the variations in plasma calcium, PTH, and in calciuria every 4 hours for 24h in C57/bl6 mice. Circadian variations of, respectively, 2.5, 40 and 20% over the 24h mean has been observed under light/dark cycles and under constant darkness. Second, the renal mRNA levels for the main partners involved in calcium reabsorption have been assessed by qPCR every 4 hours for 24 hours. TRPV5 and NCX1 mRNA levels were varying by 17 and 12% over the 24 hours mean, respectively, while calbindin-D28K and PMCA did not significantly change. NCX1 variations were confirmed at the protein level by Western Blot analysis. Third, we studied the effect of the *clock* gene on calciuria. In metabolic cages, *Clock*-deficient mice displayed higher urine calcium excretion (34.7% higher in light/dark conditions and 46.2% in constant darkness) and exhibited a disturbed circadian rhythm compared to their wildtype littermates. In *clock*-deficient mice, plasma calcium and PTH levels were not significantly different from wildtype mice. Overall, we characterized in detail the plasma calcium, PTH and calciuria circadian rhythms in the mouse and we showed that TRPV5 and NCX1 renal mRNAs expression were also varying over 24hours. In addition, our data suggest that the *clock* gene is involved in the regulation of calciuria, as *clock*-deficient mice are hypercalciuric. In order to define the cause of hypercalciuria, kidney-specific disruption of the molecular clock is awaited.

The role of micro-RNAs in beta-cell mass expansion during pregnancy

Jacovetti C.

Department of Cellular Biology and Morphology

Introduction

Diabetes mellitus is a metabolic disease characterised by impaired glucose homeostasis resulting from defective function and/or loss of beta-cells. Pregnancy is associated with diminished insulin sensitivity of maternal tissues that is compensated by an expansion of the beta-cell mass and an increase in insulin release. A better understanding of this physiological process could help identifying new possible approaches for the treatment of diabetes. MicroRNAs are small non-coding RNAs acting as translational repressors. Some of these gene regulatory molecules are known to be involved in the control of beta-cell functions, including insulin secretion and apoptosis. The aim of our study is to identify microRNAs that are differentially expressed in pancreatic islets of pregnant rats and to assess their involvement in compensatory beta-cell expansion.

Methods

We used expression profiling methods to compare the level of microRNAs in the islets of pregnant rats at d14 of gestation to non pregnant rats. Differential microRNA expression was verified by quantitative real-time PCR. The functional impact of selected microRNAs on insulin secretion, cell proliferation and survival was studied by modifying their expression level in the insulin-secreting cell lines MIN6 and INS832/13.

Results

Microarray and real time PCR analysis identified two down-regulated (miR-218 and -338-3p) and two up-regulated microRNAs (miR-144 and -451) in rat islets of pregnant rats. Interestingly, we found that miR-338-3p is also down-regulated in the islets of obese *db/db* mice and in high-fat fed mice, two other animal models characterized by compensatory beta-cell mass expansion. Reduction of miR-338-3p expression in MIN6 and INS832/13 cells using antisense molecules resulted in an increase in proliferation, as evidenced by a rise in Ki67 and BrdU staining, without any impairment in glucose-induced insulin secretion. Moreover, anti-miR-338-3p treatment protected MIN6 and INS832/13 cells from apoptosis induced by prolonged exposure to pro-inflammatory cytokines.

Conclusions

We have identified changes in microRNA expression in pancreatic islets of pregnant rats. Our data suggest that miR-338-3p might be implicated in beta-cell compensation during pregnancy and in the setting of insulin resistance in different animal models. The identification of miR-338-3p downstream signalling pathways could provide important information for the design of new microRNA-based therapeutic strategies to expand the functional beta-cell mass.

Connexin36 down-regulation by pro-inflammatory cytokines contributes to beta cell apoptosis

[1]Allagnat F., [2]Klee P., [3]Waeber G., [2]Meda P., [1]Haefliger J.-A.

Institut de Physiologie- CHUV[1], Faculté de Médecine-Université de Genève[2], Servide de Médecine Interne-CHUV[3]

Type I diabetes develops as a consequence of the autoimmune destruction of most of the insulin-producing beta cells composing the endocrine pancreas. Pro-inflammatory cytokines including the tumor necrosis factor alpha (TNFα), interleukin-1 beta (IL-1β), and interferon gamma (IFNγ) are involved in β-cells apoptosis. Connexin36 (Cx36) contributes to glucose-stimulated insulin secretion and has been shown to have anti-apoptotic properties in neuronal cell death models. Herein, we investigated the role of Cx36 in beta cells following exposure to pro-inflammatory cytokines. Knocking-down Cx36 using siRNAs increased apoptosis and caspase 3 cleavage induced by cytokines, indicating that Cx36 protects beta cell against cytotoxic attacks. A 24 hours treatment with a combination of IL-1β, TNFα and IFNγ (cytomix) strongly reduced the Cx36 mRNA and protein levels in insulin-secreting cell-lines and isolated mouse islets. To a lesser extent, IL-1β alone decreased the Cx36 levels in a dose-dependent manner whereas TNFα and IFNγ were ineffective. Cytokines have been shown to stimulate the AMP dependent kinase (AMPK) activity. Interestingly, the cytomix effects on AMPK phosphorylation and Cx36 expression were abolished following AMPK inhibition using both the chemical inhibitor compound C or the adenoviral dominant negative form of AMPK.

Taken together, our results indicate that cytokines down-regulate Cx36 gene expression through an AMPK-dependant pathway. The anti-apoptotic properties of Cx36 suggest that the Cx36 decrease contributes to the pathogenesis of type I diabetes.

Activation of the Notch pathway in human cardiac precursor cells

[1]Plaisance I., Gonzales C., Ruchat P., Demcik N., Pedrazzini T.

Experimental Cardiology Unit[1]

The heart has been considered for a long time as a terminally differentiated organ with little capacity for regeneration. Recent studies, however, have challenged this view by providing evidence for a mitotic activity in a population of cardiac precursor cells (CPCs) in the damaged heart. Nevertheless, little progress has been made about the molecular mechanisms that control the mobilization of CPCs and their proliferation. Notch signaling is a cell-to-cell communication system, which plays a crucial role in the development of the cardiovascular system and is implicated in adult self-renewing tissues. Notch prevents cardiogenic differentiation in mouse embryonic stem cells, favors proliferation of immature rat cardiomyocytes, and promotes cardiomyocytes survival. Therefore, the main goal of this study was to evaluate whether the Notch pathway could play a role in maintaining human cardiac precursors in an undifferentiated state and in stimulating their expansion in vitro. This represents a mandatory step in the production of patient-specific CPCs, which could be used in cell therapies for cardiac diseases. Therefore, a population of non-myocyte cells containing CPCs was isolated from human right atrial appendages obtained in patients undergoing cardiac surgery. CPCs expressed early cardiac markers, such as Nkx2.5, but no late cardiac markers expressed in functional cardiomyocytes. Upon induction of differentiation, these precursors have the capacity to produce cardiomyocytes and smooth muscle cells. The expression of the Notch receptors and ligands was then analyzed in cardiac atrial tissues and in CPCs. All ligands (Jagged1, Jagged2, Delta-like1, Delta-like3, Delta-like4) and all Notch receptors (Notch1 to 4) were expressed in both biological materials. Delta-like1 was the predominant ligand in starting tissues whereas Jagged1 was the most expressed ligand in CPCs. The expression of the receptors (Notch1 to 3) was similar in tissues and in CPCs. Notch2 and 3 demonstrated the highest levels. Notch4 was expressed at low levels in CPCs and was almost undetectable in atrial tissues. The activation of Notch signaling in CPCs in vitro was shown by the appearance of activated Notch1 and Notch2 intracellular domains in the nucleus, as detected by immunostaining, and by the induction of Notch target gene expression. These results suggest that the Notch pathway is active in CPCs, and could be used to expand these cells after isolation from biopsies. Ongoing experiments aim at taking advantage of immobilized soluble ligands to stimulate proliferation of CPCs in vitro in order to produce the numbers of CPCs that would be needed for cell replacement therapies in humans.

Transient Ischemic Dilation (TID) ratio measurement: Comparison between three different softwares.

[1]El hakmaoui F., [1]Malterre J., [1]Pappon M., [1]Cherbuin N., [1]Prior J., [1]Dunet V.

NUCLEAR MEDICINE DEPARTMENT[1]

Background: TID ratio indirectly reflects myocardial ischemia and is correlated with cardiac prognosis. We aimed at comparing the influence of three different software packages for the assessment of TID using Rb-82 cardiac PET/CT.

Methods: In total, data of 30 patients were used based on normal myocardial perfusion (SSS<3 and SRS<3) and stress myocardial blood flow (>2mL/min/g) assessed by Rb-82 cardiac PET/CT. After reconstruction using 2D OSEM (2 Iterations, 28 subsets, filter butterworth order 10, ρ= 0.5), data were automatically processed then manually processed to define identical basal and apical limits. Hence, TID ratio were determined with Myometrix®, ECToolbox® and QGS®. Comparisons between software results used ANOVA test and Student t-test.

Results: All of the 90 studies were successfully performed. TID ratio were not statistically different between softwares when data were processed automatically (P=0.2) or manually (P=0.17). There was a slight but significant relative overestimation of TID with the automatic processing in comparison with the manual processing using ECToolbox® (1.07 ± 0.13 vs 1.0 ± 0.13, P=0.001) and Myometrix® (1.07 ± 0.15 vs 1.01 ± 0.11, P=0.003) but not using QGS® (1.02 ±0.12 vs 1.05 ± 0.11, P=0.16).

Conclusion: Using automatic or manual mode TID estimation was not significantly influenced by software type. However, using Myometrix® or ECToolbox® TID was significantly different between automatic and manual processing, but not using QGS®. We concluded that the software type should be account for to define TID normal values as well as to compare multi-centric studies. Moreover QGS® software seemed to be the most operator-independent software package.

Myocardial blood flow quantification with 82Rb cardiac PET/CT: Impact on detection of microvascular and 3-vessel diseases

[1]Dunet V., [2]Allenbach G., [3]Klein R., [4]Camus F., [3]Renaud J., [4]Verdun F., [2]Kosinski M., [3]DeKemp R., [2]Bischoff-Delaloye A., [2]Prior J.

Nuclear Medicine-CHUV[1], Nuclear Medicine, CHUV[2], Cardiac PET Center, Ottawa, Canada [3], Radiophysics Institute, CHUV[4]

Aim:

Myocardial perfusion imaging (MPI) using semi-quantitative analysis of stress/rest [82]Rb PET/CT is a sensitive tool to detect ischemia/infarct due to epicardial coronary artery disease (CAD). However, it is limited to detect microvascular disease or balanced ischemia (3-vessel disease). We aimed to determine the impact of quantifying myocardial blood flow (MBF), myocardial flow reserve (MFR) and the prevalence of microvascular/3-vessel diseases potentially missed by semi-quantitative analysis.

Material and methods:

In total, 327 consecutive patients referred for MPI underwent [82]Rb cardiac PET/CT for suspicion or characterization of CAD. Six-minutes dynamic acquisitions were performed at rest and during adenosine stress (140μg/kg/min over 6 minutes) after injection of 1500MBq of [82]Rb. Images were assessed with ECToolbox software for semi-quantitative analysis (SRS, SSS, SDS and TID) and dynamic acquisitions were processed with the FlowQuant software to estimate average left ventricular rest-MBF, stress-MBF and MFR (stress/rest-MBF). Statistical analysis used Spearman test.

Results:

All 327 stress/rest studies were successfully performed. Of them, 132 patients had a normal perfusion in the LAD, LCX and RCA territories (SRS<3; SDS<3) on the semi-quantitative analysis. Twenty-two out of 132 patients (16.7%) with normal semi -quantitative perfusion scans had both decreased stress-MBF (<2mL/min/g) and MFR (<1.8), of whom 3 with known CABG. Of the 19 patients without known CAD/CABG, 15 patients (15/132=11.4%) had normal TID; only 4 had a TID>1.15 leading to suspect microvascular/3-vessel diseases. There was no correlation between TID and MFR (*P*=0.32) or stress MBF (*P*=0.17).

Conclusion:

Our data suggest that up to 1/10 patients referred for MPI with normal semi-quantitative myocardial perfusion scans have decrease MFR and stress-MBF due to microvascular or 3-vessel diseases that would be undetected without MBF quantification. Further studies are needed to investigate the prognosis of patients with low MFR and stress-MBF when quantified by [82]Rb-PET/CT.

Assessment of endothelial dependant coronary vasoreactivity in patients with OSA using MBF quantification with 82Rb cardiac PET

[1]Dunet V., [2]Heinzer R., [2]Rey-Bataillard V., [2]Beysard N., [2]Delaloye A., [2]Jayet P.-Y., [2]Lovis A., [1]Allenbach G., [1]Prior J.

Nuclear Medicine, CHUV[1], Center for investigation and research in sleep, CHUV[2]

Introduction: Obstructive sleep apnea (OSA) is associated with an increased risk of cardiovascular diseases. Endothelial dysfunction could underly this association. We aimed to compare endothelial dependant coronary vasoreactivity in OSA patients and controls by quantifying myocardial blood flow (MBF) response to cold pressure testing (CPT) with ^{82}Rb cardiac PET/CT.

Methods: On the morning after polysomnography (PSG), twenty-four OSA patients (2W/22M, age 57±14y, BMI 28.4±4kg/m2) with an apnea-hypopnea index (AHI)≥20/h and 9 controls (AHI<10/h) underwent a dynamic ^{82}Rb cardiac PET/CT scan at rest, during CPT and adenosine stress. In OSA patients, PSG and PET/CT were repeated 6 weeks after initiating continuous positive airway pressure (autoCPAP) treatment. Data were processed with FlowQuant software to estimate rest-MBF, CPT-MBF, stress-MBF and MFR. To reflect differences in baseline cardiac work, values were normalized according to rate pressure product (RPP). Statistical analyses were performed using t-tests and 1-way ANOVA.

Results: All of the 33 patients had normal MFR. At baseline, untreated OSA patients had a AHI of 48.6±19.5/h and showed a lower MBF response to CPT than controls (1.1±0.2mL/min/g vs. 1.3±0.4mL/min/g, *P*=0.048). CPT-MBF was not different between controls and well-treated (AHI<10/h, n=11) OSA patients (1.2±0.3mL/min/g vs. 1.3±0.4mL/min/g, *P*=0.68), but it was significantly lower for insufficiently treated (AHI≥10/h, n=10) patients (0.9±0.2mL/min/g vs 1.3±0.4mL/min/g, *P*=0.03).

Conclusion: Untreated OSA patients have an impaired coronary endothelial vasomotion as measured by MBF response to CPT compared to control subjects. This difference disappears after 6 weeks of autoCPAP therapy but only in OSA patients showing a good response to CPAP therapy (AHI<10/h). Further studies are needed to determine by which mechanism OSA and CPAP treatment influence coronary vasoreactivity.

Assessment of Coronary Vasoreactivity by MDCT: A Validation Study With 82Rb Cardiac PET/CT

[1]Dunet V., [1]Allenbach G., [2]Qanadli S., [3]Dabiri A., [2]Perrin L., [4]Mazzolai L., [3]Waeber B., [1]Bischof-Delaloye A., [3]Feihl F., [1]Prior J.

Nuclear Medicine, CHUV[1], Radiology, CHUV[2], Clinical Physiopathology, CHUV[3], Vascular Medicine, CHUV[4]

Background—Quantification of myocardial blood flow (MBF) with PET during cold pressor test (CPT) has been used to assess non-invasively endothelium-dependent coronary vasoreactivity, a surrogate marker of cardiovascular events. However, its use remains limited due to cardiac PET availability. As multi-detector computed tomography (MDCT) is widely available, we aimed at developing measurement of endothelium-dependent coronary vasoreactivity with MDCT with similar radiation burden as PET.

Materials and Methods—Twenty-eight participants without known cardiovascular risk factor (18W/10M; aged 59±6y) were enrolled. They underwent within 4 hours a cardiac PET with ^{82}Rb and unenhanced ECG-gated MDCT, at rest and during CPT. Changes in absolute MBF by PET (ml/min/g) in response to CPT were compared to relative changes in MDCT-measured coronary artery surface in the left main or left anterior descending artery using Student's t-test, linear regression analysis and non-parametric Spearman's correlation.

Results—MDCT and PET/CT could be analyzed in 18 participants (64%). Main reasons for exclusion were patient motion (n=4) and tachycardia during MDCT (n=4) (decision not to administrate any beta-blockers in these healthy participants). Hemodynamic conditions during CPT at MDCT and PET were similar (P>0.3). Relative changes in coronary artery surface in response to CPT (-2.0–21.2%) correlated to changes in MBF (-0.10–0.52mL/min/g) (ρ=0.68, P=0.02). Total effective dose was 1.3±0.2mSv for MDCT and 3.1mSv for PET/CT (P=0.01).

Conclusion—Assessment of endothelium-dependent coronary vasoreactivity using MDCT CPT is feasible. Owing to its wider availability, shorter examination times and similar radiation burden, MDCT may be attractive in clinical research to complete coronary status assessment in centers without access to cardiac PET.

Normal TID ratio determination using 82Rb quantitative cardiac PET/CT

[1]Dunet V., [1]Allenbach G., [1]Kosinski M., [1]Malterre J., [2]Verdun F., [1]Boubaker A., [1]Prior J.

Nuclear Medicine, CHUV[1], Radiophysics Institute, CHUV[2]

Aim of the study:

High transient ischemic dilation ratio (TID) is correlated with poor cardiac prognosis. Our purpose was to determine normal value of TID based on normal myocardial blood flow (MBF) and myocardial flow reserve (MFR) quantified by ^{82}Rb cardiac PET/CT.

Methods:

49 patients (21 M/ 28 F; sex ratio 0.75) with cardiovascular risk factors (smoking, hypertension, obesity, dyslipidemia and familial story) underwent a rest/stress cardiac PET/CT using a dynamic acquisition over 6 minutes after an intravenous bolus of ^{82}Rb (1600MBq). Stress acquisition was performed during infusion of adenosine over 6 minutes. Data were processed with FlowQuant using a two-compartment model (tissular+ vascular) (Lortie.EJNMMI2007;34:1765-1774) to determine MBF and MFR. Patients were selected based on normal rest/stress uptake images and normal stress MBF (> 2 mL/min/g) and MFR (> 2.0). For every patient TID was semi-automatically determined using ECToolbox software.

Results:

In total, 98 data sets were successfully performed for both quantitative analysis and for assessment of TID. All patients had a summed stress and rest score < 4 and a summed difference score <2. Mean MFR was 2.7±0.5. Mean TID was 1.01±0.12. TID was not significantly different between men and women (1.01±0.12 vs 1.01±0.11, *P*=0.86) but was between patients smoking or not (1.08±0.11 vs 0.99±0.11, *P*=0.013).

Conclusion:

Based on normal MFR, we determined TID upper limit as 1.24 (mean+1.96SD), that was higher than TID normal value previously published (Shi.NuclMedCommun2007;28(11):859-63) based on a qualitative myocardial perfusion analysis. Moreover TID value was significantly higher for smokers but none between genders.

Has TID predictive value for MBF and/or MFR abnormality when determined by 82Rb cardiac PET/CT?

[1]Dunet V., [1]Allenbach G., [1]Kosinski M., [1]Malterre J., [2]Verdun F., [1]Boubaker A., [1]Prior J.

Nuclear Medicine, CHUV[1], Institute of Radiation Physics, CHUV[2]

Aim of the study:

Our purpose was to assess the predictive value of transient ischemic dilation (TID) ratio for abnormal myocardial blood flow (MBF) and myocardial flow reserve (MFR) detection using ^{82}Rb cardiac PET/CT.

Methods:

110 patients (66 M/44 F; sex ratio 1.5) underwent a rest/stress ^{82}Rb cardiac PET/CT using a dynamic acquisition protocol. Data were processed with FlowQuant to determine MBF at rest, at stress and MFR. TID was determined by analyzing uptake images with ECToolbox software. Based on previously published study, TID ≤1.15 (1) and MFR >2.0 were defined as normal. Comparison between group with or without normal TID were analyzed using Student t test and relationship between TID and MFR was determine using regression analysis with robust computation of standard deviation.

Results:

In total, 220 data were successfully performed. 51 patients had normal MFR and 59 had decreased MFR. TID was not significantly different (P= 0.3) between patients with normal MFR and patients with decreased MFR. MFR was not statistically different according to TID abnormality or not. Therefore, rest MBF and stress MBF were statistically lower for patients with abnormal TID compared to patient with normal TID (0.9±0.3 vs 1.1±0.4 mL/min/g, P= 0.02 and 1.8±0.8 vs 2.2±0.8, P= 0.04). Moreover, there a negative correlation between TID ratio and MBF at rest (y= -0.1·x+1.2, P= 0.007) and at stress (y= -0.04·x+1.1, P= 0.021).

Conclusion:

TID assessed by ^{82}Rb cardiac PET/CT had no predictive value for decreased MFR detection. Therefore, it is inversely correlated with absolute stress MBF. Thus, we conclude that TID may be an indicator of stress MBF but cannot replace MFR measurement.

(1) Shi H, Santana CA, Rivero A et al. Normal values and prospective validation of transient ischaemic dilation index in 82Rb PET myocardial perfusion imaging. Emory University School of Medicine, Atlanta, GA 30322, USA. Nucl Med Commun. 2007 Nov;28(11):859-63.

Myocardial Blood Flow Quantification with Rubidium-82 Cardiac PET has Incremental Prognostic Value in Patients with Known or Suspected Coronary Artery Disease

[1]Dunet V., [1]Farhad H., [1]Soubeyran V., [2]Camus F., [1]Allenbach G., [1]Prior J.

Nuclear Medicine, CHUV[1], Radiophysics Institute, CHUV[2]

AIM: Cardiac PET allows non-invasively assessment of myocardial blood flow (MBF) and myocardial flow reserve (MFR). The impact of MBF and MFR in predicting major adverse cardiovascular events (MACE) has not been investigated in a prospective study, which was our aim.

MATERIAL AND METHODS: In total, 313 patients (65±11y, 36% women) with known or suspected CAD underwent both a rest and adenosine stress cardiac PET/CT with Rubidium-82. Dynamic acquisitions were analyzed semi-quantitatively computing the summed difference score (SDS) and quantitatively using the FlowQuant 2.1.3 software (MBF, MFR). Patients were stratified according to SDS, and allocated into groups of tertiles of stress MBF and MFR. For each group, annualized event rates were computed by dividing the number of annualized MACE (cardiac death, myocardial infarction, revascularisation or hospitalisation for cardiac-related event) by the sum of individual follow-up periods in years. Outcome were analyzed for each group using Kaplan-Meier event-free survival curves and compared using the logrank test. Multivariate analysis was performed in a stepwise fashion using Cox proportional hazards regression models.

RESULTS: The median follow-up was 256 days (range 168-494d) during which 42 MACE were observed. Ischemia (SDS≥2) was observed in 85 patients for whom annualized MACE rate was higher as compared tothose without (60% vs. 8%, p<0.0001). The group with the lowest MFR tertile (MFR<1.7) had higher MACE rate than the two highest tertiles (44% vs.9% and 12%, p<0.0001). Besides, the group with the lowest stress MBF tertile (MBF<1.8mL/min/g) had the highest annualized MACE rate as compared to the two others (37% vs. 21% and 3%, p=0.0001). On multivariate analysis, the addition of MFR or stress MBF to SDS significantly increased the global χ2 (from 60 to 65, p=0.02; and from 60 to 66, p=0.01). The best prognostic power was obtained by combining SDS (p<0.0001) and stress MBF (p=0.006). Interestingly, integrating stress MBF enhanced risk stratification even in absence of ischemia.

CONCLUSIONS: Quantification of MBF or MFR in Rb-82 cardiac PET/CT, over semi-quantitative assessment, provides independent and incremental prognostic information and is of significant value for risk stratification.

Alterations in microRNA expression favour the decline of function and mass of pancreatic β-cells in type 2 diabetes

[1]Nesca V., [1]Regazzi R.

Department of Cellular Biology and Morphology[1]

Background and aims:

The mechanisms underlying the development of type 2 diabetes are diverse, all leading to the decline of function and/or mass of pancreatic β-cells. MicroRNAs, a recently discovered class of non-coding RNAs, are potent regulators of key cellular processes, such as proliferation, differentiation and cell death. They are able to regulate gene expression by inhibiting the translation of target mRNAs through sequence-specific binding to the 3' untranslated region (3'UTR). In this study we evaluated the contribution of microRNAs to the decline of function and mass of pancreatic β-cells in db/db mice, a well known type 2 diabetes model.

Materials and methods:

Microarray analysis was employed to profile the expression of all known microRNAs in pancreatic islets of wild type and diabetic db/db mice. Two microRNAs showing a strong upregulation in the islets of diabetic mice were overexpressed in the mouse insulin-secreting β-cell line MIN6B1 to test for their impact on insulin secretion and cell survival. The bioinformatic tools TargetScan, miRanda and Pictar were used to search for putative targets of these microRNAs. The effect of microRNA overexpression on predicted targets was assessed by western blotting.

Results:

The expression of two microRNAs, miR-199a-5p and miR-199a-3p, was increased 12- and 9-fold, respectively, in pancreatic islets of diabetic db/db mice compared to wild type mice. Overexpression of miR-199a-5p in MIN6B1 cells led to defective glucose-induced insulin secretion while a rise in miR-199a-3p causes an increase in cell death. Western blot analysis revealed that overexpression of miR-199a-5p results in the upregulation of granuphilin a potent inhibitor of insulin secretion. On the other side, overexpression of miR-199a-3p reduced the level of mTOR, a serine/threonine kinase playing a key role in -cell survival.

Conclusion:

Our data suggest that miR-199a-5p and miR-199a-3p, two microRNAs issued from the same precursor, may contribute to -cell failure during instauration of type 2 diabetes: with miR-199a-5p causing defective insulin secretion, and miR-199a-3p having a negative effect on pancreatic β-cell survival.

Nitinol Based Artificial Muscle Independent Biventricular External Cardiac Assist Device: Bench Test Results

[1]Tozzi P., [1]Michalis A., [1]Berdajs D., [1]vonSegesser L.

CHUV[1]

Background: Ventricular assist devices (VADs) are single-ventricle pulsatile or continuous flow pumps that require anticoagulation. Thanks to artificial muscle technology a bi-ventricular assist device can restore heart muscle movement with external compression avoiding anticoagulant treatment.

Methods: Electrically driven Nitinol based artificial muscle wires are connected to an external carbon fibre scaffold that follows the heart surface at the level of the interventricular septum. This reinforced dome wraps both ventricles with a different number of fibres on the right and on the left ventricle enabling independent activation. Ejected volume and pressure gradient have been measured with afterload ranging from 25 to 150mmHg.

Results: Bench settings: preload range 5-15mmHg; afterload range 25-150mmHg; telediastolic volume 50ml; priming: 100-200ml saline. A single control unit drives both ventricles independently. Maximal systolic pressure generated by the left assist is 75mmHg and by the right assist 50mmHg. Volume ejected with a heart rate of 60/minute is 330ml/minute on the left side and 264ml/minute on the right side corresponding to an ejection fraction of 12% on the left side and 10% on the right side. The device requires a power supply of 6V, 250mA for 1.5s. The total power consumption is 10W. The pressure-volume loop shows that the ejected volume increases when afterload increases following the Starling Law.

Conclusions: External cardiac compression using dedicated artificial muscles is technically feasible. The unique design of the device described allows an independent external compression of both ventricles. It should be possible to modulate the degree of hemodynamic assistance according to the degree of right and/or left cardiac failure.

Expression of the Forbidden Gene REST Ensures the Identification of Genes Essential to Pancreatic Beta Cells

[1]Martin D., [2]Allagnat F., [3]Waeber G., [4]Meda P., [2]Haefliger J.-A.

CHUV-EPFL[1], Institut de Physiologie- CHUV[2], Medecine Interne-CHUV[3], Département de Physiologie Cellulaire et Métabolisme, CMU, Genève[4]

Background: The transcriptional repressor RE-1 Silencing Transcription factor (REST) represses a large number of genes that contain the binding motif RE-1. Because REST is ubiquitous, but absent from neurons and beta cells, it ensures that this set of genes is specifically restricted to neurons and beta cells. However, how these genes participate to beta cell function or survival is still unknown. We decided to overexpress REST in beta cells, to identify new RE-1-containing genes and assess their role in beta-cells.

Methods: We used transgenic mice that express REST specifically in pancreatic beta cells under the control of the rat insulin promoter (RIP-REST mice). Glucose tolerance test, measurements of insulin secretion, quantification of islet cell mass and immunohistochemistry were performed with mice. Adenoviral REST transduction, chromatin immuno-precipitation, qPCR, siRNA transduction and apoptotic assay were performed with INS-1E cell line.

Results: One RIP-REST founder line was intolerant to glucose, due to defects in insulin secretion, and also displayed a reduced beta cell mass. A second line of RIP-REST mice featured diabetes as a consequence of high levels of REST expression, which resulted in a major loss of beta-cell mass. Impairment of insulin release affected both phases of the insulin secretion pathway and was accounted for by decreased expression of RE-1-containing genes essential to insulin exocytosis, such as Snap25, Synaptotagmin IV and VII. Loss of beta cell mass occurred through apoptosis and was explained by decreased expression of anti-apoptotic genes containing RE-1, such as Irs2, Ib1, Cx36 and Cdk5r2.

Conclusions: Our work, accredited by the analysis of transgenic mice, have documented the need for healthy beta cells to express the whole set of RE-1-containing genes. We provided the first evidence that RE-1-containing genes are essential to beta cell life and function, *in vivo*. Especially, we identified crucial REST target genes such as Snap25 and Irs2, and also revealed the implication of novel REST target genes in insulin secretion, such as SytIV and VII and in beta-cell survival, such as Cdk5r2. We strengthen the need to perform a comprehensive identification of all RE-1-containing genes to better understand beta-cell function and life.

Critical role of Angiotensin II type 1 receptor on bone marrow-derived cells in the development of vulnerable atherosclerotic plaque in 2-Kidney, 1-Clip ApoE-/- mice

[1]Pellegrin M., [1]Aubert J.-F., [1]Bouzourène K., [2]Aubry D., [1]Nussberger J., [2]Duchosal M., [1]Mazzolai L.

Service of Angiology, CHUV[1], Service of Hematology, CHUV[2]

Background: We have previously shown that the Angiotensin II (Ang II) plays a pivotal role in the pathogenesis of atherosclerosis and vulnerable plaque development. Ang II type 1 receptors (AT1R) are expressed in a variety of cell types including bone marrow (BM)-derived cells. These are mainly constituted of macrophages and T lymphocytes which are key players in atherogenesis in general and Ang II-mediated atherosclerosis in particular. Whether Ang II drives atherogenesis via direct AT1R signaling on BM-derived cells remains unknown. To clear this issue we generated ApoE-/- mice selectively lacking AT1R on BM-derived cells. *Methods and results:* Irradiated ApoE-/- AT1R+/+ mice received BM from AT1R-/- donor mice. AT1R+/+ donor mice were used as controls. Four weeks after BM reconstitution, mouse model of Ang II-induced vulnerable plaque was generated by clipping the left renal artery (2-Kidney 1-clip renovascular hypertension model). Hemodynamic and hormonal parameters were measured 4 weeks later. Atherosclerosis characteristics were also assessed at this time point. Mean blood pressure, plasma renin concentration and activity were not different between 2K1C ApoE-/- mice receiving either AT1R-/- or AT1R+/+ BM. Atherosclerotic lesions size was significantly reduced by 69% in 2K1C ApoE-/- mice transplanted with AT1R-/- BM as compared to controls ($0.20\pm0.04\%$ vs $0.98\pm0.25\%$, $p<0.01$). Moreover, plaques of mice transplanted with AT1R-/- BM showed a more stable phenotype. Fibrous cap was thicker ($p<0.0001$), lipid core smaller ($p<0.0001$), layering, adventitia inflammation, and macrophage content ($8.0\pm2.0\%$ vs $29.9\pm3.1\%$, $p<0.0001$) were significantly decreased while smooth muscle cell content increased ($17.3\pm2.6\%$ vs $32.2\pm5.7\%$, $p<0.05$). Plaque staging also differed among the two groups of mice. Only 23% of mice lacking the AT1R in BM-derived cells developed advanced lesions (fibrofatty nodule or large necrotic/lipid core with multiple layers) compared to the 100% found in control mice ($p<0.0001$).

Conclusion: These results indicate that Ang II-mediated atherogenesis, and particularly development of vulnerable plaques, requires direct Ang II signaling via the AT1R on BM-derived cells.

Energy deficits and functional hypogonadotropic hypogonadism: A distinct clinical entity in men?

[1]Dwyer A., [1]Pitteloud N.

Service d'endocrinologie, diabétologie, et métabolisme - CHUV[1]

Background: Across species, reproduction and metabolism are tightly linked. In women, energy deficit (i.e. excessive exercise, weight loss, eating disorders) can lead to functional inhibition of the reproductive axis termed as Hypothalamic Amenorrhea (HA). Whether such a suppression of the reproductive axis exists in men is unclear.

Methods: We studied 7 men presenting with symptoms and biochemical evidence of hypogonadism in association with one or more associated factor known to predispose women to HA (i.e. excessive exercise, low body weight/weight loss, and/or psychological stress). Subjects underwent detailed hormonal profiling including an overnight frequent sampling study of LH, and DEXA scan for body composition. Men received counseling on minimizing stressors, and were followed to assess for recovery. A group of 20 age matched healthy adults with normal testosterone levels served as controls.

Results: All 7 hypogonadal men underwent complete pubertal development evidenced by full virilization and normal testicular size. The hypogonadal men had significantly lower body weight, BMI, and percent body fat compared to controls (see Table). Biochemically, sex steroids (testosterone [T] and estradiol) were significantly lower than controls yet sex hormone binding globulin was comparable. Interestingly, while LH was lower in the hypogonadal men, there were no differences in LH pulse frequency or amplitude. One hypogonadal subject exhibited a complete absence of pulses, while the others had normal pulse patterns or nocturnal entrained pulses - a pattern typically seen in HA women. Notably, Following amelioration of stressors, 3 subjects demonstrate sustained normal T (>9.4 nmol/L).

Anthropometric Characteristics	Hypogonadal Men n=7 (mean ± SD)	Healthy Men n=20 (mean ± SD)	p value
Age (yrs)	23 ± 5.7	24 ± 2.5	ns
Weight (Kgs)	64.1 ± 7.7	78.8 ± 11.9	< 0.01
BMI (Kg/M2)	20.7 ± 2.5	24.7 ± 3.3	< 0.01
Body Fat (%)	9.8 ± 2.4	17.6 ± 7.2[†]	< 0.01
Testicular Volume (mL)	21.8 ± 1.9	23.1 ± 3.4	ns
Biochemical Characteristics			
Testosterone (nmol/L)	5.8 ± 1.6	18.1 ± 4.8	< 0.001
Estradiol (pmol/L)	45.5 ± 8.4	140.3 ± 33.4	< 0.001
SHBG (nmol/L)	35.0 ± 17.4	24.6 ± 10	ns
LH (IU/L) [4.2-17]	7.2 ± 1.5	9.8 ± 2.8	< 0.05
LH pulse frequency (#/12h)	4.4 ± 2.5	5.3 ± 2.1	ns
LH pulse amplitude (IU/L)	5.6 ± 1.5	7.5 ± 2.8	ns
FSH (IU/L) [2-11]	5.0 ± 2.1	4.9 ± 1.7	ns
Inhibin B (pg/mL)	97.4 ± 43.1	180.9 ± 52.9	< 0.01

Conclusion: In men, hypogonagonadotropic hypogonadism can occur in the setting of energy deficits and psychological stress similar to HA in women. The absence of compensatory changes in LH pulse frequency or amplitude suggest a central defect in these men. Family history of HA in this cohort points to a possible genetic susceptibility to disruption of the reproductive endocrine axis. Additional follow up evaluations are underway to further assess reversibility. More of these men will need to be studied to better characterize this entity.

STAT3alpha interacts with nuclear GSK3beta and cytoplasmic RISK pathway and stabilizes rhythm in the anoxic-reoxygenated embryonic heart.

[1]PEDRETTI S., [1]RADDATZ E.

Department of Physiology[1]

Activation of the Janus Kinase 2 / Signal Transducer and Activator of Transcription 3 (JAK2/STAT3) pathway is known to play a key role in cardiogenesis and to afford cardioprotection against ischemia-reperfusion in the adult. However, involvement of JAK2/STAT3 pathway and its interaction with other signalling pathways in developing heart transiently submitted to anoxia remain unexplored.

Hearts isolated from 4-day-old chick embryos were submitted to anoxia (30min) and reoxygenation (80min) with or without the antioxidant MPG or the JAK2/STAT3 inhibitor AG490. Time course of phosphorylation of STAT3alpha^{tyr705} and Reperfusion Injury Salvage Kinase (RISK) proteins (PI3K, Akt, GSK3beta, ERK) was determined in homogenate and in enriched nuclear and cytoplasmic fractions of the ventricle. STAT3 DNA-binding was determined by EMSA. The chrono-, dromo- and inotropic disturbances were also investigated by ECG and mechanical recordings.

Phosphorylation of STAT3alpha^{tyr705} was increased by reoxygenation and reduced by MPG or AG490. STAT3 and GSK3beta were detected both in nuclear and cytoplasmic fractions while PI3K, Akt and ERK2 were restricted to cytoplasm. Reoxygenation led to nuclear accumulation of STAT3 but unexpectedly without DNA-binding. AG490 decreased the reoxygenation-induced phosphorylation of Akt and ERK2 and phosphorylation/inhibition of GSK3beta in the nucleus, exclusively. Inhibition of JAK2/STAT3 delayed recovery of atrial rate, worsened RR variability and prolonged arrhythmias compared to control hearts.

In the anoxic-reoxygenated embryonic ventricle the ROS-dependent activation of JAK2/STAT3 leads to an increase of STAT3 and inhibition of GSK3beta in the nucleus without altering transcriptional activity. Activated STAT3 interacts with cytoplasmic components of RISK pathway and in addition stabilizes heart rhythm.

Pregnancy outcome following maternal exposure to statins: a multicenter prospective study

[1]Winterfeld U., [2]Panchaud A., [3]Merlob P., [2]Rothuizen L., [4]Cuppers-Maarschalkerweerd B., [5]Vial T., [6]Stephens S., [7]Clementi M., [8]DeSantis M., [9]Pistelli A., [10]Berlin M., [11]Elefteriou J., [12]Manakova E., [1]Buclin T.

Service de Pharmacologie Clinique - CHUV[1], Drug consultation-TIS, Assaf Harofeh Medical Center, Zerifin, Israel[10], Poison Control, Bergamo, Italy[11], CZTIS, 3rd Faculty of Medicine, Charles University, Prague, Czech Republic[12], Service de Pharmacologie Clinique [2], BELTIS   Rabin Medical Center   and Sackler School of Medicine, University of Tel-Aviv,   Tel-Aviv , Israel[3], TIS, National Institute of Public Health and Environment, Bilthoven, The Netherlands[4], Centre Antipoison-Centre de Pharmacovigilance, Hospices Civils, Lyon, France[5], UKTIS, Regional Drug and Therapeutics Centre, Newcastle upon Tyne, UK[6], Servizio di Informazione Teratologica, Padova, Italy[7], Telefono Rosso-TIS, Department   of Obstetrics and Gynecology, Catholic University of Sacred Heart, Rome, Italy[8], TIS AOU Carreggi, Florence, Italy[9]

Objective: Statin use for the treatment of hypercholesterolemia in women of childbearing age is becoming increasingly common. However, published data on pregnancy outcome after exposure to statins is scarce and conflicting. This contribution addresses the safety of exposure to statins during pregnancy.

Method: In a multi-center (n = 11) observational, prospective study we compared the outcomes of 249 women exposed during the 1st trimester of pregnancy to simvastatin (n = 124), atorvastatin (n = 67), pravastatin (n = 32), rosuvastatin (n = 18), fluvastatin (n = 7) or cerivastatin (n = 1) with a control group exposed to non-teratogenic agents (n = 249). Data were collected by members of the European Network of Teratology Information Services (ENTIS) during individual risk counseling between 1990 and 2009. Standardized procedures for data collection were used by each center.

Results: There was no statistically significant difference in the rate of major birth defects between the statin exposed group and the control group (4.0% versus 2.7% OR 1.53; 95% CI 0.52-4.48, p = 0.44). The crude rate of spontaneous abortions (12.8% versus 7.1%, OR 1.90, 95% CI 1.02-3.57, p = 0.04) was higher in the exposed group. However, after adjustment to maternal age and gestational age at initial contact, the difference became statistically insignificant. The rate of elective termination-pregnancy (8.8% versus 4.4%, p = 0.05) was higher and the rate of deliveries resulting in live births was significantly lower in the statin exposed group (77.9% versus 88.4%, p = 0.002). Prematurity was more frequent in the exposed group (16.1% versus 8.5%; OR 2.07, 95% CI 1.12-3.84, p = 0.02). Nonetheless, gestational age at birth (median 39 weeks, IQR 37-40 versus 39 weeks, IQR 38-40, p = 0.27) and birth weight (median 3280 g, IQR 2835-3590 versus 3250 g, IQR 2880-3600, p = 0.95) did not differ between exposed and non-exposed pregnancies.

Conclusion: This study did not detect a teratogenic effect of statins. Its statistical power is not sufficient to reverse the recommendation of treatment discontinuation during pregnancy. At most, the results are reassuring in case of inadvertent exposure.

RB-82 GENERATOR QUALITY CONTROL

[1]El Hakmaoui F., [2]Allenbach G., [3]Champendal M., [3]Malterre J., [3]Pappon M., [3]Kosinski M., [3]Camus F., [3]Boubaker A., [3]Prior J., [3]Dunet V.

NUCLEAR MEDICINE[1], DEPARTMENT OF NUCLEAR MEDICINE chuv[2], DEPARTMENT OF NUCLEAR MEDICINE chuv[3]

Aim of the study:

High transient ischemic dilation ratio (TID) is correlated with poor cardiac prognosis. Our purpose was to determine normal value of TID based on normal myocardial blood flow (MBF) and myocardial flow reserve (MFR) quantified by ^{82}Rb cardiac PET/CT.

Methods:

49 patients (21 M/ 28 F; sex ratio 0.75) with cardiovascular risk factors (smoking, hypertension, obesity, dyslipidemia and familial story) underwent a rest/stress cardiac PET/CT using a dynamic acquisition over 6 minutes after an intravenous bolus of ^{82}Rb (1600MBq). Stress acquisition was performed during infusion of adenosine over 6 minutes. Data were processed with FlowQuant using a two-compartment model (tissular+ vascular) (Lortie.EJNMMI2007;34:1765-1774) to determine MBF and MFR. Patients were selected based on normal rest/stress uptake images and normal stress MBF (> 2 mL/min/g) and MFR (> 2.0). For every patient TID was semi-automatically determined using ECToolbox software.

Results:

In total, 98 data sets were successfully performed for both quantitative analysis and for assessment of TID. All patients had a summed stress and rest score < 4 and a summed difference score <2. Mean MFR was 2.7±0.5. Mean TID was 1.01±0.12. TID was not significantly different between men and women (1.01±0.12 vs 1.01±0.11, *P*=0.86) but was between patients smoking or not (1.08±0.11 vs 0.99±0.11, *P*=0.013).

Conclusion:

Based on normal MFR, we determined TID upper limit as 1.24 (mean+1.96SD), that was higher than TID normal value previously published (Shi.NuclMedCommun2007;28(11):859-63) based on a qualitative myocardial perfusion analysis. Moreover TID value was significantly higher for smokers but none between genders.

Long-term intermittent atrial tachycardia decreases activation recovery interval, flattens its kinetics and blunts its rate dependence before sustained atrial fibrillation

[1]Tenkorang J., [2]Jousset F., [3]Ruchat P., [4]Vesin J.-M., [5]Pascale P., [5]Fromer M., [6]Schaefer S., [7]Narayan S., [5]Pruvot E.

CHUV, Service de cardiologie[1], EPFL[2], CHUV, dept of cardiology and cardiovascular surgery[3], EFPL[4], CHUV, Service de Cardiologie[5], CHUV, Service de Pathologie[6], University of California, San Diego, USA[7]

Introduction: We recently observed in an acute ovine model of pacing-induced atrial tachycardia (PIAT) that rapid atrial capture and fibrillatory conduction were prevented by 2:1 capture mediated by decreased excitability. We hypothesize that long-term intermittent PIAT mimicking pulmonary vein tachycardia promotes rapid atrial capture beyond the ERP measured in the baseline state, fibrillatory conduction and sustained atrial fibrillation (AF) by decreasing activation recovery interval (ARI), a surrogate of action potential duration (APD).

Methods: We specifically developed a chronic ovine model of PIAT using two pacemakers (PM) each with a right atrial (RA) lead separated by ~2cm. The 1st PM (Vitatron T70) was used to record a broadband unipolar RA EGM (800 Hz, 0.4 Hz high pass filter). The 2nd was used to deliver PIAT during electrophysiological protocols at decremental pacing CL (400 beats, from 400 to 110ms) and long term intermittent RA burst pacing to promote electro-anatomical remodelling (5s of burst followed by 2s of sinus rhythm) until onset of sustained AF. ARIs, defined as the time difference between the peaks of the atrial depolarisation and repolarisation waves, were averaged over 20 consecutive beats at each pacing CL and their restitution kinetics as a function of the pacing CL were compared before (i.e. in the baseline state), during and after remodelling (i.e. the week before sustained AF occurred) using multiple-way ANOVA. A $p < 0.05$ was considered significant. Logarithmic regression was used to fit the ARI-pacing CL relationship ($y = a + b \ln(x)$).

Results: Intermittent PIAT induced sustained AF on average after 6.0 ± 3.5 weeks of burst pacing (n=8 sheep). The figure shows that ARI measured at 400 ms pacing CL before remodelling (122 ± 20 ms) was significantly decreased by intermittent PIAT during and after remodelling (99 ± 16 ms and 98 ± 20 ms respectively, $p < 0.05$). Moreover, the rate-dependence of ARI was significantly altered by intermittent PIAT from a steep kinetics (b=34.1, $p < 0.01$) before remodelling to a nearly flat relationship during (b=10.9, p=NS) and after remodelling (b=10.9, p=NS). Importantly, there was no difference in atrial structure and fibrosis as assessed by light microscopy between remodelled sheep and a set (n=4) of unremodelled control sheep.

Conclusions: Using standard pacemaker technology, atrial ARIs as a surrogate of APDs were successfully measured in vivo during the electrical remodelling process leading to AF. The facilitation of AF by pacing-induced atrial tachycardia mimicking salvos from pulmonary veins is heralded by a significant shortening of ARI, with loss of rate-dependence in the remodelled as compared to the unremodelled state.

Role of the ESCRT protein Tsg101 in the turnover of the epithelial Na+ channel in the kidney

[1]Vitagliano J.-J., [1]Staub O.

Department of Pharmacology - UNIL - Switzerland[1]

Excess salt intake is one of the primary risk factors of arterial hypertension. The kidneys play an essential role for salt homeostasis and consequently blood pressure. In the proximal tubule the bulk of the filtrate is reabsorbed constitutively, whereas in the distal region active Na^+ transport is finely tuned. This transport is regulated by various hormonal pathways including aldosterone that regulates the reabsorption at the level of the ASDN (Aldosterone Sensitive Distal Nephron), comprising the late distal convoluted tubule (DCT), the connecting tubule (CNT) and the cortical collecting duct (CCD). In the ASDN, the amiloride-sensitive epithelial Na^+ channel (ENaC) plays a major role in Na^+ homeostasis, as evidenced by gain-of function mutations in the genes encoding ENaC, causing Liddle's syndrome, a severe form of salt-sensitive hypertension. In this disease, regulation of ENaC is compromised due to mutations that delete or mutate a PY-motif (PPXY) in ENaC. Such mutations interfere with the interaction of the PY-motifs with the WW-domains of the Nedd4-2 ubiquitin-protein ligase, leading to reduced ubiquitylation and endocytosis of the channel, and consequently to increased channel activity at the cell surface. After endocytosis ENaC is targeted to the lysosome and rapidly degraded. The cellular mechanisms that are involved in lysosomal targeting are not known. Similarly to other ubiquitylated and endocytosed plasma membrane proteins (such as the EGFR), it is likely that the multi-protein complex system ESCRT is involved. To investigate the involvement of this system we tested the role of one of the ESCRT proteins, Tsg101. Co-immunoprecipitation experiments in Hek293 cells showed that Tsg101 interacts with ENaC, and that this primarily involves the ubiquitin-binding domain UEV in Tsg101. We then wanted to know if Tsg101 plays a role in ENaC degradation in renal epithelial cells and suppressed Tsg101 in $mCCD_{cl1}$ cells by shRNA. Western blots confirmed that Tsg101 was reduced and found, that ENaC subunits were higher expressed. These cells were then cultured on collagen-coated permeable filters and equivalent amiloride-sensitive currents were measured. Suppression of Tsg101 caused an increase of transepithelial currents, which could be further stimulated by aldosterone. Moreover, cell surface biotinylation experiments showed also a higher expression of ENaC subunits at the apical membrane. Taken together our data imply Tsg101 and likely the ESCRT system in ENaC degradation by the endosomal/lysosomal system.

Role of AKAP-Lbc in the activation of cardiac hypertrophy transcription factors.

[1]Del Vescovo C., [2]Cotecchia S., [1]Diviani D.

Département de Pharmacologie et de Toxicologie[1], Department of General and Environmental Physiology, University of Bari "Aldo Moro", Italy[2]

In response to various pathological stresses, the heart undergoes a remodeling process that is associated with cardiomyocyte hypertrophy and to the progression to heart failure. Our earlier work indicates that AKAP-Lbc, an A-kinase anchoring protein (AKAP) with an intrinsic Rho-specific guanine nucleotide exchange factor activity, is critical for activating RhoA and transducing hypertrophic signals downstream alpha1-adrenergic receptors (α1-ARs). To identify the effector proteins linking AKAP-Lbc to the activation of cardiomyocyte hypertrophy, we followed a proteomic approach to determine the signaling molecules associated with the AKAP-Lbc signaling complex. Analysis of AKAP-Lbc immunoprecipitates using mass spectrometry identified the nuclear factor-kappa b (NF-κB) activating kinase IKKβ as an AKAP-Lbc interacting protein. This raises the hypothesis that AKAP-Lbc might promote cardiomyocyte growth by maintaining a signaling complex that promotes the activation of the pro-hypertrophic transcription factor NF-κB. Interestingly, our results indicate that AKAP-Lbc is an important mediator of NF-κB activation as shown by the fact that suppression of AKAP-Lbc expression by infecting cells with lentiviruses encoding AKAP-Lbc-specific short hairpin RNAs strongly reduces the transcriptional activation of NF-κB induced by α1-ARs. Moreover, overexpression of a mutant form of AKAP-Lbc displaying constitutive Rho-GEF activity promotes NF-κB activation in HEK-293 cells. Importantly, AKAP-Lbc mediated NF-κB stimulation involved RhoA, Rho kinase and IKKβ since it is inhibited by the dominant negative T19N mutant of RhoA, Rho kinase inhibitors, and the dominant negative mutant K44M of IKKβ. Mapping analysis of the interaction between AKAP-Lbc and IKKβ indicates that IKKβ interacts with a region located within the Dbl homology domain of AKAP-Lbc. Altogether these results indicate that in HEK cells AKAP-Lbc can organize a transduction pathway including RhoA, Rho-Kinase and the IKK complex that is required for the activation of NF-kB. Future experiments will assess whether this complex mediates the hypertrophic responses induced by α1-ARs.

Characterization of the role of Rho activating signaling complexes in G protein-coupled receptor induced cardiac fibrosis

[1]Cavin S., [1]Diviani D.

Département de Pharmacologie et Toxicologie-UNIL[1]

Pathological cardiac remodeling is a multifactorial phenomenon characterized by the hypertrophic growth of cardiomyocytes and cardiac fibrosis. During this process, cardiac fibroblasts undergo phenotypic changes and become highly proliferative and invasive in response to specific hormones, growth factors and pro-inflammatory cytokines. These activated cells increase the secretion of extracellular matrix proteins such as collagen. This process leads over the time to an increased heart stiffness and diastolic dysfunction. Among the profibrotic factors that are secreted in the myocardium in response to stress, GPCR agonist such as angiotensin II has been shown to play a major role in mediating the cellular responses that ultimately lead to fibrosis. The small GTPase RhoA plays an important role in mediating many of the cellular responses associated with cardiac fibrosis that are induced by angiotensin II. However the exchange factors that selectively control RhoA activation during these processes are yet to be identified. We have recently shown that AKAP-Lbc, a cardiac A-kinase anchoring protein (AKAP) with an intrinsic Rho-specific guanine nucleotide exchange factor activity, is critical for activating RhoA and transducing hypertrophic signals downstream of angiotensin II receptor. Expression analysis of the RhoGEF expressed in cardiac fibroblasts revealed the presence of AKAP-Lbc as well as other RhoGEFs, including p115-RhoGEF, PDZ-RhoGEF and LARG. These findings raise the hypothesis that AKAP-Lbc and potentially additional RhoGEFs, might mediate the activation of transduction cascades that promote cardiac fibrosis. In order to determine the implication of these signaling molecules in the process of cardiac fibrosis, we have initially determined whether angiotensin II stimuli could enhance the expression of these different RhoGEFs in primary cultures of rat cardiac fibroblasts. We could then show that downregulation of selected RhoGEFs using lentivirus-delivered shRNAs could impair RhoA activation induced by profibrotic stimuli. Using a similar strategy, we are currently determining whether downregulation of the expression of these RhoGEFs can impair fibrotic responses such as fibroblast differentiation, migration and invasiveness in response to angiotensin II.

Retro controlled regulation of the Mineralocorticoid Receptor by USP2-45.

[1]FARESSE N., [1]DEBONNEVILLE A., [1]STAUB O.

Department of Pharmacology and Toxicology - UNIL[1]

Ubiquitylation (i.e. the modification of proteins with ubiquitin) is a covalent post-translational modification, comparable to acetylation, glycosylation, methylation, or phosphorylation. Besides its well known role in proteasome dependant degradation, a plethora of cellular roles has been attributed to ubiquitin, including in DNA repair, protein sorting or signaling. Usually these functions depend on the type of ubiquitylation (i.e. mono-, multi- or poly-ubiquitylation). Ubiquitin-dependent pathways play also an important role in the regulation of a number of ion channels and transport proteins including the epithelial Na$^+$ channel (ENaC), whose activity is under the control of aldosterone and the mineralocorticoid receptor. Thereby, this hormone regulates the activity or expression of different enzymes such as NEDD4-2, Sgk1 or USP2-45, which all are involved in ENaC ubiquitylation and subsequently activity of this channel.

In this study, using immobilized ubiquitin binding domains, we have identified the mineralocorticoid receptor (MR) as an ubiquitylated protein at basal conditions either in M1 cells transfected with the MR, or in mCCDcl1 cells derived from the cortical collecting duct. Activation of the receptor by aldosterone leads to the rapid deubiquitylation of the receptor. Because Usp2-45 is an aldosterone-induced deubiquitylating enzyme, we were interested to know if Usp2-45 is involved in the deubiquitylation of the receptor. Surprisingly we found that over-expression of USP2-45 dramatically decreased the level of MR due to proteasomal degradation, and conversely, RNAi dependant cell depletion of USP2-45 lead to stabilization of the receptor. This observation was confirmed *in vivo* in USP2 KO mice, where the expression of MR in the kidney is enhanced. Our results suggest a novel role for USP2-45 as a negative regulator of MR pathway that mediates the degradation of MR in response to aldosterone.

[18]FDG PET scan analysis of the mouse myocardium

Perruchoud S.

Experimental Cardiology

In nuclear medicine, ^{18}F-fluorodeoxyglucose (FDG) positron emission tomography (PET) scan is an imaging technique based on the measurement of FDG uptake in tissues. In the heart, FDG PET scan allows differentiating viable myocardium from necrotic areas in the left ventricle. This method measures the size of the infarcted area to quantify the extent of damage. Moreover, this technique, by comparing the infarcted area over time can provide information regarding the progression of the damage, which can be useful to determine the effect of treatments aimed at improving recovery after infarction. For instance, this method could be very effective to assess the potential of transplanted cardiac precursor cells in vivo, and to investigate regenerative mechanisms in the adult heart. The quality of the acquired pictures depends on myocardial uptake of the glucose analogue FDG, which itself depends on metabolic conditions. Hyperinsulinemic euglycemic clamping improves image quality. Premedication with Acipimox, a nicotinic acid derivate and hypolipidemic agent, which decreases free fatty acid mobilization, produces quality enhancement similar to clamping, and leads to a more homogenous FGD uptake. The goal of this study was then to establish the methodology in the mouse, and to evaluate whether infarct size can be precisely determined by FDG PET scan. Furthermore, we also evaluated whether Acipimox increased image quality. Mice were separated into sham-operated and myocardial infarcted groups and underwent cardiac FDG PET scan. FDG was administrated via the tail vein, and images were acquired using a microPET machine. Data were analyzed using dedicated software for quantitative image processing (PMOD Technologies Ltd) that allows the determination of localized FDG standard uptake value (SUV). Results demonstrated that myocardial viability and the extent of necrotic area can be precisely measured using FGD PET scan. Preliminary data suggested that additional Acipimox administration did not further increase uptake. However, further analysis is ongoing to evaluate whether this pharmacological treatment improve homogeneity. All together, this study establishes the conditions for a routine analysis of myocardial damage and recovery using FGD PET scan in the mouse.

GLUT9 and uric acid handling by the kidney

[1]Auberson M., [2]Thorens B., [1]Bonny O.

Department of Pharmacology and Toxicology[1], Center for Integrative Genomics[2]

Uric acid is a metabolite of purine degradation and hyperuricemia is strongly associated with gout and kidney stones, and has been linked to several other pathological conditions such as hypertension, the metabolic syndrome and inflammation. GLUT9 (SLC2A9) is a newly identified urate transporter, initially cloned by homology with the glucose transporter family. GLUT9 mutations in humans have been shown to be causative for the familial renal hypouricemia, a condition in which affected patients present hypouricemia, renal uric acid wasting, kidney stone and a propensity to acute renal failure during strenuous exercise.

The in vivo role of GLUT9 has been recently unravelled in the mouse. Mice with whole body deletion of Glut9 are hyperuricemic and display severe nephropathy that results from intratubular uric acid precipitation. Mice in which GLUT9 has been deleted only in the liver present with hyperuricemia, due to the role of GLUT9 in facilitating the entry of uric acid in the hepatocyte for its degradation by the enzyme uricase.

By contrast, the role of GLUT9 in the kidney remains largely unknown. In particular, the exact localization of GLUT9 (proximal vs. distal tubules, apical vs. basolateral side of the epithelium), and the precise mode of urate transport have not been solved yet.

In order to address these points, we generated mouse models carrying kidney-specific disruption in different parts of the tubules and showed that GLUT9 is essential for proper urate reabsorption in the mouse kidney. Indeed, tetracycline-inducible whole nephron deletion of GLUT9 led to hyperuricosuria. These results point out GLUT9 as a crucial partner in the renal handling of uric acid and designate it as a new target for uricosuric agent.

Identification of novel AKAPs involved in the regulation of the cardiac function

[1]Pérez López I., [1]Diviani D.

Department of Pharmacology and Toxicology[1]

The activity of the heart is modulated by the sympathetic system through the activation of β-adrenergic receptors that downstream activate the cyclic AMP-dependent protein kinase, PKA. This is a ubiquitous, serine/threonine kinase that after β-adrenergic stimulation phosphorylates a set of different substrates within the cardiomyocyte, changing the contractile properties of the cell. Due to the broad specificity of PKA, it is needed to target the kinase close to its substrate. Evidence collected over the last years demonstrates that compartmentalization of PKA is achieved through the association with A-kinase anchoring proteins (AKAPs). These scaffolding proteins share the capacity to bind the regulatory subunits of PKA inside cells and thanks to unique targeting domains contained within each AKAP, PKA is localized at specific subcellular regions. Several AKAPs have been identified in adult cardiac myocytes with roles as important as the control of calcium handling, cardiac contractility, the action potential duration or the regulation of cardiomyocyte hypertrophy.

For the purpose of determining the role of new AKAPs in the regulation of the cardiac activity, we followed a proteomic approach which allowed us to identify AKAP2 as a very abundant AKAP in the heart. AKAP2 also known as AKAP-KL, since it was first characterized in kidney and lung, is a broadly expressed protein whose function is still unknown. In order to characterize a possible protein complex interacting with AKAP2, we used specific antibodies against AKAP2 to perform immunoprecipitations from lysates of adult rat hearts. The immunoprecipitated proteins were then analyzed by mass spectrometry for the identification of possible AKAP2 interacting proteins. This strategy allowed us to identify the nuclear receptor coactivator 3 (NCoA-3) as protein associated with AKAP2. NCoA-3 is a member of the p160 family of steroid receptor coactivators (SRCs), and its function within the cell is to potentiate the transcriptional activity of nuclear receptors. We were able to confirm the interaction between AKAP2 and NCoA-3 by bi-directional co-immunoprecipitations. Current studies are aimed at characterizing the role of AKAP2 in the regulation of cardiac gene expression through its interaction with NCoA-3.

Involvement of the RNA-binding protein AUF1 in the cytotoxic effect of proinflammatory cytokines on pancreatic β-cells

[1]Roggli E., [1]Gattesco S., [1]Regazzi R.

DBCM - UNIL[1]

Background and aims:

During the initial phases of type I diabetes mellitus, pancreatic β-cells are exposed to proinflammatory cytokines, such as IL-1β, TNFα and IFNγ. Chronic exposure to these cytokines has a detrimental impact on the regulation of β-cell gene expression leading to impaired insulin secretion and apoptosis. AUF1 belongs to a family of proteins that control mRNA stability and translation by associating with adenosine- and uridine-rich regions in the 3'UTR of target messengers. AU-rich sequences are found in mRNAs encoding for many proteins involved in stress and/or inflammation processes. AUF1 can be activated by different signaling cascades and translocates from the nucleus to the cytoplasm to accomplish its regulatory functions. In this study, we investigated the possible involvement of AUF1 in cytokine-induced β-cell dysfunction.

Materials and methods:

The expression of the four AUF1 isoforms (p37, p40, p42, p45) was analyzed by Western blotting. AUF1 activation was assessed by following the redistribution of the isoforms from the nucleus to the cytoplasm. To test for their potential impact on insulin biosynthesis, insulin secretion and apoptosis, each isoform was overexpressed individually in the mouse insulin-secreting cell line MIN6. The contribution to cytokine-mediated β-cell dysfunction was evaluated by preventing the expression of AUF1 isoforms using specific siRNAs. The effect of AUF1 on the expression of potential targets was assessed by Western blotting.

Results:

We found that MIN6 cells and human pancreatic islets express the four AUF1 isoforms (p42>p45 >p37>p40). AUF1 isoforms were mainly localized in the nucleus but partially translocated to the cytoplasm upon 24 hours exposure of β-cells to cytokines. Over-expression of each of the isoforms did not affect glucose-induced insulin secretion but led to an increase in apoptosis. This effect was at least in part mediated by decreasing the expression of the anti-apoptotic protein Bcl2. Silencing of AUF1 isoforms restored Bcl2 levels and protected MIN6 cells and human pancreatic islet cells from cytokine-induced apoptosis.

Conclusion:

Taken together, our findings point to a contribution of AUF1 to the deleterious effects of cytokines on β-cell functions and suggest a possible role for this RNA-binding protein in the early phases of type I diabetes.

Implication of Islet Brain 1 in Endoplasmic Reticulum Stress-induced β-cell dysfunction

[1]Brajkovic S., [1]Favre D., Niederhäuser G.

DBCM[1]

Introduction: Type 2 diabetes (T2D) is the most common form of diabetes. The disease manifests when islets β-cells from endocrine pancreas fail to release sufficient insulin to compensate for insulin resistance in target tissues. Impairment of β-cell activity includes loss of glucose-induced insulin secretion and reduction in β-cell mass. It is now accepted that environmental factors as hyperglycaemia and hyperlipidemia contribute to β-cell dysfunction. In such diabetic context, β-cell has been shown to develop a stress, the endoplasmic reticulum (ER) stress, which participates in the alteration of β-cell physiology. The adverse effects of all the stressors rely on activation of the c-Jun N-terminal kinase (JNK) pathway. The prolonged JNK activity is achieved by a decrease in the contents in the MAPK8 interacting protein 1 also called JNK-interacting protein 1 (JIP-1) or Islet Brain 1 (IB1). The function of JIP-1 is to tether the kinases for activation of the JNK pathway. Our attempts are done to highlight potential link between the ER stress and JIP-1-dependent JNK activation.

Methods: mRNA expression of diabetic patients has been measured. Mouse and human islets, as well as mouse and rat insulin secreting cell lines (MIN6 and INS1E respectively), were treated with the ER stress inducers thapsigargin and tunicamycin. The protein and the mRNA contents were analysed. To study the promoter activity we used a Luciferase assay. Two proteosomal inhibitors, lactacystin and MG132, as well as the lysosomal inhibitor chloroquin, are used to test protein degradation.

Results: Western blotting revealed that thapsigargin induces ER stress in our cell models. By real time PCR we have observed that diabetic patients present a significant decrease of JIP-1, and this is associated with an increase of the ER stress marker CHOP. Tunicamycin or thapsigargin-induced ER stress result in the decrease of JIP-1 expression at protein and mRNA levels in MIN6 cells as well as INS1E cells. Similar observations have been done on mouse and human islets treated with thapsigargin. Also the promoter activity of JIP-1 was decreased by thapsigargin. Blocking the protein degradation by proteosomal and lysosomal inhibitors show that JIP-1 protein content is degraded only in the proteasome.

Conclusion: these data highlight the contribution of the ER stress in the defects of the scaffold protein JIP-1 and suggest that the downregulation may be achieved by the binding of a transcription factor and by protein degradation via the proteasome.

SHORT FISH OIL INFUSIONS MODULATE CARDIOVASCULAR AND METABOLIC RESPONSE IN PATIENTS UNDERGOING CORONARY ARTERY BYPASS SURGERY: PRELIMINARY DATA

[1]Delodder F., [1]Delodder F., [1]Khoudi D., [2]Tozzi P., [3]Tappy L.

Médecine intensive adulte [1], Service de chirurgie cardio-vasculaire [2], Institut de physiologie[3]

Rationale: Fish Oil (FO) is known to blunt inflammatory responses and to reduce arrhythmias. Cardiac surgery patients exhibit a strong inflammatory response and suffer postoperative arrhythmias. The aim of the study is to test if short infusion of FO modifies membrane composition and n-3/n-6 ratio, and clinical course of patients undergoing elective coronary artery bypass surgery. Preliminary 2009 data already showed that 2 preoperative 0.2g/kg intravenous FO infusions resulted in a significant incorporation of EPA/DHA in the cardiac tissue and platelet membranes

Methods: Prospective randomized placebo controlled trial in 30 patients, receiving 3 short infusions 0.2g/kg of FO (Omegaven, FreseniusKabi) or placebo (P). Infusion timing: evening before, at premedication and immediately after surgery. Blood samples: before and after each infusion and on day after surgery. Determination of plasma triglycerides (TG) levels, platelet & cardiac tissue fatty acid composition. Hemodynamic data: heart rate (HR), mean arterial pressure (MAP), Temperature (T°); lactate, glucose, HbCO and Norepinephrine doses (NE) were recorded during 24 hours. Stat: t-tests, Wilcoxon signed rank, Area under the curve (AUC).

Results: 22 patients aged 65±10years were enrolled. Plasma TG peaked after infusion, remaining within safe ranges. The EPA membrane composition changes were confirmed. In the FO group, HR (89 vs 94 bt/min, p<.000) and T° (36.8 vs 37.2°, p<0.0001) were lower, MAP was higher (88 vs 81 mmHg, p<.000) with the same NE dose. Glucose, Lactate and HbCO AUC were lower (p< 0.05) in the FO group. No side effects. Cytokines to come.

Conclusion: Significant increases in EPA membranes incorporation were confirmed after 2-3 FO infusions. Preconditioning with FO significantly blunted clinically observable T°, cardiovascular and metabolic responses, resulting in better patient stability.

INFLUENCE OF THE INFUSION MODE OF FISH OIL ON THE FATTY ACID COMPOSITION IN CELL MEMBRANES

[1]Delodder F., [2]Gagnon G., [2]Khoudi D., [3]Tozzi P., [4]Tappy L., [2]Berger M.

Soins intensive adulte[1], Médecine intensive adulte [2], Service de chirurgie cardio-vasculaire [3], Physiology Department[4]

Rationale: Fatty acid cell membranes composition (MC) determines structure, stability, and fluidity and related membrane functions. N-3 and N-6 classes of Poly Unsaturated Fatty Acids (PUFA) are known to directly modulate the inflammatory response. Literature suggests improvement of clinical outcome in patient receiving parenteral nutrition containing FO. While the PUFA dose is known to influence the MC, there are no data on the influence of the infusion mode (continuous versus intermittent) on MC.

Methods: Prospective randomized placebo controlled trial in patients admitted to ICU after coronary artery bypass grafting (CABG) or acute myocardial infarction (AMI) entering a pre- and post-conditioning trial. The subjects received FO (Omegaven®) or placebo (P). The FO patients received the same 0.6 g/kg FO dose over 24h: CABG patients received 3 *intermittent* infusions 0.2g/kg of FO over 2h each on the evening before, at premedication and immediately after surgery; AMI patients received a *continuous* 24h infusion with a loading dose of 0.2g /kg over 3h followed by a 21h continuous 0.4g/kg FO infusion. Blood samples: CABG before and after each infusion, AMI at baseline, then after 12h and 24h. The determination of platelet MC were performed at baseline (T0) after 12h (+/-2h for CABG) (T12) and at the end of the last infusion T24.

Stat: median and Wilcoxon

Results: A total of 34 patients were included (CBAG n=23, AMI n=11). PUFA incorporation differed between the 2 administration modes. After *intermittent* infusion EPA MC increased significantly more already at T12 (p=.004) than after *slow continuous* infusion (p=0.46), while DHA increased significantly more at T24 with the *slow continuous* infusion mode *(P=.009)* versus *intermittent* infusion *(P=0.42)*.

Conclusion: The FO infusion mode (intermittent versus continuous) appears to be one more determinant of the rate of incorporation of the different PUFAs into the cell membranes

Implication of αENaC on Whole Sodium Homeostasis in distal colon

[1]Malsure s., [2]Rossier B., [2]Hummler E.

Institute of pharmacology and toxicology,UNIL[1], Institute of pharmacology and toxicology,UNIL[2]

The epithelial sodium channel (ENaC) plays an important role in sodium balance, blood volume and blood pressure. It is composed of three sub-units α, β and γ. Although the role of ENaC in sodium reabsorption in kidney and lung is well established, less is known in colon. The aim of this project is to investigate the importance of αENaC expression in the distal colon for maintaining sodium and potassium balance. It was assessed by creating a double-transgenic mouse in which αENaC expression is deleted in the colonic crypt cells. Mice in which αENaC was selectively inactivated in colon using the *villin* promoter (El Marjou *et al.*, 2004) have been generated. Quantitative RT-PCR and protein expression analysis revealed that the knockout in distal colon is nearly complete. Following standard & low sodium diet, the mice show no difference in body weight or length of intestine. Plasma sodium and potassium electrolytes are in the normal range. Urine electrolytes show sodium retention under low sodium diet indicating compensatory mechanism from the kidney to avoid sodium loss. In contrary, these mice exhibit a highly significant decrease in amiloride-sensitive rectal potential difference that is maintained under standard and salt-deficient diets indicating that in colon, electrogenic sodium transport is mainly mediated by ENaC. This is also accompanied by a loss in cyclic variation of ENaC activity throughout the day. Using this gene targeting approach, we have observed that ENaC-mediated sodium reabsorption in colon is relevant for sodium homeostasis, but this loss can be compensated by kidney. Ongoing studies will address compensation of sodium reabsorption by the kidney.

Impact of different adiposity measures on the relation between serum uric acid and blood pressure in youth

[1]Lyngdoh T., [2]Viswanathan B., [3]Myers G., [4]Bochud M., [4]Bovet P.

Institut de Médecine Sociale et Préventive[1], Ministry of Health, Section of Noncommunicable diseases, Republic of Seychelles[2], University of Rochester Medical Center, NY, USA[3], Institut de Médecine Sociale et Préventive,CHUV[4]

BACKGROUND: Increasing evidence suggests that serum uric acid (SUA) concentration is independently associated with blood pressure (BP) in adults. We examined this association in young adults at an age where anti-hypertension treatment, co-morbidity or several other potential confounding factors are unlikely to occur.

METHODS: In 549 participants aged 19-20 years from a population-based cohort study (Seychelles Child Development Study), we measured BP, anthropometric variables including weight, height, waist circumference (WC) and fat mass (using bioimpedance), lifestyle behaviors through a questionnaire, and SUA and blood lipids.

RESULTS: Mean (SD) SUA was higher in males than females, respectively 0.33 (0.08) mmol/L and 0.24 (0.07) mmol/L. BMI was higher in females than males and BP was higher in males than females. Systolic and diastolic BP was significantly associated with SUA in males and in females. However, the magnitude of the linear regression coefficients relating BP and SUA was attenuated by up to 50% upon adjustment for waist circumference (WC) or body fat mass (BFM), while virtually unchanged upon adjustment for body mass index (BMI) or waist-to-hip ratio (WHR). The attenuating effect of WC or BFM was stronger in females than males. Further adjustment for alcohol intake or triglycerides did not alter the association between SUA and BP. In fully adjusted models, SUA remained associated with diastolic BP but not with systolic BP.

CONCLUSION: In young adults, the association between SUA and BP was largely dependent on waist circumference or fat mass, but not BMI or WHR, and only diastolic BP remained significantly associated with SUA upon full adjustment. These findings suggest a role of abdominal adiposity in the link between hyperuricemia and hypertension.

Effects of Dietary Protein and Branched Chain Amino Acids on Hepatic Steatosis in Mice

[1]Minehira Castelli K., [1]Theytaz F., [1]Sanno H., [1]Seyer P.

Department of Physiology[1]

Addition of dietary protein into high-fat diet decreases the incidence of hepatic steatosis in humans. The mechanism by which dietary protein reduces liver fat accumulation is unknown, however. To further understand this, we have been testing whether the protective effect of protein is due to increased BCAA content in the diet or not.

We fed mice with standard diet (C: fat 10 %, protein 20%), high-fat diet (HF: fat 45%, protein 20%), high-fat high-protein diet (HFHP: fat 45%, protein 40%), and high-fat high-BCAA diet (HF-BCAA: fat 45%, protein 23%, same BCAA content as HFHP) for 10 weeks.

We found that mice fed HF and HF-BCAA became obese/insulin resistant and developed severe hepatic steatosis, whereas HFHP diet protected mice from these metabolic derangements. We found that reduction in hepatic *de novo* lipogenesis in HFHP mice explained partly the protection. Further pair-feeding studies clearly demonstrated that dietary protein reduced liver fat via suppression of appetite. Unexpectedly, these effects were not observed in HF-BCAA groups, judged by monitoring food intake and the expression of neuropeptides in hypothalamus. In addition to the differential effects on appetite, these mice fed HF-BCAA presented highest *t*PAI-1 expression in the liver and the adipose tissue among other groups. These results suggest that the addition of BCAA to the HF diet renders mice prone to obesity and increases a risk of cardiovascular disease.

Our studies clarified that dietary protein reduced liver fat accumulation via reduction in hepatic *de novo* lipogenesis and appetite. Furthermore this was not due to the increased BCAA content in the diet.

Role of calcineurin/NFAT pathway in lymphatic vascular development

SABINE A.

Center of Pluridisciplinary Oncology - CHUV - UNIL

The formation of new blood and lymphatic vessels by (lymph)angiogenesis is the hallmark of many human cancers, and promotes tumor growth and metastasis. Signaling via vascular endothelial growth factors (VEGFs) and their receptor tyrosine kinases expressed on endothelial cells (VEGFRs) are essential for vascular growth and remodeling. VEGFR-2 and -3 are both implicated in (lymph)angiogenesis. The intracellular signaling pathways following VEGFR-2/3 activation on endothelial cells are not well studied in the in vivo context, although a wealth of in vitro studies have provided many important insights. In this study we focus on calcineurin/NFAT signaling pathway, which is activated by VEGF-A and VEGF-C in blood and lymphatic endothelial cells in vitro, and which we have recently shown to contribute to lymphatic development in vivo (ref.1). We have now developed several genetic mouse models, which allow tissue- and temporal-specific deletion of calcineurin to investigate requirements for calcineurin/NFAT signaling during different stages of embryonic development and in adults during tumor progression.

Reference:
1. Norrmén C., Ivanov K., Cheng J., Zangger N., Delorenzi M., Jaquet M., Miura N., Puolakkainen P., Horsley V., Hu J., Augustin H.G., Ylä-Herttuala S., Alitalo K., and Petrova T.V. (2009) FOXC2 controls formation and maturation of lymphatic collecting vessels through cooperation with NFATc1. J Cell Biol, 185 (3): 439-457.

Control of sodium and potassium transport by ENaC along the aldosterone sensitive distal nephron.

[1]Perrier R., [2]Koesters R., [1]Rossier B., [1]Hummler E.

Department of Pharmacology and Toxicoly, UNIL[1], Institure of Human Genetics, University of Heidelberg[2]

ENaC plays a critical role in sodium homeostasis as emphasized by gain-of-function mutations in patients suffering from Liddle's syndrome – a severe form of hypertension. Moreover, loss-of-function mutations are found in patients with pseudohypoaldosterism type 1 (PHA-1), which is a severe and life-threatening salt-wasting syndrome. To study ENaC function, constitutive knockout for each of the three subunits of ENaC has been developed. αENaC knockout mice display lung clearance failure, hyperkalemia and sodium loss, and β and γ ENaC knockout mice hyperkalemia and sodium loss. The aim of the present work is to study the comparative role of α and γENaC in control of Na^+ and K^+ transport in the aldosterone sensitive distal nephron.

To address this question, we crossed a double transgenic mouse (Pax8/LC1) which expresses the reverse tetracycline transactivator under the control of a Pax8 promoter (expressed along along the entire nephron) and Cre recombinase under the control of a tetracycline response element with the floxed Scnn1a or Scnn1g mouse.

After six days of doxycycline treatment, under normal salt diet, 4 week -old α and γENaC nephron-specific knockout mice kept loosing body weight, whereas wild type mice continued to gain weight. Both models develop life threatening hyperkalemia, whereas only αENaC nephron-specific knockout mice present a severe hyponatremia. This is associated with an increase in daily cumulative Na^+ loss in αENaC nephron-specific knockout mice, whereas γENaC nephron-specific knockout mice surprisingly develop a significant decreased cumulative urinary K^+ loss.

Contrary to nephron-specific *Scnn1a*-deficient, deletion of *Scnn1g* is not sufficient to alter Na^+ reabsorption, but surprisingly K^+ excretion is decreased. There is an unexpected dissociation between Na^+ and K^+ transport suggesting that ENaC mediated reabsorption is no longer coupled to ROMK mediated secretion.

PPARβ/δ involvement in the control of vascular permeability

Wawrzyniak M., Mottaz H, Michalik L

CIG Unil

Endothelial cells form a semi-permeable barrier that participates in exchange of plasma fluids, proteins and cells, and helps in maintaining the physiological function of organs as well as the circulatory homeostasis. Vascular permeability is increased in acute and chronic inflammation, cancer and wound healing. It is mediated by exposure to some vascular permeability increasing factors, such as vascular endothelial growth factor (VEGF).

The peroxisome proliferator-activated receptors (PPAR) belong to the nuclear hormone receptor (NHRs) family of ligand-activated transcription factors. Three isotypes, PPARα, PPARβ/δ and PPARγ have been identified. They are all expressed in endothelial cells (ECs), and recent data have shown that important mechanisms for vasculogenesis and angiogenesis, such as cell proliferation/differentiation, directional sensing/migration, and survival, involve PPARs. They were reported to modulate the expression of pro-angiogenic soluble factors, such as VEGF-A and may also participate in the regulation of the expression of VEGF receptors. What is more, they were shown to modulate the PKBα/Akt1 pathway (a pathway activated by most angiogenic factors). Furthermore, PPARβ/δ activates the Rho GTPases and actin dynamics, which are also involved in cell-cell junction dynamics.

Using organ culture models of rings of mouse aorta, culture of human dermal microvascular endothelial cells (HDMECs) and genetically modified mouse in vivo model, we decided to study the consequences of loss or gain in PPARβ/δ activity in endothelial cell functions. We wish to know what are the mechanisms underlying PPARβ/δ -dependent adult vessel permeability? As well as, if PPARs are pharmaceutical targets able to modulate vessel permeability?

So far, we have shown that the activation of PPARβ/δ accelerates EC migration in a monolayer scraping assay and promotes vessel sprouting in murine aorta explants. *In vivo*, we observed that dermal vessel acute permeability in response to VEGF-A stimulation is strongly impaired in PPARβ/δ -/- animals. Additionally, observation of the dermal vessel morphology showed a clear enlargement of the wild-type dermal vessels upon VEGF-A injection, whereas the vessels of the PPARβ/δ -/- animals showed almost no enlargement.

Based on the data obtained so far, we suggest that PPARβ/δ may act on intracellular signaling cascades in ECs, downstream the VEGF-A receptor. The project will be continued by addressing the mechanisms by which PPARβ/δ impact on vessel permeability in endothelial cells.

Detection and Functional Role of Sympathetic Angiotensinergic Neurotransmission in the Vasculature, Heart and Kidney

[1]Bohlender J., [2]Patil J., [1]Nussberger J., [1]Mazzolai L., [2]Imboden H.

Division of Angiology - CHUV[1], Institute of Neurobiology, University of Bern[2]

The vasculature and circulatory organs have a rich innervation by autonomic sympathetic fibers. Their efferent neurotrans-mission is by noradrenaline (NA) released together with neuropeptide co-transmitters such as neuropeptide Y (NPY) while afferent fibers release calcitonin-gene related peptide or substance P (CGRP, SP). Using a highly specific monoclonal antibody and an immunohisto-chemical staining technique with free-floating kryosections, we for the first time demonstrate the co-presence of angiotensin II (Ang-II) in autonomous efferent and afferent fibers innervating the vasculature, heart and kidney in rat, pig and human tissue samples. Tissue co-staining of Ang II with adrenergic markers tyroxine hydroxylase (TH) and dopamine-β-hydroxylase or with synaptophysin (SYN), a synaptic vesicular marker, identified (1) three subtypes of autonomic fibers depending on the presence or absence of these antigens and (2) differentiated efferent from afferent neurons. Ang-II co-localized with SYN in synaptic varicosities supporting Ang-II as a new neurotransmitter in sympathetic fibers. Ang-II fibers innervated distinct intrarenal targets corresponding to specfic subsets of neurons in the dorsal root and coeliac ganglia. There was no detectable ganglionic expression of renin mRNA but of angiotensinogen (AGT) and cathepsin D mRNA. AGT exspression co-localized with Ang II suggesting that ganglionic neurons operate a renin-free Ang-II generating system with its own regulation characteristics. Intra-renal microganglia similarly contained Ang-II positive neurons partially co-staining TH. Based on these results, a functional scheme for the angiotensinergic sympathetic innervation and its vascular and intrarenal targets is proposed. Abnormal angiotensinergic sympathetic neurotransmission may play an independent pathogenetic role in arterial dysfunction, hypertension, and cardiovascular target organ pathophysiology that has yet to be investigated comprehensively.

Zinc finger nucleases as tools for rapid engineering of knockout and knock in mice

[1]Ponce de Leon V., [1]Hummler E.

Department of Pharmacology and Toxicology[1]

Generating knockout and knock-in mice and rats is of crucial importance for the understanding of cardiovascular and metabolic disorders in humans.

Zinc fingers are peptides that are extremely common in all cells. They are transcription factors and therefore can bind specifically to DNA. By artificially combining three or four zinc fingers that each recognizes three base pairs, virtually any DNA sequence can be targeted. Zinc Finger Nucleases (ZFN) are made of a binding domain with three or four Zinc finger modules and a FokI nuclease domain that is activated upon dimerization. FokI generates double-strand DNA brakes (DSB) in the target sequence. DSBs activate endogenous DNA repair system. By providing a DNA "repair template", DSBs induce non-homologous end joining (NHEJ) of the targeted gene sequence. DSBs can stimulate recombination efficiency of several thousand folds. Without the "repair template", ZFN are used for direct gene targeting by homologous end-joining (HEJ).

Each Zinc finger module recognizes specifically three base pairs. However, the efficiency of the binding depends on external factors such as DNA folding state, and the tertiary structure of the whole protein. Therefore, it is important to generate ZFNs by creating zinc finger arrays of random sequences that are adjacent to the peptides that actually bind to the gene sequence. Quantitative and qualitative assays allow determining the binding efficiency of the array of ZFN so they can be selected for their binding capacity.

Blood Pressure and Renin-Angiotensin System Resetting in a New Transgenic Rat Model with High Plasma Val5-Angiotensinogen

[1]Bohlender J., [2]Bader M., [3]Ménard J., [4]Nussberger J.

Division of Angiology - CHUV[1], Max-Delbruck-Center for Molecular Medicine, Berlin, Germany[2], Université de Paris Descartes, Paris, France[3], Department of Angiology - CHUV[4]

Background Angiotensinogen (Ang-N) is the biosynthetic precursor of the pressor octapeptide angiotensin-II (Ang II). Increases in plasma Ang-N by genetic polymorphisms or exogenous stimuli like estrogen are associated with a blood pressure (BP) rise, salt sensitivity and cardiovascular risk. The pathophysiological links between high Ang-N, the resetting of the renin-angiotensin system, and BP still remain unclear.

Methods and Results A new transgenic rat (TGR) with targeted hepatic overexpression of native (rat) Ang-N was established to study the effects of high plasma Ang-N. The transgene harbored a mutation producing Val^5-Ang-II which was measured separately from native Ile^5-Ang-II in plasma and renal tissue by HPLC. Heterozygous male TGR and wild-type controls (CTR; n=6/group) were treated with lisinopril (0.35 mg/kg) for converting-enzyme (ACE) inhibition or vehicle. Male homozygous TGR (n=10) had high systolic BP (sBP, +26 mmHg), plasma Ang-N (~20-fold), renin activity (~2-fold), renin activity/concentration (~5-fold), total Ang-II (~2-fold, kidney 1.7-fold), and decreased concentrations of renin (-45%, kidney -85%) and Ile^5-Ang-I and II (-93%, -94% respectively) vs. CTR. Heterozygous TGR had increased plasma Ang-N (~10-fold) and sBP (+17 mmHg). Lisinopril decreased their sBP (-23 vs. -13 mmHg in CTR), kidney total Ang-II/I (~3-fold) and Ile^5-Ang-II (-70%). It increased kidney renin and Ile^5-Ang-I (≥3-fold). TGR kidney Ang-II remained higher, and renin lower vs. treated CTR documenting unequal effects

Conclusion High plasma Ang-N increases plasma and kidney Ang-II levels and amplifies the Ang-II response to changes in renal renin secretion showing increased sensitivity. This enzyme-kinetic amplification dominates the Ang-II mediated negative feed-back on renin secretion, induces a graded increase in sBP and decreases sensitivity to ACE inhibition.

Skeletal muscle mitochondrial content and electron transport chain activity in older adults at risk for type 2 diabetes: relationship to insulin sensitivity, metabolic flexibility and fatty acid oxidation

[1]Amati F., [2]Goodpaster B.

Department of Physiology-UNIL and EDM-CHUV[1], University of Pittsburgh[2]

Purpose: The extent to which skeletal muscle mitochondrial content and function contributes to metabolic dysfunction in obesity and aging is not clear. We hypothesized that lower mitochondrial content and electron transport chain (ETC) activity in human skeletal muscle are associated with reduced fatty acid oxidation and insulin resistance, a.k.a metabolic inflexibility in older overweight to obese subjects.

Methods: Fifteen older (60-75 years) obese sedentary subjects were compared to six lean physically active age-matched control subjects. Mitochondrial content (MC) was measured in muscle biopsies using Western blotting (ETC complexes) and HPLC(cardiolipin). ETC activity was determined by NADH-oxidase. Insulin sensitivity (IS) was measured with glucose clamps. Resting, insulin-stimulated and exercise-induced substrate oxidation was measured by indirect calorimetry. Metabolic flexibility was determined by ΔRQ from fasting to insulin-stimulated conditions.

Results: MC, ETC activity, IS, resting and exercise-induced fat oxidation were lower in Obese. ETC activity remained lower in Obese even after adjusting for MC (cardiolipin or ETC complexes). When all subjects were combined, MC was related to higher IS (R^2=0.36,P<0.01) and exercise-induced fat oxidation (R^2=0.80,P<0.01). ETC activity was associated with resting fat oxidation after an overnight fast (R^2=0.40,P<0.01), even after adjusting for MC. The protein content of all ETC complexes was associated with greater metabolic flexibility (R^2=0.13 to 0.25,all P<0.01).

Conclusion: Overweight to obese, physically inactive older adults have a reduced skeletal muscle mitochondria content, which is related to their insulin resistance and their metabolic inflexibility. Moreover, it appears that their lower fasting-induced fat oxidation is associated with a reduced ETC activity, even after accounting for muscle mitochondrial content.

ETUDE DE LA DOSE EFFECTIVE DELIVREE PAR LE CT A ROTATION LENTE DANS LA RECHERCHE D'EMBOLIE PULMONAIRE PAR SPECT-CT

[1]Cherbuin N., [1]Allenbach G., [2]Verdun F., [2]Baechler S., [1]BischofDelaloye A., [1]Boubaker A.

Service de médecine nucléaire - CHUV[1], Institut de radiophysique - CHUV[2]

Objectifs

Déterminer la contribution du CT "à rotation lente" dans la dose effective (DE) totale délivrée lors d'une scintigraphie pulmonaire ventilée/perfusée.

Matériels et méthodes

96 patients (40H/56F, 73±15 ans (19-98) ont bénéficié d'un SPECT-CT pulmonaire ventilé (V) et perfusé (Q) (GE « Infinia Hawkeye 4 », GE Healthcare, Milwaukee, USA). Pour (V) : inhalation d'aérosol technétié (Technegas®), préparé à partir de 1850 MBq de pertechnétate dans 0.5ml, suivie d'un SPECT. Pour (Q) : injection de 154±16 MBq (100-190) de Tc99m-MAA (Maasol®) suivie d'un SPECT-CT (axial, 140kV, 2.5mA, épaisseur 5mm). L'activité réelle inhalée est estimée à partir du rapport cps(Q)/cps(V), i.e. 53±31 MBq (4-138). Les DE sont calculées à partir des DLP indiqués par l'installation et des coefficients EUR 16262 pour le CT; de l'activité inhalée pour (V) et de l'activité injectée pour (Q), selon les coefficients ICRP 80 pour la scintigraphie.

Résultats

L'activité inhalée est très variable, difficilement prévisible et dépend du status et de la collaboration du patient.

Doses (mSv)	Moyenne	DS	Min	Max
Ventilation (V)	0.80	0.47	0.07	2.07
Perfusion (Q)	1.70	0.17	1.10	2.09
CT	2.72	0.27	1.94	3.31
Total	5.22	0.64	3.77	6.96

Conclusions

Dans le protocole utilisé, le CT "à rotation lente" double la DE totale délivrée lors d'une scintigraphie pulmonaire V/Q. Nous proposons de sélectionner les patients et de ne réaliser le CT que pour les résultats SPECT équivoques et/ou lorsque l'examen ventilé est ininterprétable.

Role of lipid droplets proteins in hepatic insulin resistance in mice and human

[1]Bouduban T., [2]Gual P., [1]Minehira K.

Département de Physiologie, UNIL[1], Equipe 8 complications hépatiques de l'obésité, Institut National de la Santé et de la Recherche Médicale, U895, Nice, France[2]

Obese and/or diabetic patients often concomitantly develop a hepatic steatosis (fatty liver), an abnormal fat accumulation in the liver. The hepatic steatosis frequently induces hepatic insulin resistance, a main cause of diabetic fasting hyperglycemia. However how exactly hepatic steatosis leads insulin resistance has not been clearly defined.

To study molecular mechanisms of insulin resistance in hepatic steatosis, we have been using a mouse model of hepatic steatosis dissociated from insulin resistance. Mice without a gene of microsomal triglyceride transfer protein ($Mttp^{\Delta/\Delta}$) in the liver develop a hepatic steatosis due to a defect of very low density lipoprotein secretion. We found that $Mttp^{\Delta/\Delta}$ mouse liver induced series of genes coding proteins existing on the surface of lipid droplets such as "Cell-death Inducing DFFA-like Effector C (*cidec*)", "Lipid Storage Droplet Protein 5 (*lsdp5*)" and "Bernardinelli-Seip Congenital Lipodystrophy 2 Homolog (*seipin*)". This is particularly interesting, since these genes are normally abundant in adipose tissue and rare function of these genes is known in the liver. In this study, we tested our hypothesis that lipid droplets proteins might protect the fatty liver against the insulin resistance.

We first studied whether these genes were involved in hepatic insulin resistance in Alfa Mouse Liver 12 (AML12) hepatocyte cell line. By downregulating *cidec* or *seipin* expression by siRNA technique, we found a defect in akt phosphorylation under insulin stimulation. It strongly suggests that the lack of lipid droplets proteins induces insulin resistance in mouse hepatocytes.

We next hypothesized that these genes were also involved in human fatty liver and insulin resistance. We analyzed their expression levels in liver biopsies from obese patients with diverse degrees of hepatic steatosis. We found that the expression of these genes was significantly increased in fatty liver. More interestingly, we found that diabetic patients significantly decreased the expression of *lsdp5* and *seipin* compared to the non-diabetic patients with the same degree of hepatic steatosis. Our results strongly argue that the lipid droplet proteins are tightly involved in human hepatic steatosis and play an important role in the development of insulin resistance.

Mapping genetic variants associated to beta-adrenergic responses in inbred mice

[1]Maurer F., [2]Peter B., [2]Hersch M., [3]Kang H., [3]Eskin E., [4]Beckmann J., [2]Bergmann S.

Service of Medical Genetics, CHUV[1], Department of Medical Genetics, UNIL and Swiss Institute of Bioinformatics[2], Department of Computer Science and Department of Human Genetics, UCLA[3], Service of Medical Genetics, CHUV and Department of Medical Genetics, UNIL[4]

The long-term goal of our research is to identify genetic variants associated with differential responses to β-adrenergic drugs. Previously, we characterized 27 cardiovascular-related traits in 23 inbred mouse strains. Mice were phenotyped either in control (ctr) condition, in response to chronic administration of a single dose of the β-blocker atenolol (ate), or under a low (iso 1) and a high (iso 10) dose of the β-agonist isoproterenol. To identify genetic segments underlying differences in trait values, we used Efficient Mixed Model Association (EMMA), which corrects for population structure and genetic relatedness in model organism association mapping. These analyses were performed on a genome-wide basis, using non-transformed trait values recorded in ca 1000 individuals and 100'152 informative SNPs. At first, individual phenotypes were analysed separately for each drug condition. The significance of the associations was evaluated with an F-test and thresholds of significance were set using the Benjamini-Hochberg correction for multiple hypotheses testing. Altogether, these analyses retrieved 6325 significant associations, 1450 of which mapped at SNPs with minor allele frequencies above 0.1 in the mouse cohort. Scans for body weight gain (iso10) and weight of the cardiac atria (ate, ctr) produced the strongest hits and the resulting QTLs were supported by several significant neighbouring SNPs. Signals above genome-wide significance were also obtained with the majority of the other traits, yet often as single, moderately significant hits. Together with the reduced number of candidate loci mapped in each analysis, these results are likely reflecting high trait complexity and limited analytical power. We then show that a data-driven pooling of related phenotypes can uncover additional significant associations, which could not be detected with a single phenotype. This suggests a new way for increasing the analytical power of a dataset of related traits.

Is organ failure and critical care of older brain dead deceased donors more challenging?

[1]Reichmuth P., [2]Guessous I., [3]Eggimann P., [3]Delodder F., [4]Pilon N., [3]REVELLY J.-P.

Ecole de Médecine[1], Community prevention unit, IUMSP, Lausanne [2], Service de Médecine Intensive Adulte, CHUV [3], Centre de Transplantation d'organes, CHUV[4]

Introduction

Many organs from increasingly older brain-dead deceased donors can be successfully transplanted. We tested the hypothesis that older patients are more vulnerable to organ dysfunction related to brain death (BD), and require more complex critical care management.

Methods

We performed a retrospective analysis of the ICU clinical information system of 80 consecutive patients admitted to our intensive care unit (ICU) between 2002 and 2009 and evolving toward BD. The following variables were determined for each patients: time to BD, diagnosis, mean arterial pressure (MAP), heart rate (HR), use of norepinephrine (NE), mean dose of NE, use of vasopressin, mean dose of vasopressin, use of vasopressin, and PaO2. In addition, status of effective donors and the organs transplanted were analysed. Patients were stratified in quartiles according to age. Comparisons between all pairs of groups were performed by Tukey-Kramer HSD and chi-square for continuous and categorical variables respectively. $p < 0.05$ was considered significant.

Results.

The quartiles (Q1 to 4) of age had the following ranges: (Q1: 16.2-36.4; Q2: 39.5-52.9; Q3: 53.0-63.4 and Q4: 63.6-86.0 years). Traumatic brain injury was more frequent in Q1, while intra-cerebral hemorrhage and post-anoxic encephalopathy were more frequent in Q4. Diabetes was more frequent in Q3 and Q4, and hypertension in Q2 to Q4. Heart rate was higher in Q1 throughout ICU stay. Mean dose of norepinephrine was lower in Q3 than in Q1 during the phase immediately preceding BD. Mean arterial pressure, doses of norepinephrine during other phases, gas exchange, ventilator settings, creatinine and time to brain death were not different between quartiles. Less hearts were donated in Q4, while the number of kidneys, livers and lungs donated and transplanted were not different between quartiles.

Conclusions

Beside minor physiological differences, and surprisingly lower mean norepinephrine doses, management of older patients suffering from brain-death was not different to that of younger patients. We observed neither a greater severity of illness, nor more complex ICU management in older patients developing BD. Old patients can be considered as potentially useful brain dead deceased donors.

The Mouse Metabolic Facility (MEF) from Cardiomet

[1]Preitner F., [1]Metref S., [1]DaCosta A., [1]Carrard M., [1]Thorens B.

Center for Integrative Genomics, UniL[1]

The MEF proposes a vast repertoire of metabolic analyses to assess the phenotype of murine models of obesity and diabetes, as well as to test the effectiveness of new therapeutic pharmacological agents. For this purpose, the MEF
• Provides services to researchers from Academia and Industry,
• Ensures the development of new investigation techniques,
• Teaches some techniques,
• Supports internal metabolic research at the Center for Integrative Genomics, thus ensuring a constant updating of equipment and expertise.

The MEF, first facility of its kind in Switzerland since 2006, offers a comprehensive and constantly evolving panel of analyses in areas of Energy metabolism, Glucose homeostasis, and the relationship between brain and periphery. Excerpts of services provided by the MEF include:
• The non-invasive and accurate analysis of body composition by MRS
• The analysis of metabolism by indirect calorimetry,
• The analysis of metabolism during exercise (treadmill) by indirect calorimetry,
• The measurement of energy content in biological samples by bomb calorimetry,
• The real-time, online measurement of food intake (cumulative and patterns),
• The real-time, telemetric measurement of body temperature and locomotor activity,
• The assessment of glucose homeostasis by insulinemic (eu-, hyper-, hypoglycemic) clamps
• Intracerebral (ICV/IHP) injections of metabolites / drugs / peptides / viruses.
• Blood chemistry (Hitachi robot) and multiplex assays of cytokines / hormones (Luminex).

The MEF, which has already been very well received by academic researchers and industrial customers alike, strives at provide customized, affordable services to the broader scientific community in a constant search for excellence and standardization.

Contacts:
Director: Prof.. Bernard Thorens, Ph.D. Bernard.Thorens@unil.ch
Supervisor: Frédéric Preitner, Ph.D. Frederic.Preitner@unil.ch
Blood analyses: Marianne Carrard Marianne.Carrard@unil.ch

Website:
http://www.cardiomet.ch/en/cmet_home/cardiomet-chercheurs/cardiomet-chercheurs-plateforme_
metabolique.htmhttp://www.cardiomet.ch/en/cmet_home/cmet-cardiomet-centre_for_cardiovascul
ar_and_metabolic_diseases-researchers/cmet-cardiomet-centre_for_cardiovascular_and_metabol
ic_diseases-researchers-metablolic_evaluation_facility-mef.htm

Perinatal nitric oxide therapy prevents adult pulmonary vascular dysfunction secondary to a perinatal exposure to hypoxia

[1]Peyter A.-C., [1]Diaceri G., [1]Marino M., [1]Muehlethaler V., [1]Tolsa J.-F.

Neonatal Research Laboratory-Department of Pediatrics-CHUV[1]

Adverse events in utero are associated with the occurrence of chronic diseases in adulthood, like cardiovascular diseases and non-insulin-dependent diabetes mellitus. In particular, humans and animals born in hypoxic conditions, or presenting neonatal pulmonary hypertension, show later in life an exaggerated pulmonary hypertensive response following a re-exposure to hypoxia.

We previously demonstrated in mice that a transient hypoxic insult in the perinatal period resulted in altered regulation of pulmonary vascular tone in adulthood. Adults born in hypoxia displayed higher right ventricular pressure compared to controls, suggesting a higher resistance state in the pulmonary circulation. Moreover, perinatal hypoxia increased the sensitivity of adult pulmonary circulation to acute hypoxia and decreased the relaxation of pulmonary arteries to the endothelium-dependent agent acetylcholine. This pulmonary vascular dysfunction was associated with permanent alterations in muscarinic receptors and their effectors, in particular phosphodiesterases, and with a marked decrease in endothelial nitric oxide synthase (eNOS) protein content.

In humans presenting neonatal pulmonary hypertension, the therapy of choice is inhaled nitric oxide (iNO). Long-term effects of neonatal iNO on adult lung vascular reactivity have not yet been investigated.

We investigated whether iNO administered simultaneously to perinatal hypoxia could have potential beneficial effects on the adult pulmonary circulation.

Pregnant mice were placed in hypoxia (13% O_2) with simultaneous administration of iNO (10 ppm) 5 days before delivery and left in these conditions with their litter for 5 days after birth. Pups were then raised in normoxia (21% O_2) until adulthood.

Acetylcholine-induced relaxation is completely restored in isolated pulmonary arteries of adults treated with iNO during perinatal hypoxia compared to mice without iNO therapy. Similarly, eNOS protein deficiency is completely reversed in pulmonary arteries of adults exposed to perinatal iNO and hypoxia compared to hypoxia alone. Therefore, **perinatal iNO therapy seems to prevent adult pulmonary vascular dysfunction following perinatal hypoxia**.

Human umbilical vessels relaxation is impaired in newborns with intrauterine growth restriction

[1]Peyter A.-C., [1]Diaceri G., [1]Muehlethaler V., [2]Vial Y., [1]Marino M., [1]Tolsa J.-F.

Neonatal Research Laboratory-Department of Pediatrics-CHUV[1], Department of Gynecology and Obstetrics-CHUV[2]

Numerous epidemiological studies have linked adverse events occurring in utero or around birth to the occurrence of chronic diseases in adulthood. In particular, limitation of nutrients or oxygen supply to the fetus, resulting in a small birthweight, is linked to an increased risk to develop cardiovascular diseases in adulthood.

Fetal growth restriction affects approximately 8% of all pregnancies and is associated with considerable perinatal mortality and morbidity. The mechanisms implicated in the development of intrauterine growth retardation (IUGR) are not yet elucidated, even if some risk factors from maternal origin have been identified, like malnutrition, maternal arterial hypertension and tobacco consuming.

We previously demonstrated in a murine model that a transient exposure to hypoxia during a critical period of development of the lung vasculature resulted in a definitive imprint leading to altered regulation of pulmonary vascular tone in adulthood. We postulate that a reduced oxygen supply in utero could influence other vascular beds, like the umbilical circulation, which present some similarities with the pulmonary circulation.

We therefore postulate that reduced delivery of oxygen and/or nutrients to the fetus in case of placental insufficiency could be in relation with alterations in regulating pathways of the umbilical circulation, contributing further to impairment of materno-fetal exchanges and therefore to the development of IUGR.

We investigated potential modifications induced in the regulation of umbilical vessels tone in case of placental insufficiency, in order to identify potential novel therapeutic strategies to limit the development of IUGR.

Umbilical cords were harvested just after birth. The vasoreactivity of umbilical vessels was tested in organ chambers: relaxation induced by the nitric oxide donor DEA/NO was investigated in vessel rings preconstricted with serotonin (10^{-5} M) or the thromboxan A2 analog U46619 (10^{-6} M).

Preliminary results show that NO-induced relaxation is reduced in umbilical vessels from newborns with IUGR.

Phosphodiesterase-5 inhibition Sildenafil prevents the development of hypoxia-induced apoptosis and hypertrophy in the heart and lungs

[1]Milano G., [1]Rochemont V., [2]Bianciardi P., [2]Samaja M., [1]vonSegesser L.

Department of Cardiovascular Surgery-CHUV[1], University of Milan, Italy[2]

Background: We have recently discovered that daily reoxyenation during chronic hypoxia (CH) markedly improved recovery of the ventricular performance, attenuated the degree of apoptosis and right ventricle pressure without appreciable differences in myocardial hypertrophy. Unfortunately, the daily reoxygenation does not apply. Here, we tested the hypothesis that Sildenafil administration reverts the negative effects led by CH in the heart and lung.

Methods: Adult male Sprague-Dawley rats were exposed to CH (10% O2) with no treatment, or with sildenafil administration (1.4 mg/kg/day, i.p.)for 2 weeks. Normoxic rats (N) breathing room air served as control. Hearts and lung were either subjected to or freeze-clamp for biochemical analyses or fixed with formalin for histological analyses. With a catheter inserted in the right ventricle and in the carotid artery we measured the right and left ventricle pressures, respectively. Apoptosis was assessed using the TUNEL techinique. Data are expressed as mean± SEM.

Results: The RV systolic pressure was elevated in CH (P<0.001). Administration of sildenafil reduced RV systolic pressure (P<0.001). The plasma level of NOx, an index of NO production, increased markedly during hypoxia from 4.5±1.0 μmol/L to 8.7±0.9 μmol/L in CH (P<0.001). *In vivo* administration of sildenafil further increased the NOx level to 13.3±1.6 μmol/L (P<0.05). Thus, whereas hypoxia increased NO production, sildenafil enabled further increase of this parameter. Both RV/LV+S ratio, an index of right hypertrophy, and lung /body weight, an index of pulmonary edema, were increased in CH with respect to normoxic hearts (P<0.001), whereas the treatment with sildenafil attenuated the increase of these ratios (P<0.05). CH induced a ~2 fold increase in TUNEL-positive apoptotic cells compared to normoxia (P<0.001) both in heart and lung tissues. Sildenafil attenuated such increase (P<0.001). For the Western blot analysis revealed a significant increase in the phosphorylation status of extracellular signal regulated kinase ½ (ERK1/2), phosphatidylinositol-3-kinase-protein kinase B (Akt) and endothelial NOS with Sildenafil versus Normoxia in the heart. In contrast in the lung Sildenafil induced an increase in phosphorylation status of ERK1/2 only and unchanged the phosphorylation of Akt and eNOS.

Conclusion: A marked decline in right ventricle hypertrophy was observed with Sildenafil, which paralleled a reduction in pulmonary edema. Sildenafil administration reverts the negative effects led by CH in the heart possibly through a nitric oxide-dependent and survival kinases pathways (Akt and ERK1/2). In contrast the beneficial effects induced by Sildenafil in the lung could be due to activation of ERK1/2 signaling only.

St3gal6, a new regulator of adipose tissue development.

[1]Sambeat A., [2]Preitner M., [2]Thorens B.

CIG, Université de Lausannne[1], CIG, Université de Lausanne[2]

In order to better understand the molecular events leading to obesity, we are interested in the biology of adipocyte, the major component of adipose tissue and particularly in adipogenesis, the process by which new mature adipocytes are created.

The aim of the initial study was to identify new genes involved in adipose tissue development and to place them into the known adipogenic network. We started from a microarray analysis comparing lean and obese mice to select genes whose expression in visceral and subcutaneous white adipose tissue is correlated with increasing body weight. In the list we obtained, we focus our attention on one gene encoding for an enzyme, the *β-galactosidase α2,3-sialyltransferase 6* (*St3gal6*), involved in sialylation, a post-translational protein modification. As the role of St3gal6 is to add a sialic acid to the glycosylated chain of proteins or lipids, we hypothesized that these changes in protein structure could have an effect on intracellular signaling or on adipocyte interactions and matrix remodeling occurring during differentiation.

First, we had showed that St3gal6 is expressed at the same level in white and brown adipose tissues. Its expression is linked to adipose tissue expansion as it is increased during differentiation. Moreover, St3gal6 belongs to a family of 20 enzymes, so we assessed the level of expression of these others members in mouse adipose tissue. It appeared that St3gal6 is the sialyltransferase the most highly expressed in white and brown adipose tissue and then it suggests a potential role in adipose tissue development.

To address the issue of the role of St3gal6 in adipocyte differentiation, first we downregulated the gene expression *in vitro* in 2 preadipocyte models that can be induced to differentiate (3T3-L1 and 3T3-F442A cells). We found that the downregulation of St3gal6 by shRNA strategy decreases adipocyte differentiation. We also assessed that the level of expression of others close members of the sialyltransferase family is not affected by the knockdown of St3gal6. So, a specific knockdown of St3gal6 inhibits adipocyte differentiation *in vitro.*

To go further, we are overexpressing in preadipocyte models the wild type form of St3gal6 and also mutated forms resistant to shRNA to check the specificity of the knockdown system. These mutants were generated by site-directed mutagenesis on cDNA sequences targetted by each shRNA. The aim is to prevent gene silencing mediated by shRNA and then to rescue the inhibitory effect by co-infecting cells with retrovirus recombined with shRNA and with the corresponding mutated cDNA. This rescue will be checked at the mRNA level but also at the protein level using a tagged form of the protein. And then, once the silencing specificity confirmed, we will observe the effect of overexpression and rescue on adipocyte differentiation by detecting lipid droplets and measuring adipogenic markers expression.

We also plan to study St3gal6 expression in white and brown adipose tissue of mice under high fat diet to reinforce the link between St3gal6 increase and adipose tissue expansion.

Investigation of Jagged1-mediated signaling pathways

[1]Metrich M., [1]Nemir M., [1]Pedrazzini T.

Experimental cardiology unit - Unil[1]

The Notch pathway is a cell-to-cell communication system between two adjacent cells. One cell expresses Notch receptors (signal-receiving cell) and one cell expresses membrane-bound Notch-receptor ligands (signal-sending cell). Notch signaling is involved in embryonic development and adult tissue renewal. The Notch1 receptor and its ligand Jagged1 (Jag1) control also the adaptive response of the heart to stress. However, the mechanism by which Notch1 regulates cardiac remodeling is unknown. In signal-receiving cells, activation of the Notch receptor induces the cleavage of Notch intracellular domain (NICD), which enters the nucleus and upregulates target gene expression, in particular of its prototypical target genes: Hes1, Hey1 and Hey2. This is thought to represent the canonical Notch pathway. However, it recently appears that a Jag1 intracellular domain (JICD) fragment is also generated upon receptor-ligand interaction, raising the possibility that Jag1-mediated signaling could be activated in signal-sending cells.

In order to identify Jag1 target genes, we generated different clones of ST2 cells stably overexpressing Jag1. Based on Hes and Hey gene expression, Notch signaling was considered either highly or minimally activated in these various clones, suggesting that some Notch-independent signaling occurs in these cells. Affymetrix microarray analyses were then performed, focusing on commonly modulated, and therefore possibly Notch-independent, genes. In these cells, Jag1 decreases the expression of cytokines and cytokine receptors such as IL-6, LIF, Toll-like receptor. Pathways activated by these factors, including NFkB-, Jak/STAT3- or TLR/IRAK4 pathways were also downregulated. Converserly, molecules involved in the regulation of cell growth and proliferation such as Cyclin D1, E2F, Elk1 were up-regulated as well as the TGFβ/Smad and the Wnt/TCF-LEF pathways. Genes involved in the regulation of the actin skeleton were also up-regulated.

In conclusion, these preliminary results suggest that Jag1 could regulate signaling pathways involved in inflammation, cellular growth and cell morphology. Given the importance of these processes during cardiac remodeling that follows cardiac injury or heart stress, ongoing experiments investigate in vitro and in vivo the relevance of these findings in the adult heart and the cardiac response to stress.

The Cardiovascular Assessment Facility at the University of Lausanne

[1]Sarre A., [1]Berthonneche C., [2]Pedrazzini T.

CAF-EMIF - CHUV[1], Dpt médecine - CHUV[2]

The number of rodent genetic models of human diseases has increased dramatically over the past years. Studying the complex cardiovascular phenotypes in these models requires standardized state-of-the-art techniques, and often calls for the development of new methods to investigate the cardiovascular system.

The Cardiovascular Assessment Facility (CAF) is a core facility of the University of Lausanne, which was recently established to offer service for researchers in the cardiovascular field. The facility aims at providing sophisticated techniques to the scientific community for the physiological assessment of the cardiovascular system in rodents. Specifically, the CAF provides investigators with the latest equipment for cardiovascular imaging, in particular a high-resolution ultrasound system allowing determination of cardiac performance and dimensions. The CAF is also equipped for the measurement of blood pressure and heart rate, and for monitoring ECG. In addition, the CAF offers a microsurgery service for producing pathophysiological models (transaortic constriction, myocardial infarction, renovascular hypertension etc.). Scientific support is provided for the design of experimental protocols as well as for the development of new techniques for the investigation of the cardiovascular system.

Services:

ECHOGRAPHY (VEVO770, VISUALSONICS): Left ventricular function and dimensions; Doppler tracing; Assessment of organ perfusion; abdominal echography; following of growth of tumor.

ELECTROCARDIOGRAPHY (EMKA): Detailed analysis of ECG complexes; Arrhythmias

BLOOD PRESSURE AND HEART RATE MEASUREMENTS (VISITECH, NOTOCORD & DSI): Noninvasive method by Tail-cuff recordings; Invasive method by direct arterial measurements, Long term measurement by telemetry.

PATHOPHYSIOLOGICAL MODELS: Myocardial infarction; Transaortic constriction (pressure overload model); Goldblatt renovascular hypertension models (1K1C; 2K1C); Carotid balloon injury.

MICROSURGICAL SERVICES: Vascular catheterization; implantation of osmotic minipump; Myocardial cell injection; etc.

Interventional cardiology: the influence of the X-ray unit settings to radiation dose

[1]Samara E.-T., [2]Staufer J.-C., [1]Verdun F.

Institute of radiation physics - CHUV[1], Department of cardiology - CHUV[2]

As the number of interventional procedures is increasing, more effort should be given to the patient radiation protection. The technology of X-ray units has improved with the introduction of the flat-panel detectors (FPD) and their ability for dose reduction. However, in bibliography it is not clear how FPDs influence patient dose. The aim of this study was to examine the differences between installations with FPDs. Three radiological units (A, B and C) were characterised with respect to entrance dose rate. Units B and C were constructed by the same company. For policy reasons, the manufacturer names are not communicated. Four PMMA phantoms with different thickness (5 - 20 cm, with a step of 5 cm) were employed. Dose rate was measured by Radcal dosimeter connected to an 11 cm^3 ion chamber (Monrovia, USA). Source-to-skin distance was set at 75 cm. The field size was 16 cm for unit A and 15 cm for units B and C at the level of the detector. Dose rate was measured for fluoroscopy (15 and 30 images/sec) and cine mode (15 images/ sec). Dose rates for the low-dose protocol (fluoroscopy mode) were found to differ 4 to 5 times between units of different manufacturers. Interestingly, differences up to 12% were estimated for units B and C. Dose rate for "paediatric" mode was found slightly lower than that of "adult". It is essential to characterize the X-ray unit in terms of image quality and radiation dose. Further optimization is required for the "paediatric" mode as children are more radiation sensitive than adults.

An iterative reconstruction method for pediatric cardiac CT examinations

[1]Miéville F., [2]Gudinchet F., [1]Verdun F.

Institute of Radiation Physics - CHUV[1], Department of Radiology - CHUV[2]

Purpose: To evaluate the benefits of the adaptive statistical iterative reconstruction (ASIR) [1] method on the diagnostic image quality of pediatric cardiac CT examinations and radiation dose reduction.

Materials and Methods: Four pediatric radiologists evaluated ten low-dose pediatric cardiac examinations (80 kVp – $CTDI_{vol}$ (4.8-7.9 mGy) – DLP (37.1-178.9 mGy·cm)). The average age of the cohort studied was 2.6 years (1 day-7 years). Acquisitions were performed on a 64-MDCT scanner. All images were reconstructed at various ASIR percentages (0%-100%). For each examination, radiologists scored 19 anatomical structures using the relative visual grading analysis method. To estimate the potential for dose reduction, acquisitions were also performed on a Catphan phantom and a pediatric phantom.

Results: The best image quality for all clinical images was obtained with ASIR 20% and 40% whereas above ASIR 50%, image quality significantly decreased. With ASIR 100%, a strong noise-free appearance of the structures reduced image conspicuity. A potential for dose reduction of about 36% is predicted for a 2-3 year-old-child when using an ASIR 40% rather than the standard filtered back projection (FBP) method.

Conclusion: A mixture of 20% to 40% of ASIR slightly improved the conspicuity of various pediatric cardiac structures in newborns and children with respect to conventional reconstruction (FBP) alone. This result is in good agreement with clinical studies performed in adults [2, 3].

References

[1] J.-B Thibault, K. D. Sauer, C. A. Bouman, and J. Hsieh, "A three-dimensional statistical approach to improved image quality for multislice helical CT," Med. Phys., Vol. 34, No. 11, pp. 4526-4544, 2007.

[2] J. Leipsic, T. M. LaBounty, B. Heilbron, J. K. Min, G. B. J. Mancini, F. Y. Lin, C. Taylor, A. Dunning, and J. P. Earls, "Adaptive Statistical Iterative Reconstruction: Assessment of Image Noise and Image Quality in Coronary CT Angiography" AJR, Vol. 195, No. 3, pp. 649-654, 2010.

Differential miRNAs and target gene expression in embryonic stem cells lacking the Notch1 receptor

Pezzuto I.

Department of Medicine-Experimental Cardiology Unit-CHUV

Cardiomyocytes derived from differentiated embryonic stem (ES) cells represent an attractive source of cells for cell-replacement therapies in cardiac disease. However, cardiogenic differentiation of ES cells requires a complete understanding of the complex molecular mechanisms controlling the differentiation process. We demonstrated that differentiation of ES cells into cardiomyocytes is favored by inactivation of the Notch1 receptor. In addition some components of the Notch pathway in ES cells are under control of miRNAs, which, therefore, play an important role in cardiogenesis. So, we aim to investigate whether the increased cardiogenic potential in ES cells lacking Notch1 could rely on the expression of particular miRNAs and the modulation of their target genes. Alternatively, Notch1 could directly induce the modulation of particular target genes independently of miRNAs. As a first approach, we use microarray analysis to identify modulated miRNAs in wild-type and Notch1-deleted ES cells. In parallel, we determined the transcriptome in both cell lines. We found approximately 20 miRNAs, which were differently expressed in Notch1-deleted ES cells as compared to wild-type ES cells. Moreover, 100 genes, predicted to be targets of the identified miRNAs using computer assignment, were also modulated in the Notch1-deleted ES cells. We confirmed the differential expression of some target genes by quantitative methods. Together, these data demonstrate that Notch1 deletion induces specific miRNAs and gene expression patterns that could regulate the commitment of ES cells toward the cardiac lineage. Ongoing experiments evaluate the importance of these genes in the mesodermal and cardiogenic commitment of ES cells. Furthermore, we will also determine whether controlled modulation of these genes can be used to force ES cell to adopt a cardiogenic commitment.

Synaptic-like microvesicle exocytosis in pancreatic β-cells exposed to glucose and other secretagogues

[1]Bergeron A., [1]Bezzi P., [1]Regazzi R.

DBCM - University of Lausanne[1]

Background/Introduction:

Pancreatic β-cells located in the islets of Langerhans secrete insulin but also other signaling molecules including several neurotransmitters. Part of these molecules is stored in insulin-containing large dense-core vesicles. However, others are located in distinct organelles with a diameter of 50-90 nm that closely resemble neuronal secretory vesicles called synaptic-like microvesicles (SLMV). The precise content of β-cell SLMVs is still unclear but they are known to store at least two major inhibitory neurotransmitters, glycine and GABA. The physiological role of these neurotransmitters in the islets is only beginning to unfold but GABA has already been shown to inhibit glucagon secretion from pancreatic α-cells and to display autocrine effects on the secretory activity and proliferation of β-cells, suggesting an important contribution in the control of pancreatic endocrine functions.

Methods:

We developed a life imaging technique to selectively monitor SLMV exocytosis in β-cells. Our approach is based on the observation that in β-cells the integral membrane protein Synaptophysin is specifically targeted to SLMVs. Our strategy consists in transfecting the cells with a fluorescent pH sensitive Synaptophysin chimera and to analyze them by Total Internal Reflection Fluorescence Microscopy (TIRFM). The pH sensitive moiety of the Synaptophysin construct is placed in the interior of the synaptic-like vesicle and undergoes a sharp increase in fluorescence when the vesicle fuses with the plasma membrane. This allows a direct detection of exocytosis and retrieval of single SLMV.

Results:

Using our life imaging approach, we could show that SLMV exocytosis is triggered by glucose and other secretagogues with kinetics comparable to those observed for insulin-containing granules. At present, the molecular mechanisms underlying SLMV release are investigated in detail using various tools including neurotoxins and siRNAs directed against potential components of the exocytotic machinery.

Conclusion:

The life imaging approach developed in our laboratory will permit to obtain new precious information about the mechanisms regulating exocytosis of SLMVs under normal and physiopathological conditions. This would help defining the role of these organelles in islet physiology and to pinpoint their possible involvement in diabetes mellitus.

Involvement of the RasGAP-derived fragment N in the resistance of pancreatic beta cells towards apoptosis.

[1]Jaccard E., [2]Walicki J., Yan J.-Y., [3]Dubuis G., [3]Widmann C.

Departement of Physiology[1], UNIGE[2], Departement of Physiology - UNIL[3]

Our laboratory has previously established *in vitro* that a caspase-generated RasGAP N-terminal moiety, called fragment N, potently protects cells, including insulinomas, from apoptotic stress by activating the Ras-PI3K-Akt pathway. We aimed to determine whether fragment N can increase the resistance of pancreatic beta cells in a physiological setting and conversely if its absence renders them more sensitive to pro-diabetogenic stimuli.

Two mouse lines have been generated, the first one bearing the rat insulin promoter followed by the cDNA encoding fragment N, called RIP-N and the second one bearing a point mutation in the caspase recognition site on position 455 on RasGAP and that is unable to generate fragment N, called D455A KI. The histology, functionality, and resistance to stress of RIP-N and D455A KI islets were then assessed.

Pancreatic beta cells of RIP-N mice express fragment N, activate Akt and block NFκB activity without affecting islet cell proliferation or the morphology and cellular composition of islets. Intraperitoneal glucose tolerance tests revealed that RIP-N mice control their glycemia similarly as wild-type mice throughout their lifespan. Moreover, islets isolated from RIP-N mice showed normal glucose-induced insulin secretory capacities. They however displayed increased resistance to apoptosis induced by a series of stresses including inflammatory cytokines, fatty acids, and hyperglycemia. RIP-N mice were also protected from multiple low-dose streptozotocin injection-induced diabetes and this was associated with reduced *in vivo* beta cell apoptosis. In contrast, mice that cannot generate fragment N were more sensitive to streptozotocin injection-induced diabetes, indicating that RasGAP cleavage is a physiological mean of protecting beta cells.

We are now currently investigating whether fragment N can decrease *in vivo* beta cell apoptosis consecutive to high-fat diet feeding.

In conclusion, fragment N efficiently increases the overall resistance of beta cells to noxious stimuli without interfering with the physiological functions of the cells. Fragment N and the pathway it regulates represent therefore a potential target for the development of anti-diabetic tools.

Cardiomyocyte protection mediated by RasGAP-derived Fragment N

KHALIL H.

Department of Physiology - Unil

Heart failure is defined as a deficiency in the capability of the heart to adequately pump blood in response to systemic demands. Heart failure is induced by a number of common disease stimuli, including: longstanding hypertension; myocardial infarction and oxidative stress. The irreversible end point in heart failure is the loss of cardiomyocytes by apoptosis. Doxorubicin (Dox) is an anthracycline antibiotic that has been used for the treatment of various types of cancer; doxorubicin induces cardiotoxicity. Resent studies suggest that apoptosis plays an important role in Dox-induced cardiotoxicity, which is at least in part mediated by the generation of peroxynitrite (PN). PN a reaction product between nitric oxide and superoxide is considered as an oxidant and nitrating mediator formed in various pathological situations. The myocardium undergoes hypertropy (hypertrophic growth in size without myocyte proliferation) as a compensatory mechanism in order to improve the contractile function. Increasing the survival potential of cadiomyocytes would be beneficial during episodes of myocardial hypertrophy which ends with loss of function. We have determined that the N-terminal fragment of RasGAP (fragment N) can efficiently protect a variety of cell types against many different stresses. In the present work we show that the anti-apoptotic properties of fragment N protect primary cardiomyocytes from cell death induced by peroxynitrite-dependent oxidative stress. In addition, we investigate the heart activity in an *in vivo* mouse model where a mutation renders RasGAP caspase resistant (D455A KI mice); these KI mice are no longer able to generate fragment N. Heart parameters in two different experimental models were studied. In the first model, pressure overload through Trans aortic constriction (TAC), which induces stress leading to hypertrophy, resembles longstanding hypertension over the left ventricle. Heart parameters were measured at 2, 4 and 6 weeks post TAC by echocardiography. In the second model mice were injected with a high dose of doxorubicin, which induces cardiotoxicity and cardiomyocyte apoptosis, Heart parameters were measured 5 days post doxorubicin injection by Millar catheter. Our results show that RasGAP cleavage and fragment N generation play a role in preserving the contractile function of the heart upon stress. D455A KI mice TAC-stressed showed an increased expression of the hypertrophy gene markers, a marked reduction in fractional shortening (%FS) and ejection fraction (%EF), in comparison to their wild type TAC-subjected controls. In the same context, doxorubicin induced left ventricular dilation (increase in both end-diastolic and end-systolic volume) and reduced left ventricular end-systolic pressure, which tended to be more marked in the D455A KI mice. Interestingly the slope of the end-systolic pressure volume relationship, or arterial elastance (a load-independent index of contractility) was significantly reduced following doxorubicin, this reduction was significantly more pronounced in the KI animals.

Cardiac-specific overexpression of the Notch ligand Jagged1 reduces cardiac hypertrophy and fibrosis in response to hemodynamic stress

M.Nemir[1], M.Metrich[1], I. Plaisance[1], M. Lepore[1], S. Cruchet[1], C. Berthonneche[2], A. Sarre[2], and T. Pedrazzini[1, 2].

[1]Experimental Cardiology Unit, Department of Medicine, and [2]Cardiovascular Assessment Facility, University of Lausanne Medical School. Lausanne, Switzerland.

Heart failure, a condition in which heart does not provide sufficient supply of oxygenated blood, constitutes a major health issue in the world. It is the result of reduced contractile capacity, after a major loss of cardiomyocytes caused by chronic or acute myocardial injury. In the mammalian heart, the dying myocytes are replaced by fibrosis, and the surviving ones become hypertrophic. These two features, cardiac hypertrophy and fibrosis, are major hallmarks of heart failure. We have previously shown that the Notch pathway, which is essential for development of the cardiovascular system, is activated in the stressed adult heart, and that its inhibition exacerbates heart failure. The Notch pathway is mediated by transmembrane receptors and ligands, the interaction of which leads to the proteolytic release of the receptor intracellular domain. The latter translocates to the nucleus where it activates expression of specific target genes. To further investigate the role of this pathway in cardiac adaptation to stress, we generated transgenic mice overexpressing the ligand Jagged1 in cardiomyocytes (TGJ1 mice). In TGJ1 mice, Notch1 receptor is activated both in myocytes and non myocyte cells. In newborn mice up to 1 week of age, proliferation is increased in TGJ1 mice, relative to their WT counterparts. As a result, the adult hearts of TGJ1 mice display increased cellular content both in the LV and RV walls, and the RV shows particularly thickened wall and increased chamber diameter, without alteration of the cardiac function. When subjected to pressure overload using aortic constriction (TAC), TGJ1 hearts developed a markedly reduced hypertrophic response both at the organ, cellular and molecular level. In addition the Akt-mTOR pathway which is activated to enhance protein synthesis in the hypertrophic hearts of WT mice is downregulated under baseline conditions and is not activated under stress conditions in hearts of TGJ1. After 1 week of TAC, WT mice developed cardiac fibrosis, which is significantly reduced in TGJ1 mice, as indicated by reduced collagen expression and deposition and expression of fibrosis regulatory factors CTGF and TGF-beta2. We have previously shown that the Notch1 receptor is essential to cardiac adaptation to stress. To determine whether Notch1 mediates the effects of Jagged1, we crossed TGJ1 mice to mice with a cardiac-specific inducible deletion of Notch1 (TGJ1-cNotch1$^{del/del}$ mice). When subjected to TAC, these mice displayed a reduced hypertrophic response, as observed with TGJ1 mice with and intact Notch1 gene indicating that Jagged1 exerts its effects independently of Notch1. Taken together, the data demonstrate that sustained activation of Notch pathway in the stressed heart, via expression of the ligand Jagged1, imparts a beneficial effect to the heart by reducing cardiac hypertrophy and fibrosis and further supports the notion that the Notch pathway controls cardiac adaptation to stress.

NEU
Neurosciences

Involvement of juxtaparanodal Kv1-channels in diabetic peripheral neuropathy

[1]Zenker J., [1]Poirot O., [1]dePreuxCharles A.-S., [1]Arnaud E., [1]Médard J.-J., [1]Chrast R.

Department for Medical Genetics - Unil[1]

Diabetes mellitus (DM) is a major cause of peripheral neuropathy. However, the underlying pathophysiological mechanisms of diabetic peripheral neuropathy (DPN) are still poorly understood. 90% of all diabetic patients suffer from type 2 DM, corresponding to more than 220 million people worldwide.

To get more insight into DPN associated with type 2 DM, we decided to use the rodent model of this form of diabetes, the db/db mice.

The progression of pathological changes in db/db mice mimics the ones observed in humans. Initially, db/db mice exhibit obesity and hyperinsulinaemia. Later they become hyperglycemic, and present reduced nerve conduction velocity and small sensory neuropathy (e.g. reduced intraepidermal nerve fiber density). After excluding any myelin related deficits in db/db mice, we further analyzed the node of Ranvier, a critical region for action potential propagation in myelinated fibers.

We observed a strong reduction of $K_v1.2$ expression in the juxtaparanodal regions. To detect if these changes will lead to any alteration in PNS function we measured compound action potentials in isolated sciatic nerves from control and diabetic animals and showed significant increase in the afterhyperpolarization phase and in excitability in db/db sciatic nerves. Using pharmacological inhibitors we demonstrated that both observations are mostly mediated by the decreased activity of K_v1-channels. Corroborating these results, we noticed aberrant action potential firing after sciatic nerve stimulation also *in vivo*, in db/db mice. Interestingly, nerve hyperexcitability has been previously described in diabetic patients and was correlated to ectopic action potential firing, ataxia, and paresthesiae suggesting that our observations may have a clinical significance.

Effect of rufinamide on gating properties of voltage-gated sodium channel Nav1.7

[1]Suter M., [2]Abriel H., [1]Decosterd I.

Department of anesthesiology[1], Dpt of Clinical Research, Bern[2]

Background: Voltage-gated sodium channels (Nav1.x) are important players in chronic pain. A particular interest has grown in Nav1.7, expressed in nociceptors, since mutations in its gene are associated to two inherited pain syndromes or insensitivity to pain. Rufinamide, a drug used to treat refractory epilepsy such as the Lennox-Gastaut syndrome, has been shown to reduce the number of action potentials in cortical neurons without completely blocking Na channels.

Aim: The goal of this study was to investigate the effect of rufinamide on Nav1.7 current.

Methods and Results: Whole-cell patch clamp experiments were performed using HEK293 cells stably expressing Nav1.7. Rufinamide significantly decreased peak sodium current by 28.3, 21.2 and 12.5% at concentrations of 500, 100 and 50µM respectively (precise EC50 could not be calculated since higher rufinamide concentrations could not be achieved in physiological buffer solution). No significant difference on the V1/2 of voltage-dependence of activation was seen; however a shift in the steady-state inactivation curve was observed (-82.6mV to -88.8mV and -81.8 to -87.6mV for 50 and 100µM rufinamide respectively, $p<0.005$). Frequency-dependent inhibition of Nav1.7 was also influenced by the drug. One hundred µM rufinamide reduced the peak sodium current (in % of the peak current taken at the first sweep of a train of 50) from 90.8 to 80.8% (5Hz), 88.7 to 71.8% (10Hz), 69.1 to 49.2% (25Hz) and 22.3 to 9.8% (50Hz) (all $p<0.05$). Onset of fast inactivation was not influenced by the drug since no difference in the time constant of current decay was observed.

Conclusion: In the concentration range of plasma level in human treated for epilepsy, 15µM, rufinamide only minimally blocks Nav1.7. However, it stabilizes the inactivated state and exerts frequency-dependent inhibition of Nav1.7. These pharmacological properties may be of use in reducing ectopic discharges as a causal and symptom-related contributor of neuropathic pain syndrome.

The brain's internal noise determines discrimination sensitivity

[1]Bernasconi F., [2]Manuel A., [3]MMurray M., [4]Spierer L.

NPR; Community Psychiatry Service, CHUV[1], NPR,Community Psychiatry Service, CHUV[2], NPR,CIBM, Radiology Service; CHUV; Vanderbilt University Medical Center, Nashville, TN, USA[3], NPR,CHUV[4]

Variation in stimulus-related behavior and brain responses is commonplace and typically attributed to the random variability in neural responses ("internal noise"). Computational models indicate that internal noise is sufficient to engender perceptual differences, in turn suggesting that identical stimuli can be (mis)perceived as being different. In the case of signal detection theory (SDT), internal noise is quantified as the ratio between an observer's discrimination threshold and sensitivity (d').

The present study investigated the contribution of internal noise to conscious perception and discrimination abilities. Participants were instructed to indicate which sound of a pair of identical pure tones was of higher pitch, being unaware that sounds were actually physically identical. In order to ensure that participants know what pitch differences referred to, they also underwent an above-threshold frequency discrimination task. With the aim to determine whether and how spontaneous activity can engender different percepts, AEPs to the identical sounds were compared as a function of perceived pitch, yielding a "High perceived pitch" vs. "Low perceived pitch" design. AEPs modulated topographically 92-115ms post-stimulus onset as a function of perceived pitch, indicative of the engagement of distinct intracranial sources; LAURA source estimations indicated that it followed from a modulation within the left temporo-parietal areas. Activity within this cluster negatively correlated with the participant's sensitivity in pitch discrimination measured in the pre-test session. Collectively, our results indicate that the brain's spontaneous internal noise engenders perception and determines sensitivity.

Spatio-temporal brain dynamics mediating post-error behavioral adjustments

[1]Manuel A., [1]Bernasconi F., [2]Murray M., [3]Grivel J., [4]Spierer L.

Neuropsychology and Neurorehabilitation service; Community Psychiatry Service, CHUV[1], Neuropsychology and Neurorehabilitation service; Radiology Departement, CHUV; Electroencephalography Brain Mapping Core, Center for Biomedical Imaging[2], Community Psychiatry Service, CHUV[3], Neuropsychology and Neurorehabilitation service; CHUV[4]

Optimal behavior relies on rapid and flexible adaptation to environmental requirements, notably based on the detection of errors. The impact of error-detection on subsequent behavior typically manifests as a slowing down of response time following errors. This effect has been attributed to shifts to more cautious response mode or to distraction induced by the infrequent error trials. However, how errors impact the processing of subsequent stimuli and in turn shapes behavior remains unresolved.

To address these questions, we used a speeded auditory spatial Go/NoGo task and contrasted auditory evoked potentials (AEPs) to left-lateralized "Go" and right "NoGo" stimuli as a function of performance on the preceding Go stimuli, generating a 2x2 design with "Preceding Performance" (accurate; inaccurate) and Stimulus type (Go; NoGo) as within-subjects factors.

Behaviorally, we replicated post-error slowing effects. Electrophysiologically, AEPs modulated topographically as a function of preceding performance 80-110ms post-stimulus onset and then as a function of stimulus type 110-140ms, indicative of changes in the underlying brain networks. Source estimations of these effects revealed a stronger activity of prefrontal regions to stimuli after successful than error trials, followed by a stronger response of parietal areas to the NoGo than Go stimulus.

We interpret these results in terms of a shift from a fast-automatic to a slow-controlled form of inhibitory control induced by the detection of errors, manifesting during low-level integration of subsequent stimuli, which in turn influences response speed.

Effect of a neuroprotective agent on the inflammatory response during cerebral ischemia

[1]Benakis C., [2]Vaslin A., [2]Pasquali C., [2]Bonny C., [1]Hirt L.

Department of Clinical Neurosciences, CHUV[1], Xigen Pharmaceuticals, Lausanne[2]

After an ischemic event affecting the brain, glial cells become activated and numerous inflammatory cells infiltrate the site of the lesion secreting a large variety of cytokines and chemokines. It is less known whether this brain inflammation is detrimental or beneficial for tissue recovery. Here, we evaluated if a strong neuroprotective peptide XG-102 (formely D-JNKI1) modulates post-ischemic inflammation in animal models of stroke.

XG-102 (0.1mg/kg) or vehicle (saline) was administered intravenously 3 h after transient middle cerebral artery occlusion (MCAO) in mice. Lesion size at 48 h was significantly reduced in the treated group. Quantification of the average intensity of CD11b positive microglia (infra-red emission) within the ischemic tissue showed no significant difference between groups.

The secretion of inflammatory mediators in the brain and systemic circulation was analysed by ELISA at 4 h, 7 h, 24 h, 48 h and 5 days in sham, MCAO and MCAO+XG-102 mice. Our results show that in the plasma samples of vehicle mice, Interleukin-6 (IL-6) and Keratinocyte Chemokine (KC/CXCL1) were secreted early after ischemia and return to basal level at late time points. XG-102 showed a trend towards reducing plasma levels of IL-6 but not KC. Interestingly, we found a significant release of IL-6 and KC only at 48 h in the brain of treated mice, compared with untreated mice, which decrease 5 days after the occlusion.

These findings suggest that neuroprotection of XG-102 may be linked, at least partly, to the inflammatory response. Further experiments will show whether the neuroprotective agent infuences downstream events activated by IL-6 (JAK-STAT pathway).

Tracking dynamic impacts of digestive hormones on brain mechanisms of food evaluation following gastric bypass surgery

[1]Lietti C., [2]Saugy J., [3]Egli L., [3]Campos V., [4]Murray M., [5]Tappy L., [6]Giusti V., [7]Toepel U.

Radiologie[1], Neuropsychologie et Neuroréhabilitation, CHUV-UNIL[2], Institut de Physiologie, UNIL[3], Radiologie, Neuropsychologie et Neuroréhabilitation, CHUV-CIBM[4], Endocrinologie, diabète et métabolisme, CHUV- Institut de Physiologie, UNIL[5], Endocrinologie, diabète et métabolisme, CHUV[6], Radiologie, Neuropsychologie et Neuroréhabilitation, CHUV[7]

Food intake and nutritional behaviour are known to be regulated by several gastro-intestinal (ghrelin, GLP-1, PYY) and endocrine (insulin, leptin) factors in animals. In terms of human nutritional behaviour, direct links and correlations between gastrointestinal (GI) or endocrine signals and reactions of the central nervous system have so far been seldom investigated. In this interdisciplinary study, combining methods for the monitoring of gastric hormones linked to glucose homeostasis and electrical neuroimaging, we aim to determine the parallels between Roux-en-Y gastric bypass (RYGB) - and its associated effects on gastric hormone levels and eating behaviour - and brain activity during pre-ingestion discrimination of food images. In particular, hormone blood measures are correlated with neural responses as measured by electroencephalography (EEG) in healthy normal-weighted and obese controls without surgery, as well as in RYGB patients before and after food intake. Preliminary results of this ongoing study will be presented.

Postsynaptic site reorganization at cortical glutamatergic synapses in Alzheimer's disease: PSD-95 and NMDA receptors expression changes in relation to pat

[1]Leuba G., [2]Savioz A., [1]Vernay A., [3]Kraftsik R., [1]Riederer I., [1]Riederer B.

Department of Psychiatry, Lausanne[1], Department of Psychiatry, Geneva[2], Department of Cell Biology and Morphology, Lausanne[3]

Background:
In Alzheimer's disease (AD), synaptic alterations play a major role and are correlated with the extension of cognitive changes. Modifications in presynaptic and postsynaptic proteins occur and the increase in postsynaptic protein PSD-95 suggests some degree of postsynaptic reorganization in AD (Leuba et al., 2008). In order to better understand how synaptic modifications are related to cognitive activity, we studied further PSD-95 together with possible alterations in NMDA receptors expression, in the entorhinal cortex (EC) and frontal cortex (FC; area 9) from ten patients with AD compared to ten age-matched controls. These changes were related to pathological markers such as ß-amyloid, including Aß oligomers, AD2 and ubiquitin proteins.

Methods:
We used quantitative immunohistochemical methods for synaptic proteins, NMDA receptors R1, R2A and R2B, and AD markers. Western blot analysis was also used for some proteins.

Results:
In both the entorhinal and frontal cortex, the immunostaining of the NMDAR1 receptors subunit was significantly increased in AD, in parallel to that of PSD-95, mainly in the neuropile (puncta). In addition, numerous neurons - mostly pyramidal - were also marked, significantly more in AD than in controls. This was particularly the case in layer 2 in EC, projecting to the hippocampus, while changes in FC were obvious in layers 2-3. The immunostaining of NMDAR2A and R2B receptors subunits was mostly not significantly different between AD and controls in puncta, in spite of a tendency to increase in AD. But significantly more neurons were stained in controls than in AD cases, contrarily to NMDAR1 and PSD-95 staining. Pyramidal neurons positive for NMDAR1 and PSD-95 staining were often positive for AD2 and ubiquitin and some degree of colocalization between PSD-95 and Aß oligomers was noticeable in positive puncta.

Conclusions:
On the whole, these data suggest that the postsynaptic site of glutamatergic synapses is the place of significant reorganization in AD cortex, particularly in relation to PSD-95 protein and NMDA receptors, and that the NMDA receptor itself could undergo expression changes of its subunits, leading to altered synapses and cognitive deficit

The role of the right parietal cortex in sound localization: a chronometric single-pulse TMS study

[1]At A., [2]Spierer L., [2]Clarke S.

CHUV, Service de Neuropsychology/Neuroréhabilitation[1], CHUV[2]

Auditory spatial functions, including the ability to discriminate between the position of nearby sound sources, are subserved by a large temporo-parieto-frontal "where" network. With the aim of determining whether and when the right parietal cortex is critical for auditory spatial discrimination, we applied single pulse transcranial magnetic stimulation (TMS) on right parietal regions 20, 80, 90 and 150ms post-sound 1 onset while participants (n= 15 in Exp 1 and n= 13 in Exp 2) completed a two-alternative forced choice auditory spatial discrimination task between pairs of sounds presented within the left (Exp 1) or right hemispace (Exp 2). Our results reveal that transient TMS disruption of right parietal activity impairs spatial discrimination when applied at 20 ms post-stimulus onset for sounds presented in the left controlateral hemispace and at 80 ms for sound presented in the right ipsilateral hemispace. We interpret our finding in terms of a critical role for controlateral temporo-parietal networks over initial stages of the building-up of auditory spatial representations and for a right hemispheric specialization in integrating the whole auditory space over subsequent, higher-order processing stages.

Early Benefit of Thrombolysis is Limited to Strokes of Minor and Moderate Severity

[1]Ntaios G., [2]Faouzi M., [3]Michel P.

Service de Neurologie - CHUV[1], Preventive and Social Medicine - CHUV[2], Service de Neurologie - CHUV[3]

Introduction: A large number of parameters have been identified as predictors of early outcome in patients with acute ischemic stroke. The present work analyzes a wide range of demographic, metabolic, physiological, clinical, laboratory and neuroimaging parameters in a large population of consecutive patients with acute ischemic stroke and aims to identify independent predictors of early clinical course.

Subjects and methods: We used prospectively collected data from the Acute STroke Registry and Analysis of Lausanne (ASTRAL). All consecutive patients between 01/2003 and 12/2008 admitted to our stroke unit and/or intensive care unit with ischemic stroke within 24 hours after onset of symptoms were analyzed. Univariate and multivariate analysis was performed to identify significant association with NIHSS score at admission and 24 hours. We also sought for any interactions between identified predictors.

Results: 1446 patients were included in the analysis. In multivariate analysis, NIHSS at 24 hours was associated with NIHSS at admission ($\beta=1$, $p<0.001$), initial glucose ($\beta=0.05$, $p<0.002$) and thrombolytic intervention ($\beta=-2.91$, $p<0.001$). There was a significant interaction between thrombolysis and NIHSS at admission ($p<0.001$), indicating that the latter does not improve early clinical course in patients with severe stroke.

Conclusions: Thrombolytic treatment, lower initial glucose and lower initial stroke severity predict favourable early clinical course. However, the effect of thrombolysis was limited to minor and moderate stroke, and was absent in patients with severe stroke.

Recanalization and collaterals predict outcome in proximal MCA occlusion, but neither penumbra nor core of stroke

[1]Le Corre-Laliberté C., [1]Michel P.

Service de Neurologie - CHUV[1]

Introduction: Data on new predictors of outcome include penumbra core or collaterals.

Objective: To test the predictive value of recanalization, collaterals, penumbra and core of ischemia for functional outcome in a large group of patients with MCA occlusion.

Method: Consecutive events included prospectively in the Acute Stroke Registry and Analysis of Lausanne from April 2002 to April 2009 with an acute stroke due to proximal MCA occlusion (M1) were considered for analysis. Acute CTA were reviewed to grade the collaterals (dichotomized in poor <= 50% or good >50% compared to the normal side) and localization of M1 occlusion (proximal or mid-distal). Acute CTP were reviewed and reconstructed to determine penumbra, core and stroke index (penumbra/penumbra+core) of brain ischemia. Good outcome was defined by mRS 0-2 at 3 months.

Results: Among 242 events (115 male, mean NIHSS 18.1, SD 5.8, mean age 66, SD 15), 42% were treated with intravenous thrombolysis, and 3% with intraarterial thrombolysis. Collateral status was rated as poor in 53% of events and proximal M1 occlusion was present in 64%. Recanalization determined at 24 hours with CTA was complete in 26% events and partial/absent in 54%.CTP was available for 212 events. Mean penumbra was 88.6 cm^3 (median 84.4, SD 53.8), mean core was 54.1 cm^3 (median 46.2, SD 45.7) and stroke index was 64% (median 68%, SD 25%). Good outcome was observed in 87 events (36%) and was associated in multivariate logistic regression with thrombolysis (p=0.02, OR=2.5, 95% CI 1.2-5.4), recanalization (p<0.001, OR=4.1, 95% CI 1.9-8.9), lower NIHSS (p<0.001, OR=0.84, 95% CI 0.78-0.91), male gender (p=0.01, OR=2.8, 95% CI 1.3-5.9), mRS prior to stroke (p=0.02, OR=0.5, 95% CI 0.28-0.9) and good collateral status (p=0.005, OR=3, 95% CI 1.4-6.4). Nor penumbra, nor core, nor stroke index were significant in the multivariate model, even if an association was present in the univariate model between good functional outcome and penumbra (p=0.004, OR=1.008, 95% CI 1.003-1.01), core (p<0.001, OR=0.98, 95% CI 0.976-0.99) and stroke index (p<0.001, OR=16.7, 95% CI 4.6 59.9).

Conclusion: MCA recanalization is the best predictor for good functional outcome, followed by collateral status. CTP data did not predict the functional outcome in our large group of M1 occlusion.

Multimodal Predictors of Massive Ischemic Stroke

[1]Zufferey P., [1]Bill O., [2]Faouzi M., [1]Michel P.

Neurology Service - CHUV[1], Institute of Social and Preventive Medicine - CHUV[2]

Introduction:

Severe stroke carries a high short and long term disability and fatality rate. Nevertheless, the profile of these patients in the acute phase is poorly defined. The aims of this study are to determine the characteristics of patients with severe ("massive") ischemic stroke at onset regarding a large range of clinical and paraclinical parameters.

Methodology:

Using a prospectively constructed acute ischemic stroke databank (Acute STroke Registry and Analysis of Lausanne, ASTRAL), we compared all patients with massive stroke defined as a NIHSS ≥ 20 at admission with all other patients. The variables included in a univariate and then in a multivariate analysis included demographic factors, vascular risk factors, clinical presentation, stroke mechanism, previous clinical or silent ischemic events, medication and acute radiological and metabolic findings.

Results:

Among 1915 acute ischemic patients, 243 (12.7%) had massive strokes. On multivariate analysis massive stroke patients had higher prestroke modified Rankin Scale (OR=1.28, 95%CI=1.04/1.56, p<0.019), more unknown onset (>1h but less than 24h) (OR=2.35, 95%CI=1.14/4.83, p<0.02), more early ischemic CT/MRI findings (OR=2.65, 95%CI=1.79/3.92, p<0.000), less chronic radiological infarcts (OR=0.43, 95%CI=0.25/0.71, p<0.001), more arterial occlusions in the ischemic territory on admission vascular imaging (OR=0.03, 95%CI=0.01/0.08, p<0.000), lower Hb concentration (OR=0.97, 95%CI=0.96/0.98, p<0.000), higher WBC (OR=1.05, 95%CI=1.00/1.11, p<0.045), and more cardio-embolic stroke mechanism (OR=1.74, 95%CI=1.19/2.54, p<0.004), With this profile, the area under the ROC curve showed a trade-off between sensitivity and specificity of 86%.

Conclusion:

Stroke severity is predicted by multiple clinical, radiological and laboratory anomalies of which several are modifiable. Interestingly, age, admission blood pressure and past history are not associated with severe stroke. This study confirms the necessity to consider a broad range of clinical and laboratory values in the acute phase of ischemic stroke, including detailed neuroimaging. The predictors of poor or good outcome in these patients still need to be studied.

TITLE: Predictors and accuracy of abnormal CT perfusion in 1296 consecutive acute ischemic stroke patients

[1]Nuno I., [2]Meuli R., [2]Maeder P., [3]Faouzi M., [4]Wintermark M., [5]Michel P.

Service de Neurologie - CHUV [1], Service de Radiologie CHUV[2], Medecine Sociâle - CHUV[3], CHUV[4], Service de Neurologie - CHUV[5]

INTRODUCTION: Diagnosis, localization and acute treatment of acute ischemic stroke is most frequently based on noncontrast cerebral CT (NCCT). CT perfusion (CTP) may improve the performance of NCCT. We aim to describe prevalence and predictors of pathological CTP in a large series of consecutive stroke patients and to determine its accuracy in predicting infarction on follow-up imaging.

METHODS: All consecutive patients arriving within 24 hours in our hospitals and then admitted to the stroke unit and/or intensive care were entered in a prospective registry (Acute STroke Registry and Analysis of Lausanne, ASTRAL). All patients with a good quality CTP (usually 4 or 16 slices) performed within 24 hours from January 2003 to March 2010 were included in the present analysis. Demographic, clinical, radiological and follow-up imaging (CT and/or MRI > 24h after initial imaging) were analysed. We used univariate logistic regression analysis to test the association of different factors associated with focal hypoperfusion on CTP. Significant predictors (at p<20%) were used to fit a multivariable model.

RESULTS: Of 1296 patients undergoing acute CTP, 455 (35%) had early ischemic changes on NCCT, and 943 (73%) had a focal hypoperfusion on CTP. Initial NIHSS, aphasia and neglect, cardioembolic stroke mechanism, bilateral carotid territory strokes, other non-lacunar supratentorial territories, increased glucose level, quicker time from symptoms onset to CT, early ischemic changes on NCCT, presence of silent infarcts, and presence of significant arterial pathology were independently associated with a positive CTP. The calculated sensitivity of CTP with regards to an infarction on follow-up imaging was 80.5% and the specificity was 51.3% .

CONCLUSION: Focal hypoperfusion on CTP is frequent in acute ischemic stroke and is predicted by higher NIHSS, earlier imaging, non-lacunar cardiogenic supratentorial infarcts, increased glucose levels, and the presence of arterial pathology in the ischemic territory. Sensitivity for subsequent infarct is high, and specificity moderate. Adding CTP to acute CT-based imaging may improve recognition of stroke and its localization, interpret arterial pathology, and therefore improve stroke management.

Early predictive metabolic biomarkers for lesion after transient cerebral ischemia

[1]Berthet C., [2]Lei H., [2]Gruetter R., [1]Hirt L.

Department of Clinical Neurosciences, Neurology Service, CHUV[1], Laboratory of Functional and Metabolic Imaging, EPFL; Department of Radiology, UNIL[2]

Background and Purpose:

Despite the improving imaging techniques, it remains challenging to predict the outcome early after transient cerebral ischemia. The aim of this study was thus to identify early metabolic biomarkers for outcome prediction.

 Methods:

We modeled transient ischemic attacks and strokes in mice. Using high field magnetic resonance spectroscopy, we correlated early changes in the neurochemical profile of the ischemic striatum with histopathological alterations at a later time-point.

Results:

A significant increase in glutamine was measured between 3h and 8h after all ischemic events followed by reperfusion independently of the outcome and can thus be considered as an indicator of recent transient ischemia. On the other hand, a reduction of the score obtained by summing the concentrations of N-acetyl aspartate, glutamate and taurine was a good predictor of an irreversible lesion as early as 3h after ischemia.

Conclusion:

In conclusion, we identified biomarkers of reversible and irreversible ischemic damage which can be used in an early predictive evaluation of stroke outcome.

Metabolism of brain glycogen after cerebral ischemia

[1]Piazza Y., [1]Berthet C., [2]Allaman I., [2]Magistretti P., [1]Hirt L.

Department of Clinical Neurosciences, Neurology Service, CHUV[1], Brain and mind institute, EPFL[2]

Brain contains glycogen stores, mainly localized in astrocytes. These stores are completely depleted during ischemia, but get synthesized again later, even to higher levels, showing an overcompensation of glycogen which accumulates around the lesion at 24h and 48h after middle cerebral artery occlusion (MCAO) in mice. The aim of this study was to understand the mechanisms leading to this overcompensation of glycogen, using an *in vivo* model of 60 min MCAO in mice and an *in vitro* model of oxygen and glucose deprivation (OGD) on rat organotypic hippocampal slices.

In vivo, western blots analysis on mouse brain extracts after MCAO showed that glycogen synthase (GS) is activated (dephosphorylated) in the ischemic hemisphere at early time points after MCAO. Using immunohistochemistry on mouse brain slices, we saw an increased expression of GS around the lesion and –interestingly- of its inactive form in some cortical neurons.

Our *in vitro* model shows the same evolution after ischemia with depletion of glycogen stores directly after OGD followed by resynthesis. We observed significantly higher glycogen stores after OGD compared to controls at 48h. Addition in the medium of 4 mM L-lactate directly after OGD tended to abolish the overcompensation.

These results open the discussion to establish if the purpose of glycogen overcompensation is to prevent further energy depletion or if it does simply reflect a metabolic perturbation.

Imaging life: two-photon microscopy and advanced tools for intra-vital optical imaging development at the Cellular Imaging Facility.

[1]Lamy C., [2]Chatton J.-Y.

DBCM[1], DBCM - CIF[2]

Many fields of biology seek to monitor biological processes over time with a cellular resolution in intact organs. Neurosciences pioneered *in vivo* cellular imaging two decades ago by developing the two-photon microscope to allow imaging of fluorescent probes deep inside the brain. These microscopes are not easily accessible as the cost of ownership and maintenance is high and precludes their widespread use by individual labs. This has led to the installation of shared commercial instruments. These shared microscopes are well suited for endpoint measurements; however they lack the flexibility and availability to accommodate longer time-lapse imaging experiments with living specimens. In addition, they usually offer limited options to monitor non-imaging signals synchronously with image acquisition, thus limiting their use for more elaborate experimental protocols.

To overcome these limitations and make the technology more readily available, the Cellular Imaging Facility UNIL-CHUV has launched a project, supported by the FBM, to develop a custom-made two-photon microscope. This instrument was assembled using off-the-shelf parts and without the need of purchasing an actual microscope stand. The software was implemented using the LabView programming environment.

The two-photon microscope we developed is now operational. Extensive imaging testing showed that optical properties and robustness of this instrument are comparable to that of commercial counterparts. The software offers advanced features and allows making time-series, line-scans and z-stacks. Nonetheless, the interface was kept simple and resembles that of typical confocal microscope already familiar to our users. This system offers many advantages over a commercial microscope: the investment is only a fraction of that of a brand name system, the maintenance is done locally at a minimal cost, the modular design allows for easy add-ons, there is ample space around the sample to accommodate any kinds of experimental accessories and, last but not least, both the hardware and software can be modified at will to fit specific user's needs.

We plan to make this instrument accessible to CIF users in a near future. To this purpose, we are now seeking input from researchers interested in using it or who would like to evaluate whether this kind of technology would benefit their research. Accordingly, we will aim at providing a microscope ready for experiments. If the need arises, we might duplicate this microscope. Other lines of development will be pursued towards implementation of latest technologies on our microscopes, such as fast 3D scanning, second harmonic generation imaging, stimulated emission imaging, adaptive optics, or fiber optics microscope for freely-moving animal imaging. Finally, we could provide guidance to researchers who wish to duplicate this kind of microscope in their own laboratory.

The HeCo Mouse, a unique mouse model of cortical band heterotopia associated with a lowered epileptic threshold

[1]Kleeberg J., [2]Kleeberg J., [1]Kielar M., [2]Kielar M., [3]Quairiaux C., [2]Welker E., [4]Fritschy J.-M., [5]Croquelois A., [2]Croquelois A.

Unit of neuropsychology and neurorehabilitation - CHUV[1], DBCM - UNIL[2], DNF -UNIGE[3], Institute of Pharmacology and Toxicology – UZH [4], Unit of neuropsychology et neurorehabilitation - CHUV[5]

Subcortical band heterotopia (SBH) belongs to the spectrum of neuronal migration disorders and is characterized by the presence of large clusters of neurone within the white matter underlying a relatively normal cortex. In patients, SBH is associated with developmental delay, mental retardation, and epilepsy. Despite recent advances, especially in genetics, our understanding of the underlying molecular mechanisms of SBH is still insufficient and no curative treatment exists yet, mainly due to the lack of appropriate animal models. We described previously the mouse mutant HeCo, a unique mouse model of SBH, which shares with its human counterpart the morphology of the heterotopia, developmental delay and a lowered epileptic threshold (1). Here we present recent data of on-going electrophysiological and neuronal migration/proliferation studies and analysis of the GABA system in the HeCo mouse.

Analysis of the GABA system by immunostaining for parvalbumin, calretinin and calbindin and the GABA A receptor subunits alpha 1, alpha 2, alpha 3, alpha 4 and beta 2 revealed that GABA cell subpopulations and GABA A receptors distributions did not differ between cerebral cortex of control mice and the homotopic cortex of the mutant HeCo. Furthermore, the labelling intensity within the heterotopia and layer II-III of the homotopic cortex was not significantly different for all the antibodies tested.

Combined EEG/EMG/video recordings in freely moving animals showed trains of 15-20Hz spike activity associated with typical behavioural changes including tonic head movement, myoclonic jerks and freezing in 5 out of 8 HeCo mice but in none of the 5 control mice. A pilot experiment using 16-epicranial electrodes in head restraint animals showed persistent burst suppression pattern under deeper isoflurane anaesthesia in the Heco but not in the control mouse.

Birthdates study and immunochemistry for layer-specific markers revealed that the HeCo formation is due to a transit problem in the intermediate zone affecting both radial and tangential migrating neurons. Neurons within the heterotopia are generated at relatively late embryonic stages and share their phenotype with neurons in superficial layers of the homotopic cortex, which are affected in terms of cell density and layer thickness. Pulsed injection (1 hour) of 5-bromo-2-deoxyuridine (BrdU) combined with Tbr1 immunolabelling (marker of deep cortical layers) as well as GFP plasmids electroporation followed by time-lapse microscopy demonstrated an increased neuronal proliferation within the intermediate zone.

In conclusion, preliminary results of the EEG recordings give further support for the assumption that the HeCo mouse has a tendency to spontaneous seizure activity. However, an involvement of the GABA system in the seizure activity seems less likely. The formation of the SHB in the HeCo mouse is the result of both migration and cell proliferation alterations.

Ref.: 1. Croquelois A, Giuliani F, Savary C, Kielar M, Amiot C, Schenk F, Welker E. Cereb Cortex. 2009 Mar;19(3):563-75.

Influence of MRI slice orientation in evaluating spinal stenosis through surface measurements or morphology grading

[1]Schizas C., [1]Lucy H., [2]Richarme D., [2]Theumann N., [1]Kulik G.

Department of Orthopedics and Trauma surgery[1], Radiology, CHUV[2]

Introduction

Lumbar spinal stenosis (LSS) treatment is based primarily on clinical criteria providing that imaging confirms radiological stenosis. It has been recently shown that grading stenosis based on the morphology of the dural sacs as seen on axial T2 images better reflects severity of stenosis than measurements of dural sac cross-sectional area (DSCA). Our aim was to study the variability of surface measurements and morphological grading of stenosis for varying degrees of angulation of the T2 axial images relative to the disc space as observed in clinical practice.

Materials and Methods

Lumbar spine TSE T2 three dimensional (3D) MRI sequences were obtained from 32 consecutive patients presenting with either suspected spinal stenosis or low back pain. Axial reconstructions using the OsiriX software at 0, 10, 20 and 30 degrees relative to the disc space orientation were obtained. For each image, surface area (DSCA) was digitally measured and stenosis was graded according to the recently-published 4-point (A-D) morphological grading by two observers. Interobserver agreement was analyzed using kappa statistics. Statistical analysis of DSCA measurements was performed using t-tests.

Results

A good interobserver agreement was found in grade evaluation (kappa = 0.71) of stenosis.
DSCA varied significantly as the slice orientation increased from 0 to +10, +20 and +30 degrees at each level examined (P <0.0001). More specifically DSCA varied from -15.48% to +31.89% (SD 18.40%) at 10 degrees, -24.00% to +143.82% (SD 20.45%) at 20 degrees and -29.35% to +231.13% (SD 26.52%) at 30 degrees of slice orientation. At 13 disc levels, DSCA was of less than 100mm^2 at 0 degrees slice orientation, but changed to values of more than 100mm^2 in three cases at 10 degrees orientation, in five cases at 20 degrees and in ten cases at 30 degrees orientation. In only two out of 97 levels studied did the morphological grading change as the angle increased.

Discussion

Even though 30 degrees of slice orientation is less frequently encountered, the need to obtain continuous slices using the classical 2D MRI acquisition technique entails often at least a 10 degree slice inclination relative to one of the studied disc spaces due to physiological lordosis. Such an inclination could have an important influence on surface measurements but much less in morphological grading which also better reflects nerve tissue impingement and has been shown to be of prognostic value. In conclusion, the axial MRI slice angle variation significantly affects DSCA, and thus potentially management decisions. Morphological grading seems to offer an alternative means for assessing severity of spinal stenosis that is little affected by image acquisition technique.

Consciousness Impairment In Acute Ischemic Stroke

[1]Puricel S.-G.,

Faculté de Biologie et Medecine[1]

Background and objectives: Decreased level of consciousness (LOC) at ischemic stroke onset is infrequent and associated with a poor prognosis. Its causes and mechanisms are insufficiently understood. We aimed at finding predictors and topographic correlations for such strokes.

Methods: In an acute hospital based registry of consecutive acute ischemic strokes admitted within 24 hours after last proof of wellbeing(Acute STroke Registry and Analysis of Lausanne, ASTRAL), decreased level of consciousness was defined as a value of value ≥ 1 on the corresponding NIHSS item on initial neurological assessment. Acute status epilepticus was excluded by EEG if suspected. Demographic, clinical, etiological, radiographic, arterial imaging and outcome factors were considered. Poor prognosis was defined as a modified Rankin Scale score of ≥3 at 3 months. In a first multivariate logistic regression analysis of predictors of decreased LOC, we entered all significant variables except initial NIHSS. The second multivariate logistic regression analysis considered only significant variables concerning anatomical localisation and arterial territories.

Results: In 1'436 acute ischemic strokes, 139 (9.7 %) had a decreased LOC on admission, of whom only one was attributable to early mass effect. These patients showed significantly poorer prognosis (OR 7.8, 95% CI 5.09-11.84) and higher mortality rate at three months (OR 4.67, 95% CI 3.15-6.92). On multivariate analysis, they had more frequently one or more previous strokes (OR 5.1, 95% CI 2.79-9.31), more frequently early ischemic changes on radiology (OR 1.74, 95% CI 1.10-2.75) and a higher frequency of arterial stenosis or occlusion in the ischemic territory (OR 2.87, 95% CI 1.6-4.91). Lacunar mechanism (OR 0.11, 95% CI 0.04-0.36) and stroke with an uncertain cause (OR 0.37, 95% CI 0.18-0.71) were less frequent. Regarding localisation, patients with pure basilar strokes (OR 1.83, 95% CI 1.15-2.90), bilateral (OR 2.05, 95% CI 1.00-4.19), mixed supra- and infratentorial strokes (OR 6.11, 95% CI 3.02-12.35), large hemispheric infarction, and involvement of midbrain simultaneous with at least one other posterior circulation structure (OR 4.99, 95% CI 2.13-11.65) showed decreased LOC. Limiting the multivariate analysis to stroke localization, LOC was more frequently normal in left sided infarctions (OR 0.56, 95% CI 0.36-0.88) and in supratentorial strokes without cortical involvement (OR 0.23, 95% CI 0.10-0.54).

Conclusion: Decreased level of consciousness at ischemic stroke onset is related to the presence of previous strokes, current stroke mechanism, early ischemic changes on acute imaging and acute arterial occlusions. Lesions have to be distributed in specific patterns and widespread in infra- and supratentorial structures in order to decrease LOC, suggesting distributed networks for its maintenance.

ODE
Oncology and Development

Involvement of a RasGAP-derived peptide in cell migration

Barras D.

Department of Physiology

Metastases are the main causes of death in cancer patients. Cells from primary tumor have first to escape from the tumor, to travel in the bloodstream, to home to the new location and to promote angiogenesis among others. In a therapeutic point of view, it is more relevant to target the first step of this sequential process, which is cell adhesion modulation.

In 2004, our group developed a cell permeable peptide derived from a caspase-cleaved fragment of RasGAP (TAT-RasGAP317-326). This peptide was already shown to sensitize, efficiently and specifically, cancer cells against chemotherapy-induced cell death. We recently assessed that this peptide was also able to inhibit cell migration and to increase cell adherence on cell culture plates. Theses observations make us think that the TAT-RasGAP317-326 peptide could be used as a potential compound for anti-metastatic therapy.

Targeting renal cell carcinoma with NVP-BEZ235 a dual PI3K/mTOR inhibitor in combination with sorafenib

[1]Roulin D., [1]Waselle L., [1]Dormond-Meuwly A., [1]Demartines N., [1]Dormond O.

Department of Visceral Surgery,CHUV[1]

Background: NVP-BEZ235, a PI3K/mTOR inhibitor, reduces the growth of renal cell carcinoma (RCC) in vitro and in vivo. However, NVP-BEZ235 has little effect on tumor angiogenesis in renal carcinoma xenografts. We therefore hypothesized that the antitumor efficacy of NVP-BEZ235 on RCC would be potentiated in combination with anti-angiogenic therapy such as sorafenib.

Materials and Methods: RCC cell lines 786-0 and Caki-1 were treated with various concentrations of NVP-BEZ235 and/or sorafenib, and tumor cell proliferation and apoptosis were investigated in vitro. Moreover, treatment efficacy of NVP-BEZ235 alone, or in combination with sorafenib, was evaluated on RCC xenografts in athymic nude mice.

Results: NVP-BEZ235 or sorafenib reduced cell proliferation and increased cell apoptosis in vitro, and reduced tumor xenograft growth in vivo. Combination of both drugs in vitro resulted in significant RCC growth inhibition and increased apoptosis compared to monotherapy. This synergistic effect was also observed on tumor progression in vivo.

Conclusions: Our findings indicate that the simultaneous use of NVP-BEZ235 and sorafenib provides greater antitumor benefit compared to either drug alone and may thus provide a treatment strategy in RCC.

POLYMORPHISM F144I IN NATURAL VARIANTS OF EBV-ENCODED LMP1 LEADS TO ENHANCED NF-KAPPAB ACTIVATION

[1]Zuercher E., [1]Martinez R., [1]Telenti A., [1]Rothenberger S.

Institute of Microbiology - CHUV[1]

Background. Epstein-Barr Virus (EBV) infects more than 90% of human adults worldwide. Not only EBV causes Infectious Mononucleosis, but it is linked with several kinds of cancers such as Hodgkin's lymphoma. Latent Membrane Protein 1 (LMP1) is the major key player in the transformation of cells by EBV. LMP1 activates NF-kappaB transcription factor that, if upregulated, is associated with carcinogenesis. We mapped one polymorphism –F144I– on a natural variant of LMP1, which allows the protein to activate NF-kappaB at higher levels (3-fold more) than the prototype B95-8 LMP1. We further hypothesized that natural LMP1 variants containing this polymorphism are able to activate NF-kappaB at higher levels than the prototype LMP1 B95-8.

Methods. To address this question, 31 full length LMP1 variants were isolated from 100 genomic DNA samples extracted from PBMC of HIV infected individuals included in the Swiss HIV Cohort Study (SHCS). Variants were amplified in a single PCR, fully sequenced and sequences analyzed. LMP1 genes were cloned into mammalian expression vector in order to test them by gene reporter assay for their levels of NF-kappaB activation.

Results. Among the 31 LMP1 variants characterized, 5 carry the polymorphism of interest. When tested by gene reporter assay, all the 5 are able to activate NF-κB at levels higher than the prototype B95-8 LMP1. Analysis of phylogenetic tree based on LMP1 sequences revealed a second cluster of variants that display a similar phenotype with respect to NF-kappaB activation. New candidate determinants based on these results are currently under investigation.

Conclusions. The identification of polymorphisms associated with increased NF-kappaB signaling is of crucial importance for evaluating the role of LMP1 gene variation in the development of EBV-associated tumors.

Chitosan/alginate nanogels as vectors for siRNA-mediated survivin silencing in human neuroblastoma cell lines

[1]Lagopoulos L., [2]Muehlethaler A., [3]Rossi N., [3]Kaeuper P., [3]Laue C., [2]Gross N.

Research in Pediatric Oncology, DMCP, CHUV and Medipol, PSE-EPFL, Lausanne [1], Research in Pediatric Oncology, DMCP, CHUV, Lausanne [2], Medipol, PSE-B, EPFL, Lausanne [3]

High stage neuroblastoma is one of the most aggressive solid childhood tumor which is still associated to a poor outcome, despite intensive and multimodal treatments. Moreover, children represent a population of cancer survivors at high risk to develop late side effects of current treatments, for who the development of less toxic therapies is essential. The recent developments in cancer nanotechnology offer unique drug delivery systems, showing efficient drug targeting and delivery properties. These new options have not yet been developed for neuroblastoma.

Neuroblastoma cells overexpress molecules such as survivin, which are involved in their development and progression, and thus represent potential valuable therapeutic targets. In this study chitosan/alginate designed nanogels (Hynosphere[TM]) formulated with a "model siRNA drug" have been assayed in vitro as vectors for the delivery of survivin siRNAs in two relevant neuroblastoma cell lines (SH-EP and LAN-1). Immunofluorescence-labelled nanogels were shown to bind and enter NB cells within 6h with a cell line-dependent efficiency. Survivin siRNA loaded nanogels had no significant toxicity, as measured by viability assay. The ability of different Hynosphere[TM] formulations to target cells and reduce the cellular level of survivin was measured by western blot in cell lines. Survivin levels could be specifically reduced up to by 70 % in different cells after exposure to siRNA-loaded nanogels with survivin siRNA concentrations corresponding to 80nM. The silencing efficiency was thus comparable to that of classical siRNA transfection agents, however not suitable for use in the clinics.

These preliminary results indicate that chitosan-nanogels represent promising vectors which are currently further characterized and developed for the targeted delivery of silencing molecules in neuroblastoma.

Treatment with antigen-loaded recombinant CD1d proteins leads to sustained iNKT cell reactivity, attenuated PD-1 expression and tumor protection

[1]Donda A., [1]Corgnac S.

Department of Biochemistry[1]

Invariant Natural Killer T cells (iNKT) are potent activators of Natural Killer (NK) cells, dendritic cells (DC) and T lymphocytes, and their anti-metastatic activity through NK cell transactivation has been well demonstrated. iNKT cells can be readily activated by a single injection of the high affinity CD1d superagonist ligand alpha-galactosylceramide (αGalCer). However, this activation is only short-lived, followed by long-term iNKT cell anergy, limiting the therapeutic use of αGalCer. Upregulation of Program Death-1 (PD-1) on iNKT cells was shown to be largely responsible for the onset of iNKT cell unresponsiveness, as it could be reversed by PD-1/PD-L1 blockade. As a promising alternative, we have demonstrated that when αGalCer is loaded on recombinant soluble β2m-CD1d molecules (aGalCer/sCD1d), repeated injections led to sustained iNKT cell activation associated with continued cell proliferation and IFNγ secretion. Importantly, the retained reactivity of iNKT cells allowed prolonged antitumor activity when the αGalCer/sCD1d was fused to an anti-HER2 or anti-CEA scFv antibody fragments. Potent growth inhibition was obtained against established tumors expressing the relevant antigen, whereas free αGalCer had no effect. The capacity of recombinant CD1d fusion proteins to keep iNKT cells reactive was associated with low PD-1 upregulation even after six injections, in contrast to high PD-1 expression reached already after one injection of αGalCer alone. These results suggest that activation of NKT cells by soluble CD1d fusion proteins does not require iNKT-APC interaction, thus escaping the co-inhibitory control of PD-1/PD-L1, PD-L2. Preliminary experiments with human iNKT cells indicate that they react similarly to their murine counterparts. Indeed, while free αGalCer requires the presence from CD1d-expressing APCs, soluble αGalCer-loaded CD1d proteins are able to directly activate human iNKT cell clones.

Altogether, the proposed innovative strategy of cancer immunotherapy combines two promising characteristics, first the targeting of the immune response to the tumor site by CD1d fusion to an antitumor scFv and second, the sustained reactivity of iNKT cells by preventing the co-inhibitory signal of PD-1/PD-L1.

INVOLVEMENT OF THE CXCL12/CXCR4/CXCR7 AXIS IN THE MALIGNANT PROGRESSION OF HUMAN NEUROBLASTOMA

[1]Liberman J., [1]Flahaut M., [1]Muhlethaler A., [1]Coulon A., [2]Joseph J.-M., [1]Gross N.

Pediatric Oncology Research Unit-CHUV[1], Pediatric Surgery Unit-CHUV[2]

Neuroblastoma (NB) is a devastating childhood neoplasm for which no efficient treatment is available for high stage tumours. Chemokines and their receptors, in particular the CXCR4/CXCL12 axis, have been involved in tumour progression. We previously reported a tumour type-specific and microenvironment-related growth-promoting role for the CXCR4 receptor. Such growth-promoting effects were highly significant only when NB cells were orthotopically injected in the adrenal gland of nude mice. This finding highly suggested a pivotal cross-talk between the CXCR4-expressing aggressive tumour cells and the associated microenvironment. The recent description of CXCR7 as a second CXCL12 receptor, add to the CXCL12/CXCR4 chemokine/receptor axis a new player, which function remains to be determined.

In search for specific microenvironment-related effects, which might cooperate with CXCR4-mediated NB tumour growth, we addressed the role and participation of CXCR7. Although reported to confer atypical properties to cancer cells, the role of CXCR7 in NB development and the cross-talk with the microenvironment is still unknown. A preliminary screening of a small panel of NB tissues of different stages and histology types for CXCR7 expression revealed a selective CXCR7 staining on the more differentiated cells of the tumour and on the associated adrenal tissue. In contrast, CXCR7 was only moderately expressed on NB cell lines, but was found to increase upon exposition of cells to differentiation agents.

From these preliminary observations, we propose that CXCR4 and CXCR7 may display two distinct and atypical roles in NB. Rather than a metastatic-promoting role identified in several other tumour systems, our data favour a tumour type-specific and growth-promoting influence for CXCR4, while CXCR7 may be implicated in NB maturation and interactions with the environment. These preliminary findings open new research perspectives for the role of the CXCL12/CXCR4/CXCR7 axis in the behaviour of NB, that will be further explored *in vitro* and *in vivo*.

INDIVIDUAL CASPASE-10 ISOFORMS PLAY DISTINCT AND OPPOSING ROLES IN THE INITIATION OF DEATH RECEPTOR-MEDIATED TUMOUR CELL APOPTOSIS

[1]Mühlethaler-Mottet A., [2]Flahaut M., [2]Balmas Bourloud K., [2]Auderset Nardou K., [2]Coulon   A., [2]Liberman J., [3]Thome M., [2]Gross N.

Peadiatric Department-CHUV[1], Department of Paediatrics-CHUV[2], Department of Biochemistry[3]

The cysteine protease caspase-8 is an essential executioner of the death receptor apoptotic pathway. The physiological function of its homologue caspase-10 remains poorly understood, and the ability of caspase-10 to substitute for caspase-8 in the death receptor apoptotic pathway is still controversial. Here we analysed the particular contribution of caspase-10 isoforms to death receptor-mediated apoptosis in neuroblastoma cells characterized by their resistance to death receptor signalling.

Silencing of caspase-8 in TRAIL-sensitive neuroblastoma cells resulted in complete resistance to TRAIL, which could be reverted by overexpression of caspase-10A or caspase-10D. Overexpression experiments in various caspase-8 expressing tumour cells also demonstrated that caspase-10A and caspase-10D isoforms strongly increased TRAIL and FasL sensitivity, whereas caspase-10B or caspase-10G had no effect or were weakly anti-apoptotic.

Further investigations revealed that the unique C-terminal end of caspase-10B was responsible for its degradation by the ubiquitin-proteasome pathway and for its lack of pro-apoptotic activity compared to caspase-10A and caspase-10D.

These data highlight in several tumour cell types, a differential pro- or anti-apoptotic role for the distinct caspase-10 isoforms in death receptor signalling, which may be relevant for fine tuning of apoptosis initiation.

Therapeutic Drug Monitoring (TDM) of Imatinib: Effectiveness of Bayesian dose adjustment for CML patients enrolled in the I-COME study

[1]Gotta V., [2]Widmer N., [2]Csajka C., [2]Decosterd L., [3]Duchosal M., [4]Chalandon Y., [5]Heim D., [6]Gregor M., [1]Buclin T.

Division of Clinical Pharmacology and Toxicology - CHUV [1], Division of Clinical Pharmacology and Toxicology, CHUV [2], Service and Central laboratory of Hematology, CHUV[3], Service of Hematology, HUG[4], Hematology, USB[5], Service of Hematology, LUKS[6]

Introduction: As imatinib pharmacokinetics are highly variable, plasma levels differ largely between patients under the same dosage. Retrospective studies in chronic myeloid leukemia (CML) patients showed significant correlations between low levels and suboptimal response, as well as between high levels and poor tolerability. Monitoring of trough plasma levels, targeting 1000µg/L and above, is thus increasingly advised. Our study was launched to assess prospectively the clinical usefulness of systematic imatinib TDM in CML patients. This preliminary analysis addresses the appropriateness of the dosage adjustment approach applied in this study, which targets the recommended trough level and allows an interval of 4-24h after last drug intake for blood sampling.

Methods: Blood samples from the first 15 patients undergoing 1st TDM were obtained 1,5 -25h after last dose. Imatinib plasma levels were measured by LC-MS/MS and the concentrations were extrapolated to trough based on a Bayesian approach using a population pharmacokinetic model. Trough levels were predicted to differ significantly from the target in 12 patients (10 <750µg/L; 2 >1500µg/L along with poor tolerance) and individual dose adjustments were proposed. 8 patients underwent a 2nd TDM cycle. Trough levels of 1st and 2nd TDM were compared, the sample drawn 1,5h after last dose (during distribution phase) was excluded from the analysis.

Results: Individual dose adjustments were applied in 6 patients. Observed concentrations extrapolated to trough ranged from 360 to 1832 µg/L (median 725; mean 810, CV 52%) on 1st TDM and from 720 to 1187 µg/L (median 950; mean 940, CV 18%) on 2nd TDM cycle (figure 1).

Conclusion: These preliminary results suggest that TDM of imatinib using a Bayesian interpretation is able to target the recommended trough level of 1000µg/L and to reduce the considerable differences in trough level exposure between patients (with CV decreasing from 52% to 18%). While this may simplify blood collection in daily practice, as samples do not have to be drawn exactly at trough, the largest possible interval to last drug intake yet remains preferable to avoid sampling during distribution phase leading to biased extrapolation. This encourages the evaluation of the clinical benefit of a routine TDM intervention in CML patients, which the randomized Swiss I-COME trial aims to.
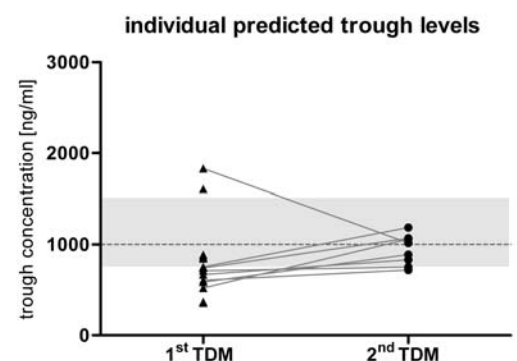

Figure 1: Comparison of extrapolated trough levels on 1st TDM cycle (14 patients, triangles) and afterwards on 2nd TDM cycle (8 patients, dots). *Dashed line:* target of 1000 ng/ml. *Pattern:* tolerance interval with lower limit of 750 ng/ml and upper limit of 1500 ng/ml (only if accompanied by poor tolerability).

The TRAF interacting protein (TRAIP) regulates keratinocyte proliferation.

[1]Chapard C., [1]Almeida S., [1]Hohl D., [1]Huber M.

Dermatology - CHUV[1]

TRAIP is an E3 ubiquitin ligase which undergoes auto-ubiquitination and is reported to interact with TNF-receptor associated factors (TRAF) and two tumor suppressors (CYLD, SYK). TRAIP is necessary for mice development since TRAIP knock-out mice die in utero at day 6.5 caused by aberrant regulation of cell proliferation and apoptosis. Physiological substrates of TRAIP are not known. Over-expression of TRAIP in 293T cells inhibits TNF-α-induced NF-κB activation. We showed that TRAIP mRNA expression was strongly down-regulated in cultured primary human keratinocytes undergoing differentiation triggered by high cell density or high calcium. Short-term phorbol-12-myristate-13-acetate (TPA) treatment or inhibition of phosphatidylinositol-3 kinase signaling in proliferative keratinocytes suppressed TRAIP transcription. Inhibition by TPA was protein kinase C dependent. Keratinocytes undergoing KD of TRAIP expression by lentiviral short-hairpin RNA (shRNA; T4 and T5) strongly reduced proliferation rates compared with control shRNA. Furthermore, cell-cycle analysis demonstrated that TRAIP-KD caused growth arrest in the G1/S phase. Keratinocytes with TRAIP-KD resembled differentiated cells consistent with the augmented expression of differentiation markers keratin 1 and filaggrin. Luciferase-based reporter assays showed no increase in NF-κB activity in TRAIP-KD keratinocytes, indicating that NF-κB activity in keratinocytes was not regulated by TRAIP. TRAIP mRNA expression was increased by ~2-fold in basal cell carcinomas compared with normal skin. To understand the mechanisms in which TRAIP is implicated, dynamics of TRAIP protein expression and subcellular localization during the cell cycle was examined. In HeLa cells and human epidermal keratinocytes transiently over-expressing a TRAIP-GFP fusion protein, the fluorescent protein localized mainly to the nucleolus. In summary, these results underline the important role of TRAIP in the regulation of cell cycle progression and the tight linkage of its expression to keratinocyte proliferation.

A novel mechanism of drug resistance in human leukemia/lymphoma

[1]Nahimana A., [1]Aubry D., [1]Duchosal M.

Service of Hematology, CHUV[1]

Leukemic cells are highly prone to become resistant to treatment. Polychimiotherapies, by attacking leukemic cells through various pathways are aimed at preventing cell resistance development and also at maximizing killing effects. For these reasons, development of new cell targeting therapies, i.e. those modifying metabolic pathways is most warranted. In this context, we demonstrated the tremendous antitumor activity of a novel agent, APO866: an inhibitor of NAD biosynthesis, in numerous leukemic and lymphomatous cells. Treatment with APO866 decreased intracellular NAD and adenosine triphosphate (ATP) at 24 hours and 48 to 72 hours, respectively. The NAD depletion led to cell death. APO866-mediated cell death occurred in a caspase-independent mode, and was associated with mitochondrial dysfunction and autophagy. Although, the in-vitro and in-vivo studies demonstrate that most leukemic cells are sensitive to APO866-mediated cell death without significant toxicity to normal cells, we recently observed that some cells became refractory to this agent. We made a seminal observation that sensitive leukemic cells cultured in conditioned medium (CM; supernatant) obtained from APO866 resistant malignant cells, become also resistant to APO866 treatment. Interestingly, preliminary results confirm that APO866 resistance could be transferred in vivo as it was observed in vitro. These findings suggest that drug resistant malignant cells secrete unknown or unidentified factor(s) that can promote the tumor resistance and that drug resistance could be transferred in-vivo from resistant to sensitive malignant cells. We are currently characterizing the secreted molecule(s) by APO866 resistant malignant cells and data from these investigations are presented.

MFGE-8 promotes the growth of mammary epithelial cells and enhances their in vivo tumorigenicity

[1]Carrascosa C., [1]Obula R., [2]DeLorenzi M., [3]Lehr H.-A., [4]Mazzucchelli L., [5]Rüegg C., [1]Mariotti A.

CHUV/CePO/UNIL[1], SIB, Lausanne[2], IUP, CHUV[3], ICP, Locarno[4], Université de Fribourg[5]

Milk fat globule-EGF factor 8 (MFG-E8) is a secreted glycoprotein that is expressed in breast carcinomas and is present in the serum of patients with aggressive breast cancer. By performing a meta-analysis of publicly available gene expression data of breast cancer biopsies we have found that MFG-E8 is highly expressed in breast cancer and its expression is significantly associated with low levels of ErbB2 and of Estrogen receptor. We have then confirmed MFG-E8 expression in a series of breast cancer biopsies by immunohistochemistry analysis. To investigate the function of MFG-E8 we have overexpressed it in non-transformed mouse mammary epithelial cells NMuMG. We have observed that MFG-E8 increases in vitro proliferation and anchorage-independent growth of NMuMG cells and it promotes their proliferation and branching in Collagen I gels. Moreover, overexpression of of MFG-E8 in mouse mammary carcinoma cells that have low endogenous levels of the protein promotes their in vivo growth when injected orthotopically in immunosuppressed mice. In line with these results, we have also found that MFG-E8 downregulation enhances the epithelial phenotype of mammary carcinoma and Ras-transformed mammary cells, and decreases the in vivo growth of the latter. In addition, expression of a mutated version of MFG-E8 unable to bind integrins decreases in vivo tumorigenicity of mammary carcinoma cells. These results demonstrate that MFGE8 promotes mammary gland carcinoma growth in vivo and and identify this molecule as a potential therapeutic target in breast cancer.

Nuclear localization of lactadherin in melanoma cells

[1]Obula R., [1]Carrascosa C., [1]Mariotti A.

CHUV/CePO/UNIL[1]

Lactadherin is a secreted glycoprotein that was shown to promote melanoma progression by enhancing cell survival and invasion abilities and by stimulating immune suppression. We have analyzed the expression of lactadherin in human melanoma biopsies obtained from tumors at different progression stages by immunohistochemistry (IHC). We have observed that while in most cells lactadherin is localized in the cytoplasm and at the cell membrane, in some cells it is present in the nuclei. To confirm this observation we have then examined lactadherin localization in a series of melanoma cell lines by immunofluorescence staining with different anti-lactadherin antibodies and we have detected this protein in the nuclei of several melanoma cell lines. We have found that the number of cells in which lactadherin is present in the nucleus varies depending on the cell line, with some cell lines being highly positive (> 90% of lactadherin-positive nuclei), some consisting of a mixture of cells with lactadherin positive and lactadherin-negative nuclei, and others presenting only cytoplasmic and membrane staining. We have observed no correlation between lactadherin nuclear localization and the degree of aggressiveness of the analyzed cell lines. We have confirmed lactadherin nuclear localization by western blotting of nuclear extracts of melanoma cells. This observation suggests that lactadherin function may be more complex than what described so far. Ongoing experiments are addressing the biological significance and functional role of nuclear lactadherin in the development of melanoma.

Phosphorylation induces genome-wide reprogramming of FOXC2-mediated transcription

[1]Agalarov Y., [1]Ivanov K., [2]Valmu L., [1]Maby-ElHajjami H., [3]Norrmen C., [4]Houhou N., [4]Delorenzi M., [1]Samuilova O., [1]Jaquet M., [5]Miura N., [3]Alitalo K., [6]Yla-Herttuala S., [1]V.Petrova T.

Division of Experimental Oncology, CePO, CHUV and University of Lausanne[1], University of Helsinki, Department of Clinical Medicine, Biomedicum, Division of Clinical Chemistry, Helsinki, Finland[2], University of Helsinki, Biomedicum Helsinki, Molecular/Cancer Biology Program, Helsinki, Finland[3], Swiss Institute of Bioinformatics (SIB), Lausanne, Switzerland[4], Hamamatsu University School of Medicine, Department of Biochemistry, Hamamatsu, Shizuoka, Japan[5], University of Eastern Finland, AI Virtanen Institute, Kuopio, Finland[6]

Lactadherin is a secreted glycoprotein that was shown to promote melanoma progression by enhancing cell survival and invasion abilities and by stimulating immune suppression. We have analyzed the expression of lactadherin in human melanoma biopsies obtained from tumors at different progression stages by immunohistochemistry (IHC). We have observed that while in most cells lactadherin is localized in the cytoplasm and at the cell membrane, in some cells it is present in the nuclei. To confirm this observation we have then examined lactadherin localization in a series of melanoma cell lines by immunofluorescence staining with different anti-lactadherin antibodies and we have detected this protein in the nuclei of several melanoma cell lines. We have found that the number of cells in which lactadherin is present in the nucleus varies depending on the cell line, with some cell lines being highly positive (> 90% of lactadherin-positive nuclei), some consisting of a mixture of cells with lactadherin positive and lactadherin-negative nuclei, and others presenting only cytoplasmic and membrane staining. We have observed no correlation between lactadherin nuclear localization and the degree of aggressiveness of the analyzed cell lines. We have confirmed lactadherin nuclear localization by western blotting of nuclear extracts of melanoma cells. This observation suggests that lactadherin function may be more complex than what described so far. Ongoing experiments are addressing the biological significance and functional role of nuclear lactadherin in the development of melanoma.

Vaccination-induced functional competence of circulating human self/tumor-specific CD8 T-cells

[1]Baumgartner P., [1]Jandus C., [2]Rivals J.-P., [1]Derré L., [1]Lövgren T., [1]Baitsch L., [1]Guillaume P., [1]Luescher I., [2]Matter M., [1]Rufer N., [2]Michielin O., [1]Speiser D.

Ludwig Institut for Cancer Research [1], University Hospital Center and University of Lausanne (CHUV)[2]

T-cells specific for foreign (e.g. viral) antigens can give rise to strong protective immune responses, whereas self/tumor antigen-specific T-cells are thought to be less powerful. However, synthetic T-cell vaccines composed of Melan-A/MART-1 peptide, CpG and IFA can induce high frequencies of self/tumor-specific circulating CD8 T-cells in melanoma patients. Here we analyzed the functional competence of these T-cells directly ex vivo, by multiparameter flow cytometry. The production of multiple cytokines (IFNγ, TNFα, IL-2) and upregulation of LAMP-1 (CD107a) by tumor (Melan-A/MART-1) specific T-cells was comparable to virus (EBV-BMLF1) specific CD8 T-cells. Phosphorylation of STAT1, STAT5 and ERK1/2, and expression of CD3 zeta chain were also similar in tumor- and virus-specific T-cells, demonstrating functional activatory signaling pathways. Interestingly, high frequencies of functionally competent T-cells were induced irrespective of patient's age or gender. Thus, vaccination with peptide and CpG activated multifunctional tumor-specific human CD8 T-cells in vivo, despite that Melan-A is a self-antigen. This is strikingly different to tumor-specific T-cell responses arising spontaneously or upon vaccination without CpG, which typically show low T-cell frequencies, inefficient cytokine production and cytotoxicity, and blunted signaling. Our demonstration of robust T-cell responses encourage further development and phase III trials assessing the clinical efficacy of this vaccination strategy.

Crosstalk between Tumor Necrosis Factor-alpha and Estrogen signaling pathways in endometrial epithelial cells

[1]Gori I., [1]Pellegrini C., [1]Staedler D., [1]Russell R., [1]Jan C., [1]Canny G.

Dept. of Gynecology, Obstetrics and Medical Genetics, CHUV[1]

TNF-α, a major pro-inflammatory cytokine and the female hormone estrogen have been implicated in the pathophysiology of two gynaecological diseases: endometriosis and endometrial adenocarcinoma.

The aim of this study was to examine crosstalk between TNF-α and ER signaling in endometrial epithelial cells.

The action of TNF-α on ER-mediated signaling was compared to the classical ligand estrogen by means of an ERE luciferase assay. We demonstrated that TNF-α induced luciferase expression in the absence of E2 and augmented the effect of E2 with maximal activation after 3h of exposure.

TNF-α activity on estrogen signaling appeared to be dependent on the ERK pathway, since E2 increased TNF-α stimulated phosphorylation of ERK1/2.

Furthermore, TNF-α increased the expression of c-fos mRNA, an estrogen regulated gene, and potentiated the E2 mediated activation.

Using siRNA againt ERα we also demonstrated that TNF-α activates specifically ER signaling through this receptor.

Our results suggest that a combination of TNF-α and estrogen inhibitors might be useful for the treatment of these pathologies.

THE
Therapeutic Procedures

Neurally Adjusted Ventilatory Assist (NAVA) improves patient-ventilator synchrony in patients undergoing non invasive ventilation.

[1]Piquilloud L., [2]Bialais E., [3]Lambermont B., [2]Roeseler J., [4]Vignaux L., [5]Sottiaux T., [1]Jolliet P., [4]Tassaux D.

SMIA-CHUV[1], Cliniques universitaires St-Luc- Bruxelles[2], CHU Sart-Tilman-Liège[3], HUG-Genève[4], Clinique Notre dame de grâce-Gosselies[5]

Rationale

Neurally adjusted ventilatory assist (NAVA) is an assisted ventilatory mode using electrical activity of the diaphragm or Eadi recorded through esophageal electrodes to trigger the ventilator, deliver assistance in proportionality to inspiratory demand and cycle off the ventilator. NAVA improves patient-ventilator synchrony in intubated patients in comparison with pressure support (PS). Under non invasive ventilation (NIV), because of the presence of leaks which interfere with the triggering and cycling, patient-ventilator synchrony is difficult to achieve, which can lead to NIV failure and intubation. Using Eadi, a signal independent from leaks and respiratory mechanics, could be promising.   The aim of this study is to determine if, compared to PS, NAVA can improve patient-ventilator synchrony in intensive care patients undergoing NIV.

Methods

Randomized comparative study during PS with clinician determined ventilator settings and NAVA with gain (proportionality factor between Eadi and delivered pressure) set as to obtain the same peak airway pressure as the total pressure obtained in PS. A 20 minute continuous recording of airway pressure, flow and Eadi with each ventilatory mode was performed in a randomized order allowing determination of Trigger delay (Td), patient neural inspiratory time (Tin), duration of pressurization by the ventilator (Tiv), excess duration of pressurization (Ti excess = Tiv-Tin / Tin X100) and number of asynchrony events by minute. Results between both groups were compared by paired T-test or Wilcoxon test if needed and given as mean ± SD. p was considered significant if < 0.05.

Results

Preliminary results (mean ± SD): 7 patients (age 64.7 ± 4.9 yr ,1 M/6F, BMI 24.5 ± 6.6 kg/m^2, SAPS II 34 ± 9) , 3 patients with COPD, 1 with mixed obstructive and restrictive disease.   Ventilator settings: FIO_2 32.9 ± 9.1%, PEEP 6.1 ± 1.6 cmH_2O, PS 9.3 ± 2.4 cmH_2O, Trigger in PS: 6 flow/ 1 pressure , Cycling off criteria in PS between 30 and 55%. NAVA gain between 0.2 and 1 µV/cmH_2O, trigger NAVA 0.5 µV.
Under NAVA, 87 ± 8.1% of ventilator cycles were triggered and 96 ± 3.1% were cycled off by the Eadi signal.

	PS	NAVA	p
Leaks (mean value) *l/min*	2.5 ± 2.5	2.2 ±2.0	0.140
Td *ms*	193 ± 62	46 ± 23	< 0.001
Tiexcess *ms*	192 ± 126	131 ± 25	0.275
Total number of asynchronies *n/min*	6.8 ± 6.5	2.3 ± 1.6	0.12
Double triggering *n/min*	2.5 ± 3.8	0.3 ± 0.3	0.078
Ineffective effort *n/min*	0.7±0.9	0	0.082
Late cycling *n/min*	0.7±1.6	0	0.125
Premature cycling *n/min*	0.8 ± 0.8	0	0.035
Autotriggering *n/min*	2.0± 2.1	1.9 ± 1.5	0.915

Conclusion

Compared with PS, NAVA improves patient ventilator synchrony under NIV by reducing Td and premature cycling. With NAVA ineffective efforts, late or premature cycling were absent. There is also a strong trend towards reducing total asynchrony events. This ongoing trial should provide evidence that NAVA can improve patient-ventilator synchrony in patients undergoing NIV.

Aging and storage of erythrocyte concentrates

Delobel J.

Service Régional Vaudois de Transfusion Sanguine

Introduction

Red Blood Cell (RBC) concentrate is the main labile blood product used in transfusion medicine. Numerous efforts are made to ensure quality and security of blood products from collection to transfusion. Non-physiological cold-storage may provoke RBC alterations, well described in the literature as "RBC storage lesions". Those lesions includes morphological, biomechanical and biochemical alterations. How theses lesions affect transfusion efficiency is not yet clearly understood. Among the different storage lesions, RBCs are subjected to oxidative stress, which leads to the oxidation of part of their protein content. We focus on how oxidative lesions are involved in RBC *in vitro* aging and *in-vivo* clearance.

Materials and Methods

Erythrocyte concentrates are obtained from voluntary blood donation from Lausanne and Bern blood transfusion centers. Briefly, whole blood donations are collected into anticoagulant solution. Plasma, platelets and leukocytes are removes and RBC concentrates are stored in additive solution for up to 49 days at 4°C. Only RBC concentrates stored in SAGM and refused for transfusion medicine were used here.

Cytoplasmic content is extracted by hypotonic lysis with or without previous density-based fractionation of RBCs populations through Percoll centrifugation. High-density fraction is thought to be enriched in old erythrocytes and low-density fraction in young ones.

Carbonylation content is here spectrophotometrically investigated. The assay is based on carbonylated proteins dérivatisation by 2,4-dinitrophenylhydrazine. This reaction leads to formation of protein-hydrazone complexes of which optical density at 375 nm allows quantitaion of protein carbonylation.

Since hemoglobin has absorption peak at the wavelength used for this assay, cytoplasmic extracts are previously hemoglobin-depleted by nickel-based IMAC column.

Results

Preliminary results show a storage time-related increase of the carbonylated protein content that seems to be constant from day one to day 14 (around 2 nmol/mg), then present an important increase at day 14 (from 1.7nmol per mg of protein to 3.2nmol/mg), with a maximum at day 22 (3.7nmol/mg), and seems to stay relatively constant with a little decrease until day 42 (2.7nmol/mg).

The age-related fractionation reveals that the supposed old-population enriched fraction presents lower protein carbonylation content than the young-population enriched one. It's however interesting to note that the ration between lower-density and higher-density fractions is constant at around 1 from day 1 to day 16, then increases until the end of the storage period.

Conclusions

RBC cytoplasmic carbonylation content shows an increasing profile from day 14, and a decrease in the end of the storage. Contrary to expected, results show that population lower density population (supposed to be younger RBCs) have higher carbonylation content. In our hands, it appears that number of RBC microparticles increases during storage. A possible explanation could be that microparticulation allows harmful components elimination, of which carbonylated proteins possibly belong. Further experiments on microparticles and oxidation will be conduct to support these results.

Determination of oseltamivir and oseltamivir carboxylate in human plasma_by liquid chromatography-tandem mass spectrometry

Manel A.

Clinical Pharmacology-CHUV

Introduction: Oseltamivir phosphate (OP), the prodrug of oseltamivir carboxylate (OC; active metabolite), is marketed since 10 years for the treatment of seasonal influenza flu. It has recently received renewed attention because of the threat of avian flu H5N1 in 2006-7 and 2009-10 A/H1N1 pandemics. However, relatively few studies have been published on OP and OC clinical pharmacokinetics. The disposition of OC and the dosage adaptation of OP in specific populations, such as young children or patients undergoing extrarenal epuration, have also received poor attention. An analytical method was thus developed to assess OP and OC plasma concentrations in patients receiving OP and presenting with comorbidities or requiring intensive care.

Methods: A high performance liquid chromatography coupled to tandem mass spectrometry method (HPLC-MS/MS) requiring 100-µL aliquot of plasma for quantification within 6 min of OP and OC was developed. A combination of protein precipitation with acetonitrile, followed by dilution of supernant in suitable buffered solvent was used as an extraction procedure. After reverse phase chromatographic separation, quantification was performed by electro-spray ionization–triple quadrupole mass spectrometry. Deuterated isotopic compounds of OP and OC were used as internal standards.

Results: The method is sensitive (lower limit of quantification: 5 ng/mL for OP and OC), accurate (intra-/inter-assay bias for OP and OC: 8.5%/5.5% and 3.7/0.7%, respectively) and precise (intra-/inter-assay CV%: 5.2%/6.5% and 6.3%/9.2%, respectively) over the clinically relevant concentration range (upper limits of quantification 5000 ng/mL). Of importance, OP, as in other previous reports, was found not to be stable *ex vivo* in plasma on standard anticoagulants (i.e. EDTA, heparin or citrate). This poor stability of OP has been prevented by collecting blood samples on commercial fluoride/oxalate tubes.

Conclusions: This new simple, rapid and robust HPLC-MS/MS assay for quantification of OP and OC plasma concentrations offers an efficient tool for concentration monitoring of OC. Its exposure can probably be controlled with sufficient accuracy by thorough dosage adjustment according to patient characteristics (e.g. renal clearance). The usefulness of systematic therapeutic drug monitoring in patients appears therefore questionable. However, pharmacokinetic studies are still needed to extend knowledge to particular subgroups of patients or dosage regimens.

Is there a role for I-123-hippuran renography (RG) in the assessment of live kidney donors?

[1]Nicod Lalonde M., [2]Venetz J.-P., [3]Matter M., [1]BischofDelaloye A., [1]Boubaker A.

Service de Médecine Nucléaire- CHUV[1], Centre de transplantation d'organes- CHUV[2], Service de chirurgie viscérale-CHUV[3]

Aim: to assess the role of RG in the evaluation of renal function in live kidney donors.

Methods: From 2002 to 2008, 109 patients (35M, 74F; 49±12y) were evaluated for kidney donation. Creatinine clearance (Ccr) was estimated by Cockroft, and abbreviated modification of diet in renal disease (MDRD) equations (n=108), and 24h urine collection (UCcr) (n=100). During RG, individual renal function was measured by an accumulation index (AI) defined as the percent of injected activity extracted 30-90 sec after heart peak and effective renal plasma flow (ERPF) was measured using the single blood sample method at 44 min (Tauxe). Accepted lower limit of Ccr is 80ml/min. Normal AI is 11±2 per kidney.

Results: Of 109 patients, 78 patients have donated a kidney, 19 patients were excluded, 12 are still under investigation. We observed a progressive decrease of ERPF with age, whereas AI decreased after 60y only. Cockroft, MDRD and UCcr were higher in donors under 40y, but did not vary significantly after 40y.

Age	*N*	AI donated kidney	AI remaining kidney	ERPF	UCcr	Cockroft	MDRD
≤40	21	10.2±1.6	10.9±1.9	597±69	115±25	111±25	92±16
41-60	43	9.7±1.8	10.6±1.6	546±83	101±22	87±23	80±17
≥60	14	8.8±1.4	9.7±1.6	465±76	102±18	86±15	87±11

41 donors (53%) had a Cockroft and/or MDRD <80ml/min. In these 41 donors, UCcr was normal in 35, ERPF in 39, AI of the remaining kidney was ≥9 in 33. The best functioning kidney was left in 56 donors

Conclusions: In our population, based on Cockroft and/or MDRD, 53% of potential donors would not have been eligible, indicating an additional method is needed to better assess renal function. RG (ERPF, AI) and UCcr provided more reliable renal function evaluation. In addition, RG is useful to decide on the side of nephrectomy, leaving the best functioning kidney in the donor.

In Vivo Synergism of Ceftobiprole in Combination with Vancomycin Against Experimental Endocarditis due to Vancomycin-Intermediate Staphylococcus aureus

[1]Vouillamoz J., [1]Entenza J., [1]Coelho-Veloso T., [1]Giddey M., [1]Moreillon P.

Department of Fundamental Microbiology[1]

Background: Several studies have reported in vitro synergy between beta-lactams and vancomycin (VAN) against methicillin-resistant *S. aureus* (MRSA) and vancomycin-intermediate *S. aureus* (VISA) isolates. Nevertheless, attempts to use such combinations against VISA in animal infection models have yielded conflicting results, probably due to the relatively weak affinity of the beta-lactams used for penicillin-binding protein 2A (PBP2A). Ceftobiprole (BPR), a novel cephalosporin with improved affinity for PBP2A, showed in vitro synergism with VAN against MRSA and VISA (Entenza et al. ECCMID 2010). Here we further explored this synergism in vivo against two VISA clinical isolates in the model of experimental endocarditis (EE).

Methods: Rats with aortic vegetations (veg) were inoculated with 10^6 CFU of VISA strains PC3 or Mu50. Infected rats were treated for 3 days with drug dosages simulating the following treatments in humans: (i) BPR 750 mg intravenously (i.v.) bid (Cmax: 49 mg/L), (ii) BPR 125 mg i.v. bid (Cmax: 10 mg/L; a low dosage purposely used to help detect positive drug interactions), (iii) VAN 1 g i.v. bid and (iv) BPR 125 combined with VAN.

Results: MICs (mg/L) of BPR for VISA PC3 and Mu50 were 2 and 1 mg/L, respectively, and MICs of VAN were 8 mg/L for both strains. Results of therapy were:

	VISA PC3	VISA Mu50
Groups	Infected veg/total (%)	Infected veg/total (%)
Control	10/10 (100)	10/10 (100)
BPR 750	2/14 (14)*	3/13 (23)*
BPR 125	8/8 (100)	15/15 (100)
VAN 1	7/7 (100)	8/8 (100)
BPR 125 + VAN 1	2/9 (22)**	8/14 (57)**

 * $P < 0.05$ vs control and VAN

 ** $P < 0.05$ vs control, BPR125 and VAN

Conclusions: BPR monotherapy, modeled on approved standard doses, was active against EE caused by VISA. Moreover, low-dose BPR strongly synergized with inactive VAN to restore treatment efficacy. Combining BPR with VAN merits further study as an option for difficult-to-treat VISA infections especially when drug penetration at the infected site is an issue.

Neurally Adjusted Ventilatory Assist can improve arterial oxygenation

[1]Piquilloud L., [2]Roeseler J., [3]Vignaux L., [2]Bialais E., [1]Jolliet P., [3]Tassaux D.

SMIA-CHUV[1], Cliniques universitaires St-Luc, Bruxelles[2], HUG-Genève[3]

INTRODUCTION

Neurally Adjusted Ventilatory Assist (NAVA) (1) is a new spontaneous-assisted ventilatory mode which uses the diaphragmatic electrical activity (Eadi) to pilot the ventilator. Eadi is used to initiate the ventilator´s pressurization and cycling off. Delivered inspiratory assistance is proportional to Eadi. NAVA can improve patient-ventilator synchrony (2) compared to pressure support (PS), but little is known about its effect on minute ventilation and oxygenation.

OBJECTIVES

To compare the effects of NAVA and PS on minute ventilation and oxygenation and to analyze potential determinant factors for oxygenation.

METHODS

Comparison between two 20-minute periods under NAVA and PS. NAVA gain (proportionality factor between Eadi and delivered pressure) set as to obtain the same peak pressure as in PS. FIO_2 and positive end-expiratory pressure (PEEP) were the same in NAVA and PS. Blood gas analyses were performed at the end of both recording periods. Statistical analysis: groups were compared with paired t-tests or non parametric Wilcoxon signed-rank tests. $p < 0.05$ was considered significant.

RESULTS (mean ± SD):

22 patients (age 66 ± 12 yr, 7 M/ 15 F, BMI 23.4± 3.1 kg/m^2), 8 patients with COPD. Initial settings: PS 13 ± 3 cmH$_2$O, PEEP 7 ± 2 cmH$_2$O, NAVA gain 2.2 ± 1.8. Minute ventilation and PaCO$_2$ were the same with both modes (p=0.296 and 0.848 respectively). Tidal volume was lower with NAVA (427 ±102 vs.477 ± 102 ml, p< 0.001). In contrast respiratory rate was higher with NAVA (25.6 ± 9.5 vs. 22.3 ± 8.9 cycles/min). Arterial oxygenation was improved with NAVA (PaO$_2$ 85.1 ± 28.9 vs. 75.8 ± 11.9mmHg, p=0.017, PaO$_2$/FIO$_2$ 210 ± 53 vs.195 ± 58 mmHg, p=0.019). Neural inspiratory time (Tin) was comparable between NAVA and PS (p=0.566). Among potential determinant factors for oxygenation, mean airway pressure (Pmean) was lower with NAVA (10.6 ± 2.6 vs 11.1 ± 2.4 cmH$_2$O, p = 0.006), as was the Pressure time product of the ventilator (PTP) (6.8 ± 3.0 vs. 9.2 ± 3.5 cm H$_2$O x sec, p=0.004). There were less asynchrony events with NAVA (2.3 ± 2.0 vs 4.4 ± 3.8, p= 0.009).Tidal volume variability was higher with NAVA (variation coefficient: 30 ± 19.5 vs. 13.5 ± 8.6, p< 0.001). Inspiratory time in excess (Tiex) was lower with NAVA (56 ± 23 vs. 202 ± 200 ms, p= 0.001).

CONCLUSION

Despite lower Pmean and PTP of the ventilator in NAVA, arterial oxygenation was improved compared to PS. The increase in VT variability with NAVA could be an explanation for improved oxygenation. Further studies should now be performed to confirm the potential of NAVA in improving arterial oxygenation and explore the underlying mechanisms.

REFERENCES

(1) Sinderby et al. Nat Med. 1999 Dec;5(12):1433-6.
(2) Spahija J et al. Crit Care Med. 2010 Feb;38(2):518-26.

Neurally Adjusted Ventilatory Assist increases tidal volume variability and improves coupling between tidal volume and patient ventilatory demand compared

[1]Piquilloud L., [2]Moorhead K., [2]Desaive T., [3]Roeseler J., [4]Chase J., [5]Vignaux L., [3]Bialais E., [5]Tassaux D., [6]Lambermont B., [7]Jolliet P.

SMIA-CHUV[1], Centre de recherche cardio-vasculaire, université de Liège, Liège[2], Soins intensifs, Cliniques universitaires St Luc, Bruxelles[3], Department of Mechanical Engineering, University of Canterbury, Christchurch[4], HUG-Genève[5], Soins intensifs médicaux, CHU Sart-Tilman, Liège[6], CHUV-Lausanne[7]

INTRODUCTION: Neurally Adjusted Ventilatory Assist (NAVA) is a new ventilatory mode in which ventilator settings are adjusted based on the electrical activity of the diaphragm (Eadi). This mode offers significant advantages in mechanical ventilation over standard pressure support (PS), since ventilator input is determined directly from patient ventilatory demand. Therefore, it is expected that tidal volume (Vt) under NAVA would show better correlation with Eadi compared with PS, and exhibit greater variability.

OBJECTIVES: To compare tidal volume variability in PS and NAVA, and it's correlation with patient ventilatory demand (as characterized by Eadi).

METHODS: A comparative study of patient-ventilator interaction was performed for 22 patients during standard PS with clinician determined ventilator settings; and NAVA, with gain set to ensure the same peak airway pressure as the total pressure obtained in PS. A 20 minute continuous recording was performed in each mode. Respiratory rate, Vt, and Eadi were recorded. Tidal volume variance and Pearson correlation coefficient between Vt and Eadi were calculated for each patient. A periodogram was plotted for each ventilator mode and each patient, showing spectral power as a function of frequency to assess variability.

RESULTS: Median, lower quartile and upper quartile values for Vt variance and Vt/Eadi correlation are shown in Table 1. The NAVA cohort exhibits substantially greater correlation and variance than the PS cohort.

Table 1. Variance and Correlation metrics for PS and NAVA

Patient Cohort	Variance in Vt		Correlation (Eadi vs Vt)	
	PS	NAVA	PS	NAVA
Lower quartile	793	5218	0.0405	0.5971
Median	3043	10798	0.2563	0.6618
Upper Quartile	5398	23715	0.3517	0.7618

Figure 1. Power Spectrum for Vt and Eadi under PS (above) and NAVA (below)
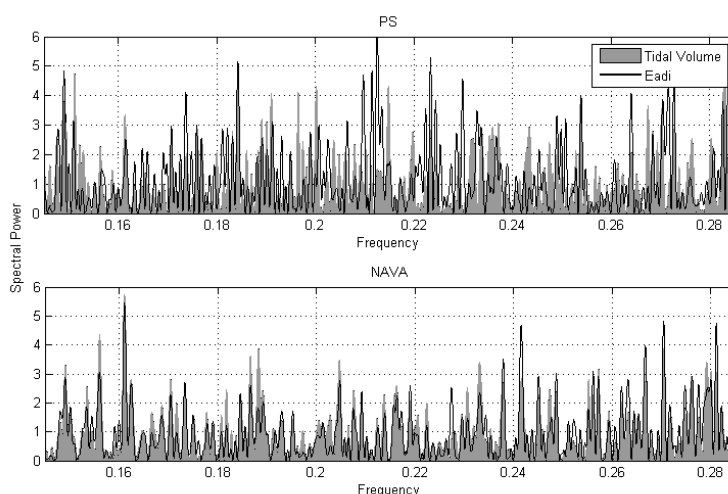
Power spectrums for Vt and Eadi are shown in Figure 1 (PS and NAVA) for a typical patient.

CONCLUSIONS: There is greater variability in tidal volume and correlation between the tidal volume and the diaphragmatic electrical activity with NAVA compared to PS. These results are consistent with the improved patient-ventilator synchrony reported in the literature.

Authors' Index

*Main author in **thick***

BICHAT ARNAUD MCV-63
BILL OLIVIER NEU-138
BISCHOF-DELALOYE ANGELIKA MCV-75/MCV-77/MCV-111/THE-164
BIZZINI ALAIN **IMI-17**/IMI-35
BOBST MARTINE IMI-24
BOCHUD MURIELLE IMI-33/MCV-102
BOCHUD PIERRE-YVES IMI-29/IMI-37
BOHLENDER JÜRGEN **MCV-107**/**MCV-109**
BOILLAT BLANCO NOÉMIE **IMI-37**/**IMI-42**
BOITTIN FRANÇOIS-XAVIER MCV-65
BONAFÉ LUISA MCV-48/MCV-49/MCV-50
BONNEAU JUSTINE EHU-7
BONNY CHRISTOPHE NEU-132
BONNY OLIVIER MCV-70/MCV-95
BONTEMS OLYMPIA IMI-22
BOUBAKER ARIANE MCV-78/MCV-79/MCV-88/ MCV-111/THE-164
BOUDUBAN THIERRY **MCV-112**
BOURQUIN CÉLINE **EHU-1**
BOUZOURÈNE KARIMA MCV-84
BOVET PASCAL EHU-3/MCV-64/MCV-66/MCV-102
BRAISSANT OLIVIER MCV-49/MCV-50
BRAJKOVIC SASKA **MCV-98**
BRAUN MARION **IMI-46**
BRUCHEZ F. **EHU-168**
BUCLIN THIERRY MCV-87/ODE-153
BULLIARD JEAN-LUC **EHU-7**/EHU-168/ENA-10
BURNIER MICHEL MCV-67
BÜRGISSER PHILIPPE IMI-40
CALANDRA THIERRY IMI-16/IMI-18/IMI-20/IMI-21/IMI-29
CALMET GAUTIER **EHU-4**
CAMPOS VANESSA NEU-133
CAMUS FABRICE MCV-75/MCV-80/MCV-88
CANELLINI GIORGIA IMI-40
CANNY GERALDINE IMI-45/ODE-160
CARIOLATO LUCA **MCV-69**
CARRARD MARIANNE MCV-115
CARRASCOSA CORALIE **ODE-156**/ODE-157
CAVASSINI MATTHIAS IMI-37/IMI-40
CAVIN SABRINA **MCV-92**
CENTENO GABRIEL MCV-70
CHALANDON YVES ODE-153
CHAMPENDAL MÉLANIE MCV-88
CHAPARD CHRISTOPHE **ODE-154**
CHAPUIS-TAILLARD CAROLINE **IMI-25**
CHASE J. GEOFFREY THE-167
CHATTON JEAN-YVES NEU-142
CHERBUIN NICOLAS MCV-74/**MCV-111**
CHIOLERO ARNAUD **MCV-66**
CHRAST ROMAN NEU-128
CISSÉ OUSMANE H. **EHU-5**
CLARKE STEPHANIE NEU-135
CLEMENTI M. MCV-87
COELHO-VELOSO TIAGO RAFAEL THE-165
CORGNAC STÉPHANIE **ODE-150**
CORNUZ JACQUES GEN-11/MCV-59

COSTE ALIX IMI-29
COTECCHIA SUSANNA MCV-91
COULON AURELIE ODE-151/ODE-152
CRISANTE GIOVANNA **IMI-43**
CROQUELOIS ALEXANDRE NEU-143
CROXATTO ANTONY ENA-9
CRUCHET STEEVE MCV-169
CSAJKA CHANTAL ODE-153
CUPPERS-MAARSCHALKERWEERD B. MCV-87
D'ANGELO FABRIZIA **IMI-23**
DABIRI AMIN MCV-77
DACOSTA ANABELA MCV-115
DAMNON FRANÇOISE IMI-45
DANG THANH IMI-33
DARIOLI ROGER MCV-62
DARLING KATHARINE IMI-40
DAVIN CAROL MCV-56
DEBONNEVILLE ANNE MCV-93
DECOSTERD ISABELLE NEU-129
DECOSTERD LAURENT A. ODE-153
DECRAUSAZ LOANE IMI-24
DEGUEURCE GWENDOLINE **GEN-12**
DEKEMP ROBERT MCV-75
DEL VESCOVO COSMO DAMIANO **MCV-91**
DELALOYE ALINE MCV-76
DELOBEL JULIEN **THE-162**
DELODDER FREDERIK **MCV-99/MCV-100**/MCV-114
DELORENZI MAURO ODE-156/ODE-158
DEMARTINES NICOLAS ODE-147
DEMCIK NATHALIE MCV-5/MCV-73
DEPAIRON MICHÈLE MCV-62
DEPREUXCHARLES ANNE-SOPHIE NEU-128
DERRÉ LAURENT ODE-159
DESAIVE THOMAS THE-167
DESANTIS M. MCV-87
DESSEN PIERRE MCV-63
DIACERI GIACOMO MCV-116/MCV-117
DIVIANI DARIO MCV-69/ MCV-91/MCV-92/MCV-96
DOMINGOS-PEREIRA SONIA **IMI-24**
DONDA ALENA ODE-150
DORMOND OLIVIER ODE-147
DORMOND-MEUWLY ANNE ODE-147
DUBUIS GILLES MCV-126
DUCHOSAL MICHEL MCV-84/ODE-153/ODE-155
DUNET VINCENT MCV-68/MCV-74/**MCV-75/MCV-76/MCV-77/MCV-78/MCV-79**/MCV-80/MCV-88
DUPASQUIER RENAUD IMI-30
DUQUENNE PHILIPPE EHU-2
DWYER ANDREW **MCV-85**
DÉNÉRÉAZ MARIE-LAURE **GEN-14**
EGGER MATTHIAS IMI-33
EGGIMANN PHILIPPE **IMI-16**/IMI-18/**IMI-19**/MCV-114
EGLI DELPHINE MCV-48

EGLI LÉONIE NEU-133
EL HAKMAOUI FATIMA **MCV-74/MCV-88**

ELEFTERIOU J. MCV-87
ENTENZA JOSÉ MANUEL IMI-36/**THE-165**
ESKIN ELEAZAR MCV-113
FAOUZI MOHAMED NEU-136/NEU-138/NEU-139
FARESSE NOURDINE **MCV-93**
FARHAD HOSHANG **MCV-68/MCV-80**
FAVRE DIMITRI MCV-98
FEIHL FRANÇOIS MCV-51/MCV-77
FICHE MARYSE IMI-45
FIRSOV DMITRI MCV-70
FLAHAUT MARJORIE ODE-151/ODE-152
FLUECKIGER URSULA IMI-18
FRANCIOLI LAURENT ENA-10
FRANÇOIS PATRICE IMI-21
FRATTI MARINA IMI-22
FRITSCHY JEAN-MARC NEU-143
FROMER MARTIN MCV-89
FURUSTRAND ULRIKA **IMI-27/IMI-28**/IMI-42
GAGNON GHISLAINE MCV-100
GATTESCO SONIA MCV-97
GEDEON JUDE EHU-3
GIACOBINO ARIANE MCV-63
GIDDEY MARLYSE IMI-15/IMI-36/THE-165
GIULIERI STEFANO IMI-37
GIUSTI VITTORIO NEU-133
GLAUSER FRÉDÉRIC **MCV-62**
GONZALES CHRISTINE **MCV-52**/MCV-73
GOODPASTER BRET MCV-110
GORI ILARIA IMI-45/**ODE-160**
GOTTA VERENA **ODE-153**
GRAF ROLF IMI-16
GRANDMAISON GAËL IMI-20
GREGOR MICHAEL ODE-153
GREUB GILBERT ENA-9/IMI-32
GRIVEL JEREMY NEU-131
GROSS NICOLE ODE-149/ODE-151/ODE-152
GRUETTER ROLF NEU-140
GUAL PHILIPPE MCV-112
GUDINCHET FRANÇOIS MCV-123
GUESSOUS IDRIS MCV-114
GUILLAUME PHILIPPE ODE-159
GUPTA BHAWNA **IMI-34**/IMI-39
HAEFLIGER JACQUES-ANTOINE MCV-65/MCV-72/MCV-83
HANLEY JAMES A. MCV-66
HAUSER PHILIPPE EHU-5/IMI-18
HAZAN RONEN IMI-15
HE JIANXIN IMI-15
HEBEISEN MICHAEL **IMI-41**
HEIM DOMINIK ODE-153
HEINZER RAPHAEL MCV-76
HENRY HUGUES MCV-50
HERSCH MICHA MCV-113
HIRT LORENZ NEU-132/NEU-140/NEU-141
HOHL DANIEL IMI-44/ODE-154
HOTZ PHILIPP EHU-2

HOUHOU NAWAL ODE-158
HUBER MARCEL ODE-154
HUMMLER EDITH GEN-14/MCV-67/MCV-101/MCV-105/MCV-108
IANCU EMANUELA MARINA IMI-34/**IMI-39**
IBBERSON MARK GEN-12
IMBODEN HANS MCV-107
IRVING MELITA IMI-41
IVANOV KONSTANTIN ODE-158
JACCARD EVRIM **MCV-126**
JACOVETTI CÉCILE **MCV-71**
JAN CAROLINE ODE-160
JANDUS CAMILLA ODE-159
JAQUET MURIEL ODE-158
JATON KATIA IMI-25/IMI-42
JAYET PIERRE-YVES MCV-76
JICHLINSKI PATRICE IMI-24
JILEK TERRASSE SAMANTHA **IMI-30**
JOLLIET PHILIPPE THE-161/THE-166/THE-167
JOSEPH CHRISTINE IMI-19
JOSEPH JEAN-MARC ODE-151
JOUSSET FLORIAN MCV-89
KAEUPER PETER ODE-149
KANG HYUN MIN MCV-113
KASAS SANDOR IMI-17
KAUFMANN ANNATINA **IMI-40**
KENFAK-FOGUENA ALAIN IMI-40
KESARWANI MEENU IMI-15
KHALIL HADI **MCV-127**
KHOUDI DORRA MCV-99/MCV-100
KIELAR MICHEL NEU-143
KLEE PHILIPPE MCV-72
KLEEBERG JOERG **NEU-143**
KLEIN RAIN MCV-75
KNAUPREYMOND MARLIES IMI-20
KOESTERS ROBERT MCV-53/MCV-105
KOSINSKI MAREK MCV-75/MCV-78/MCV-79/MCV-88
KRAFTSIK RUDOLF NEU-134
KULIK GERIT **NEU-144**
KUMAR RAJESH **IMI-45**
KUTALIK ZOLTAN GEN-11
LAGOPOULOS LUCIENNE **ODE-149**
LAJAUNIAS FREDERIC IMI-16
LAMBERMONT BERNARD THE-161/THE-167
LAMOTH FREDERIC IMI-18
LAMY CHRISTOPHE **NEU-142**
LATGÉ JEAN PAUL IMI-29
LAUE CARSTEN ODE-149
LAURENT JULIEN IMI-39
LE CORRE-LALIBERTÉ CELINE **NEU-137**
LEHR HANS-ANTON ODE-156
LEI HONGXIA NEU-140
LEPORE MARIO MCV-169
LEROY DIDIER IMI-20/IMI-21/IMI-29
LEUBA GENEVIÈVE **NEU-134**
LEVI F. EHU-168

LEYVRAZ SERGE IMI-39
LIAUDET LUCAS IMI-16/MCV-51
LIBERMAN JULIE **ODE-151**/ODE-152
LIENARD JULIA **ENA-9**
LIETTI CLAUDIA **NEU-133**
LOFFING DOMINIQUE MCV-53
LOFFING JOHANNES MCV-53/MCV-67
LOVIS ALBAN MCV-76
LUCY HENDERSON NEU-144
LUESCHER IMMANUEL F. ODE-159
LUGRIN JÉRÔME **IMI-20/IMI-21**
LYNGDOH TANICA MCV-64/**MCV-102**
LÖVGREN TANJA ODE-159
MABY-ELHAJJAMI HELENE   ODE-158
MADELEINE GEORGE MCV-66
MAEDER PHILIPPE NEU-139
MAGISTRETTI PIERRE NEU-141
MAILLARD MARC MCV-67
MAILLARD MICHEL IMI-23
MAISON DAMIEN GEN-14
MAJIC IVANA IMI-28
MALSURE SUMEDHA **MCV-101**
MALTERRE JEROME MCV-74/MCV-78/MCV-79/MCV-88
MANAKOVA E. MCV-87
MANEL AOURI **THE-163**
MANUEL AURÉLIE NEU-130/**NEU-131**
MANUEL ORIOL IMI-25
MARCELINO GISELA MCV-54/MCV-61
MARCHETTI OSCAR IMI-18/IMI-25
MARINO MATHIEU MCV-116/MCV-117
MARIOTTI AGNESE ODE-156/ODE-157
MARQUES-VIDAL PEDRO **GEN-11/MCV-54/MCV-55/MCV-56/MCV-57/MCV-58/MCV-59/MCV-60/MCV-61**
MARTIN DAVID **MCV-83**
MARTINEZ RAQUEL ODE-148
MASCLAUX FRÉDÉRIC **EHU-2**
MATTER MAURICE ODE-159/THE-164
MAURER FABIENNE **MCV-113**
MAZZOLAI LUCIA MCV-62/ MCV-65/MCV-77/MCV-84/MCV-107
MAZZUCCHELLI LUCA ODE-156
MEDA PAOLO MCV-65/MCV-72/MCV-83
MELICH-CERVEIRA JOÃO MCV-54/MCV-59/MCV-61
MELITA IRVING IMI-41
MERILLAT ANNE-MARIE GEN-14
MERLOB P. MCV-87
METREF SALIMA   MCV-115
METRICH MELANIE **MCV-120**/MCV-169
MEULI RETO NEU-139
MEYLAN PASCAL IMI-25/IMI-39
MICHALIK LILIANE GEN-12/MCV-106
MICHALIS ALEXANDRE MCV-82
MICHEL PATRIK NEU-136/NEU-137/NEU-138/NEU-139
MICHETTI PIERRE IMI-23
MICHIELIN OLIVIER IMI-34/ IMI-39/IMI-41/ODE-159
MILANO GIUSEPPINA **MCV-118**
MILON ANTOINE EHU-7/ENA-10

MINEHIRA CASTELLI KAORI **MCV-10**/MCV-112
MIURA NAOYUKI ODE-158
MIÉVILLE FRÉDÉRIC **MCV-123**
MOCCOZET LAURENT ENA-10
MOHAMED FAOUZI NEU-139
MONOD MICHEL IMI-22/IMI-29
MOODYCLIFFE ANGUS IMI-44
MOORHEAD KATE THE-167
MORADPOUR DARIUS IMI-40
MORDASINI DAVID **MCV-67**
MOREILLON PHILIPPE IMI-16/IMI-36/THE-165
MOTTAZ HELENE MCV-106
MUEHLETHALER VINCENT MCV-116/MCV-117
MURRAY MICAH NEU-130/ NEU-131/NEU-133
MYERS GARY MCV-64/ MCV-102
MÉDARD JEAN-JACQUES NEU-128
MÉNARD JOEL MCV-109
MÜHLETHALER-MOTTET ANNICK ODE-149/ODE-151/**ODE-152**
NAHIMANA AIMABLE **ODE-155**
NARAYAN SANJIV MCV-89
NARDELLI-HAEFLIGER DENISE IMI-24
NEGRO FRANCESCO IMI-33
NEMIR MOHAMED MCV-120/**MCV-169**
NESCA VALERIA **MCV-81**
NICOD LALONDE MARIE **THE-164**
NICOD PASCAL MCV-63
NICULITA-HIRZEL HÉLÈNE **ENA-8**
NIEDERHÄUSER GUY MCV-98
NIKOLAEVA SVETLANA MCV-70
NORRMEN CAMILLA ODE-158
NTAIOS GEORGIOS **NEU-136**
NUNO INACIO **NEU-139**
NUSSBERGER JÜRG MCV-84/MCV-107/MCV-109
OBULA RAMPRASAD ODE-156/**ODE-157**
OPPLIGER ANNE EHU-2/ENA-8
ORASCH CHRISTINA IMI-18
PACCAUD FRED GEN-11/MCV-54/MCV-55/MCV-56/MCV-58/MCV-59/MCV-61/MCV-66
PAGANI JEAN-LUC IMI-19
PAGNI MARCO EHU-5
PANCHAUD A. MCV-87
PANTALEO GIUSEPPE IMI-30
PAPPON MARTIN MCV-74/MCV-88
PARADIS GILLES MCV-66
PASCALE PATRIZIO MCV-89
PASQUALI CHRISTIAN NEU-132
PATIL JASPAL MCV-107
PEDRAZZINI THIERRY MCV-52/ MCV-73/MCV-120/MCV-121/MCV-169
PEDRETTI SARAH **MCV-86**
PELLEGRIN MAXIME MCV-84
PELLEGRINI CHIARA ODE-160
PELTZE NIEVES **GEN-13**
PERRIER ROMAIN **MCV-105**
PERRIN LUDOVIC MCV-77
PERRUCHOUD STÉPHANIE MCV-52/**MCV-94**
PETER BASTIAN MCV-113

PEYTER ANNE-CHRISTINE **MCV-116/MCV-117**
PEZZUTO IOLE **MCV-124**
PHILIPPE MAEDER NEU-139
PIAZZA YVO **NEU-141**
PIERRE-YVES BOCHUD IMI-33
PILON NATHALIE MCV-114
PIQUILLOUD LISE **THE-161/THE-166/THE-167**
PISTELLI A. MCV-87
PITTELOUD NELLY MCV-85
PLAISANCE ISABELLE MCV-52/**MCV-73/** MCV-169
PLUMETTAZ CHLOÉ **EHU-3**
POIROT OLIVIER   NEU-128
PONCE DE LEON VERONICA **MCV-108**
PREITNER FREDERIC **MCV-115**
PREITNER MARIA   MCV-119
PRIOR JOHN MCV-68/ MCV-74/MCV-75/MCV-76/MCV-77/MCV-78/MCV-79/MCV-80/MCV-88
PROBST ARNOLD **IMI-33**/IMI-37
PRUVOT ETIENNE MCV-89
PURICEL SERBAN-GEORGE **NEU-145**
PYTHOUD CATHERINE IMI-23
PYTHOUD CHRISTELLE **IMI-38**
PÉREZ LÓPEZ IRENE **MCV-96**
QANADLI SALAH DINE MCV-77
QUAIRIAUX CHARLES NEU-143
QUE YOK AI **IMI-15/** IMI-16/IMI-36
RADDATZ ERIC MCV-86
RAFFOUL WASSIN MCV-51
RAHME LAURENCE G. IMI-15
REAVEY MICHELLE MCV-60
REGAZZI ROMANO MCV-81/MCV-97/MCV-125
REICHMUTH PHILIPP **MCV-114**
RENAUD JENNIFER MCV-75
RETO MEULI NEU-139
REVELLY JEAN-PIERRE IMI-19/MCV-114
REXHAJ EMRUSH **MCV-63**
REY-BATAILLARD VINCIANNE MCV-76
RICHARME DELPHINE NEU-144
RIEDERER BÉAT NEU-134
RIEDERER IRÈNE NEU-134
RIGNAULT STEPHANIE MCV-51
RIMOLDI STEFANO MCV-63
RIVALS JEAN-PAUL ODE-159
ROCHEMONT VIVIANE MCV-118
ROESELER JEAN THE-161/THE-166/THE-167
ROGER THIERRY IMI-16/IMI-20/IMI-21/IMI-29
ROGGLI ELODIE **MCV-97**
ROMERO PEDRO IMI-34/IMI-39/IMI-46
RONZAUD CAROLINE **MCV-53**
ROSENBLATT-VELIN NATHALIE **MCV-51**
ROSSI NATHANAEL ODE-149
ROSSIER BERNARD MCV-101/MCV-105
ROTHENBERGER SYLVIA ODE-148
ROTHUIZEN L. MCV-87
ROULIN DIDIER **ODE-147**
RUBINO IVANA **IMI-29**

RUCHAT PATRICK MCV-52/ MCV-73/MCV-89
RUFER NATHALIE IMI-34/IMI-39/IMI-41/ODE-159
RUSCONI BRIGIDA **IMI-32**
RUSSELL RONAN ODE-160
RYSER STEPHAN **IMI-44**
RÜEGG CURZIO ODE-156
SABINE AMÉLIE **MCV-104**
SAMAJA MICHELE MCV-118
SAMARA ELENI-THEANO **MCV-122**
SAMBEAT AUDREY **MCV-119**
SAMUILOVA OLGA ODE-158
SANNO HITOMI MCV-103
SARRE ALEXANDRE **MCV-121/** MCV-169
SARTORI CLAUDIO MCV-63
SAUGY JEREMY NEU-133
SAVIOZ ARMAND NEU-134
SCHAEFER STEPHAN MCV-89
SCHERRER URS MCV-63
SCHIZAS CONSTANTIN NEU-144
SCHLUEP MYRIAM IMI-30
SCHMID DAPHNE IMI-41
SCHRENZEL JACQUES IMI-21
SCHWARZ KATRIN IMI-46
SCHÜTZ FRÉDÉRIC GEN-12
SEYER PASCAL MCV-103
SHAMLAYE CONRAD EHU-3
SIEGEMUND MARTIN IMI-18
SINGY PASCAL EHU-1/EHU-6
SOTTIAUX THIERRY THE-161
SOUBEYRAN VINCENT MCV-80
SPEISER DANIEL IMI-34/IMI-39/IMI-41/IMI-46/ODE-159
SPIERER LUCAS NEU-130/NEU-131/NEU-135
STAEDLER DAVIDE ODE-160
STAUB OLIVIER MCV-53/MCV-90/MCV-93
STAUFER JEAN-CHRISTOPHE MCV-122
STEPHENS S. MCV-87
STIEFEL FRIEDRICH EHU-1
STUBER MATTHIAS MCV-47
STOKES JOHN B MCV-53
STUBER MATTHIAS **MCV-47**
SUAREZ PHILIPPE **IMI-31**
SULSTAROVA BRIKELA **EHU-6**
SURBECK ISABELLE IMI-45
SUTER MARC **NEU-129**
TAPPY LUC MCV-99/ MCV-100/NEU-133
TASSAUX DIDIER THE-161/THE- 166/THE-167
TELENTI AMALIO ODE-148
TENKORANG JOANNA **MCV-89**
THEUMANN NICOLAS NEU-144
THEYTAZ FANNY MCV-103
THOME MARGOT ODE-152
THORENS BERNARD MCV-95/MCV-115/MCV-119
THÉVENIN MARIE-JOSÉPHINE IMI-19
TISSOT FREDERIC **IMI-18**
TOEPEL ULRIKE NEU-133

TOLSA JEAN-FRANÇOIS MCV-116/MCV-117
TOZZI PIERGIORGIO **MCV-82**/MCV-99/MCV-100
TRAMPUZ ANDREJ IMI-17/IMI-27/IMI-28/IMI-35/IMI-42
ULLRICH NINA MCV-52
V.PETROVA TATIANA ODE-158
VALMU LEENA ODE-158
VASLIN ANNE NEU-132
VELIN DOMINIQUE IMI-23
VELOSO TIAGO **IMI-36**
VENETZ JEAN-PIERRE THE-164
VERDUN FRANCIS MCV-75/MCV-78/MCV-79/MCV-111/MCV-123/MCV-122
VERNAY ANDRÉ NEU-134
VERNEZ DAVID EHU-7/**ENA-10**
VERRIER JULIE **IMI-22**
VESIN JEAN-MARC MCV-89
VIAL T. MCV-87
VIAL YVAN MCV-117
VICARI MANUELA IMI-45
VIGNAUX LAURENCE THE-161/ THE-166/THE-167
VINCENT ZOETE IMI-41
VISWANATHAN BHARATHI EHU-3/MCV-64/MCV-102
VITAGLIANO JEAN-JACQUES **MCV-90**
VOGT BRUNO MCV-67
VOIROL PIERRE IMI-19
VOLLENWEIDER PETER GEN-11/MCV-55/MCV-56/MCV-58/MCV-59
VON SEGESSER LUDWIG K MCV-82/MCV-118
VOUILLAMOZ JACQUES IMI-36/THE-165
VUILLEUMIER LAURENT ENA-10
WAEBER BERNARD MCV-51/MCV-77
WAEBER GÉRARD GEN-11/MCV-55/MCV-56/MCV-58/MCV-59/MCV-65/MCV-72/MCV-83
WAELTIDACOSTA VRENELI IMI-37
WAHLI WALTER GEN-12
WALICKI JOEL MCV-126
WANG QING MCV-67
WASELLE LAURENT ODE-147
WAWRZYNIAK MARTA **MCV-106**
WELKER EGBERT NEU-143
WIDMANN CHRISTIAN MCV-126
WIDMER NICOLAS ODE-153
WIECKOWSKI SÉBASTIEN IMI-34/IMI-39
WINTERFELD URSULA **MCV-87**
WINTERMARK M. NEU-139
XENARIOS IOANNIS GEN-12
YAN JIANG-YAN MCV-126
YANG BAOLI MCV-53
YLA-HERTTUALA SEPPO ODE-158
ZANETTI GIORGIO IMI-19
ZAVADOVA VLASTA **MCV-70**
ZENKER JENNIFER **NEU-128**
ZHANG JIANGWEN IMI-15
ZIMMERLI STEFAN IMI-18
ZIMMERLI WERNER IMI-28
ZOETE VINCENT IMI-43
ZUERCHER EMILIE **ODE-148**
ZUFFEREY PHILIPPE **NEU-138**